The Transport Properties of Carbon Dioxide

V. Vesovic and W. A. Wakeham

IUPAC Transport Properties Project Centre, Department of Chemical Engineering and Chemical Technology, Imperial College, London SW7 2BY, United Kingdom

G. A. Olchowy[a] and J. V. Sengers

Institute for Physical Science and Technology, University of Maryland, College Park, Maryland 20742

J. T. R. Watson

National Engineering Laboratory, G75 0QU, East Kilbride, Glasgow, United Kingdom

J. Millat

Sektion Chemie, Wilhelm-Pieck Universität Rostock, Buchbinderstrasse 9, Rostock, DDR-2500, German Democratic Republic

The paper contains new, representative equations for the viscosity and thermal conductivity of carbon dioxide. The equations are based in part upon a body of experimental data that have been critically assessed for internal consistency and for agreement with theory whenever possible. In the case of the low-density thermal conductivity at high temperatures, all available data are shown to be inconsistent with theoretical expectation and have therefore been abandoned in favor of a theoretical prediction. Similarly, the liquid-phase thermal conductivity has been predicted owing to the small extent and poor quality of the experimental information. In the same phase the inconsistencies between the various literature reports of viscosity measurements cannot be resolved and new measurements are necessary. In the critical region the experimentally observed enhancements of both transport properties are well represented by theoretically based equations containing just one adjustable parameter. The complete correlations cover the temperature range 200 $K \leqslant T < 1500$ K for viscosity and 200 $K \leqslant T \leqslant 1000$ K for thermal conductivity, and pressures up to 100 MPa. The uncertainties associated with the correlation vary according to the thermodynamic state from $\pm 0.3\%$ for the viscosity of the dilute gas near room temperature to $\pm 5\%$ for the thermal conductivity in the liquid phase. Tables of the viscosity and thermal conductivity generated by the representative equations are provided to assist with the confirmation of computer implementations of the calculation procedure.

Key words: carbon dioxide; critical phenomena; thermal conductivity; thermal diffusivity; transport properties; viscosity.

Contents

[a] Present address: Department of Chemistry, University of Toronto, Toronto, Ontario, M5S 1A1, Canada

Appendix I   List of All Available Data from Measurements of the Thermal Conductivity of Carbon Dioxide

Appendix II   List of All Available Data from Measurements of Viscosity of Dense Carbon Dioxide

Appendix III   Deviation Plots of the Experimental Data from the Correlation

Appendix IV   Tabulations of the Transport Properties of Carbon Dioxide

List of Figures

1. Introduction

Carbon dioxide is a material with an increasing number of industrial applications, and its physical properties have been the subject of intensive study for a considerable period of time. New industrial interest in the substance has been generated by its application as a solvent in supercritical extraction[1] and as a coolant in gas-cooled nuclear reactors.[2] Scientific interest in the fluid state originates with Andrews' original studies of the behavior of carbon dioxide in an equilibrium near-critical state. Because the critical state of carbon dioxide occurs under readily realized experimental con-

ditions ($T_c = 304.107$ K, $P_c = 7.3721$ MPa) the fluid is still employed as a prototype for the application of modern theories of critical phenomena in both equilibrium and transport properties.[3,4] The dual importance of the fluid implies that definitive statements of its physical properties are of considerable value and that they should be regularly updated as new experimental information and more rigorous theory become available.

The most recent critical reviews of the viscosity of carbon dioxide date from 1972, by Altunin and Sakhabetdinov[5] and from 1976 by Watson.[6] For thermal conductivity, Watson[7] produced recommended values in 1976 and Ulybin and Bakulin[8] provided a further compilation in 1978. A decade has therefore elapsed since a comprehensive review of either property was conducted, within which period there have been significant developments in the measurement of the thermal conductivity of fluids leading to important new results. In the same period, our theoretical understanding of transport properties in the neighborhood of the critical point of a pure fluid has greatly improved. Thus, the new critical evaluation of the transport properties of carbon dioxide presented in this paper incorporates all of this modern information into the preparation of recommended data and representative equations.

In general, the data and their representations that emerge from the new study enjoy a higher level of confidence than earlier evaluations because they are founded on more accurate experiments and more complete theory. However, in the case of the liquid-phase viscosity of carbon dioxide, the present review revealed a large discrepancy between old and new sources of experimental information.

The original works provide no evidence on which to base a judgement of the relative merits of the various sets of results. Furthermore, there is no theoretical guidance as to the value of the liquid-phase viscosity. Thus, it is not possible to resolve this problem without independent information. Van der Gulik and his collaborators[9] have made new viscosity measurements to provide just that information but have so far been unable to measure at temperatures below 290 K where the greatest discrepancies arise. In this paper we therefore cannot attempt to resolve this discrepancy. Instead, we accept that some, or all, of the liquid viscosity data at low temperatures may be burdened with a substantial error and choose to weight it equally in a representation that itself is then necessarily burdened with a similar uncertainty. This is done in the recognition that the consequent representation may be refined when new experimental data are available. The form of representation of the transport properties adopted throughout this work is arranged to make such refinements straightforward.

2. Methodology

For both fundamental, physical reasons and for practical purposes, either the total viscosity of a fluid $\eta(\rho,T)$ or the total thermal conductivity $\lambda(\rho,T)$ may be expressed as a sum of three independent contributions. Thus, writing $X(\rho,T)$ for either transport property we have

$$X(\rho,T) = X^0(T) + \Delta X(\rho,T) + \Delta_c X(\rho,T) . \quad (1)$$

Here, the first term, $X^0(T) = X(0,T)$, is the contribution to the transport property in the limit of zero-density, where only two-body molecular interactions occur. The final term, $\Delta_c X(\rho,T)$, the critical enhancement, arises from the long-range fluctuations that occur in a fluid near its critical point which contribute to divergences of both the viscosity and thermal conductivity at that singular point. Finally, the term $\Delta X(\rho,T)$, the excess property, represents the contribution of all other effects to the transport property of the fluid at elevated densities including many-body collisions, molecular-velocity correlations, and collisional transfer.

The identification of these three separate contributions to a transport property is useful because it is possible, to some extent, to treat both $X^0(T)$ and $\Delta_c X(\rho,T)$ theoretically. In addition, it is possible to derive unequivocal information about $X^0(T)$ from experiment. In contrast, there is almost no theoretical guidance concerning $\Delta X(\rho,T)$, so that its evaluation must be based entirely on experiment. For these reasons the general approach adopted for the representation of the transport properties of carbon dioxide is first to seek to establish the functions $\eta^0(T)$ and $\lambda^0(T)$ using a combination of experiment and theory. Subsequently, a first estimate of the 'background' transport property:

$$\bar{X}(\rho,T) = X^0(T) + \Delta X(\rho,T) , \quad (2)$$

is established from experimental data to which $\Delta_c X(\rho,T)$ contributes negligibly, that is data obtained far from the critical region. The subtraction of $\bar{X}(\rho,T)$ from all experimental data then yields first-iterate values of the critical enhancement $\Delta_c X(\rho,T)$ to which the appropriate theory may be applied to determine a single, disposable parameter within it. The subsequent, improved estimate of $\Delta_c X(\rho,T)$ is then used to obtain a refined estimate of the 'background' properties $\bar{X}(\rho,T)$ and the process repeated until convergence.

It is obvious that the analysis described above must be applied to the best available experimental data for both the viscosity and thermal conductivity. Thus, a prerequisite to the analysis is a critical assessment of the experimental data. For this purpose we define two categories of experimental data: primary data employed in the development of the correlation and secondary data used simply for comparison purposes. Ideally, the primary data set comprises those results determined in instruments for which a full working equation exists and in which a high precision in the measured variables was achieved.[10] In practice, such a narrow definition would limit the range of the data representation unacceptably. Consequently, within the primary data set it is also necessary to include results that extend over a wide range of conditions, albeit with a poorer accuracy, provided that they cannot be demonstrated to be inconsistent with other more accurate data or with theory. In all cases the accuracy claimed for the final recommended data must reflect the estimated uncertainty in the primary information.

In the following sections we treat the individual contributions to the viscosity and thermal conductivity separately, in each case subjecting all of the relevant available experimental data to a critical scrutiny in order to compile the primary data set. Subsequently, a representation of the indi-

vidual contributions is developed using the links between contributions, where necessary, to yield a global correlation of $\eta(\rho,T)$ and $\lambda(\rho,T)$.

3. The Zero-Density Limit

Because the value of the properties in the limit of zero density may be obtained from experimental data and analyzed independently of other contributions to the total property, we begin with a recapitulation of the results of earlier related studies in this area.[11-13]

3.1 The Viscosity

Trengove and Wakeham[11] have reported the results of a critical review of the viscosity of carbon dioxide in the limit of zero density. In their review, they employed viscosity data from four groups of workers: Smith and his collaborators,[14,15] Bailey,[16] Kestin and his co-workers,[17-29] and Iwasaki and Takahashi.[30] Together, these data cover the temperature range 203–1497 K and a representation of them with an estimated accuracy of $\pm$ 1.5% at the lowest temperature, $\pm$ 0.3% near room temperature, and $\pm$ 2% at 1500 K was developed. Since the work for the original correlation was completed, a new set of measurements of the viscosity of carbon dioxide at low densities has been reported by Vogel and Barkow.[31] These measurements were performed in an oscillating-disk viscometer with a proven record of accuracy.[32] Consequently, it has been thought necessary to add these new data to the primary data set for the zero-density viscosity and to repeat the correlation. The methodology adopted was exactly that described earlier[11] so that here we merely quote the final result. The form adopted for the corre-

TABLE 1. Coefficients of the correlation of the zero-density transport properties of carbon dioxide. T in K; λ in mW m^{-1} K^{-1}; η in μPa s

i	a_i	b_i	c_i
0	0.235156	0.4226159	$\cdots$
1	-0.491266	0.6280115	2.387869×10^{-2}
2	5.211155×10^{-2}	-0.5387661	4.350794
3	5.347906×10^{-2}	0.6735941	-10.33404
4	-1.537102×10^{-2}	0.0	7.981590
5	$\cdots$	0.0	-1.940558
6	$\cdots$	-0.4362677	$\cdots$
7	$\cdots$	0.2255388	$\cdots$

lation, which is valid for the range 200 K$\leqslant T \leqslant$1500 K, is

$$\eta^0(T) = \frac{1.00697 T^{1/2}}{\mathfrak{S}_\eta^*(T^*)}, \tag{3}$$

in which the viscosity η^0 is measured in μPa s and the temperature in K. Here the reduced effective cross section, denoted by $\mathfrak{S}_\eta^*(T^*)$, is represented by the equation

$$\ln \mathfrak{S}_\eta^*(T^*) = \sum_{i=0}^{4} a_i (\ln T^*)^i, \tag{4}$$

with

$$T^* = kT/\epsilon, \tag{5}$$

and the energy and length scaling parameters are

$$\epsilon/k = 251.196 \text{ K} \quad \text{and} \quad \sigma = 0.3751 \text{ nm}, \tag{6}$$

respectively. The coefficients a_i of Eq. (4) are listed in Table 1.

+ ref 14; ▲ ref 15; ⊙ ref 16; ✳ ref 17–19;
△ ref 31;
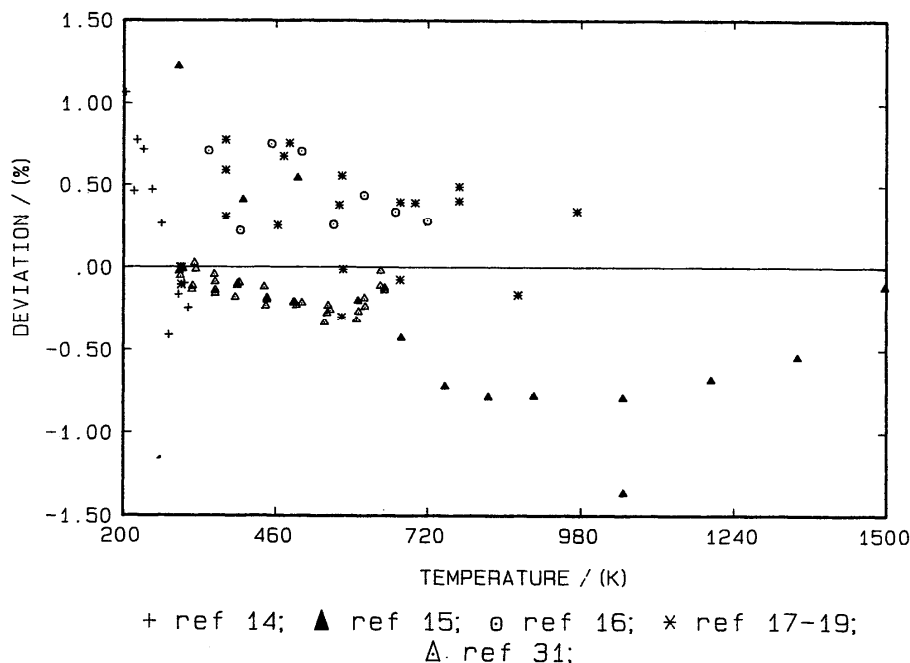
FIG. 1. Deviations of the experimental zero-density viscosity data from correlation of Eqs. (3) to (6).

It should be noted that we adopt here the more modern symbolism in terms of effective cross sections, $\mathfrak{S}_\eta^*$ rather than the collision integrals, Ω_η^*, employed earlier.[11] This is because the new notation renders the treatment of the zero-density thermal conductivity more compact. In fact, the relationship between the two quantities is straightforward:

$$\Omega_\eta^* = (5/4)\mathfrak{S}_\eta^* .$$ (7)

The correlation of Eqs. (3) to (6) differs by no more than ± 0.3% at any temperature from that given earlier and the estimated uncertainty associated with it is exactly the same as given earlier. The two correlations are consistent within their mutual uncertainty. Figure 1 shows the deviations of the complete set of primary data[14-31] for the zero-density viscosity from the new correlation. In each case the deviations are essentially consistent with our estimate of the experimental error of each author's data.

3.2 The Thermal Conductivity

Appendix I lists the literature sources for the entire accessible set of thermal-conductivity data for carbon dioxide over the entire range of thermodynamic states.[12,33-91] The bibliography is annotated to indicate the range of states covered and the experimental method employed. Figure 2 contains the plot of most of the zero-density data derivable from these experimental results as a function of temperature which cover the range $186\,K \leqslant T \leqslant 1350\,K$. Especially at ele-
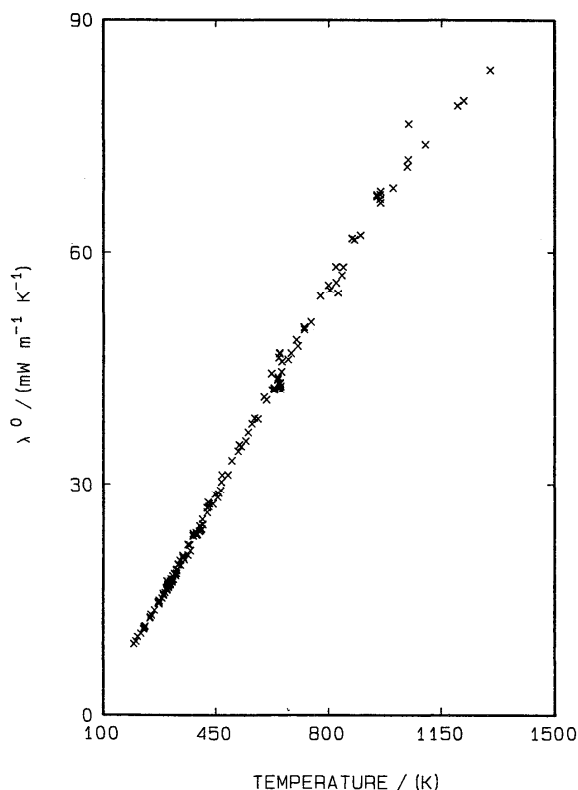
TABLE 2. Set of primary data used for correlating zero-density thermal conductivity

Source	T range/K	Number of points	Ascribed uncertainty
1. Millat *et al.*[12]	308–380	5	± 0.5%
2. Johns *et al.*[90,91]	302–470	7	± 1.0%
3. Clifford *et al.*[89]	301	1	± 0.5%
4. Dickins[34]	285	1	± 1.0%
5. Lenoir and Comings[47]	314–340	3	± 1.0%
6. Johnston and Grilly[40]	285–380	7	± 1.0%
7. Johnston and Grilly[40]	186–285	8	± 5%
8. Bakulin *et al.*[84]	226–285	8	± 5%
9. Keyes[53]	210–273	2	± 5%
10. Franck[48]	197	1	± 5%
11. Theoretical prediction	285–1000	28	± 2.0%

vated temperatures, there is a spread of experimental results amounting to 12%. This is typical of the situation for most gases and reflects the fact that many earlier measurements have rather large errors associated with them because of inadequacies in the theoretical description of the experimental technique.[92] The modern implementation of the transient hot-wire technique[92] has overcome most of these deficiencies and has been shown to yield accurate thermal conductivity data within the temperature range to which it has been applied, $T \leqslant 470\,K$. Thus, in order to establish the primary data for the zero-density thermal conductivity data of carbon dioxide we first adopt those results obtained in transient hot-wire instruments[12,89-91]. Subsequently, we employ the results of an analysis of these data to assist with the decision on the reliability of other, more extensive experimental data within the set of those available.

Table 2 includes the four sources of transient hot-wire measurements of the zero-density thermal conductivity of carbon dioxide.[12,89-91] The table includes our estimate of the uncertainty in the experimental data. The zero-density value of the thermal conductivity has in each case been quoted by the authors as a result of a statistical analysis of the density dependence of the experimental data and we have found no reason to change their quoted values. However, we note that for carbon dioxide the first density coefficient of thermal conductivity is relatively small, whereas the overall density dependence of the thermal conductivity is rather steep. In consequence, it is rather more difficult to determine an accurate zero-density thermal conductivity than for some other gases. For this reason we have increased the authors' estimates of the uncertainty in the zero-density thermal conductivity.

To these sets of data from the transient hot-wire technique we have added the small set of results from Dickins,[34] Lenoir and Comings,[47] and those of Johnston and Grilly[40] above 285 K. All of these data were found to be consistent with the transient hot-wire data. In particular, the data of Johnston and Grilly[40] agree with the transient hot-wire data to within ± 0.5%. We therefore assign an estimated uncertainty of ± 1% to those three sets of data. It should be noted that all of these estimates of uncertainty are employed to determine *relative* weights in the fitting procedure. How-

FIG. 2. The zero-density thermal conductivity of carbon dioxide as a function of temperature determined by various authors showing the spread of the results.

ever, they are also used to determine the overall error bounds attached to the final correlation.

3.2.a. Analysis

In order to provide a basis for the assessment of experimental thermal-conductivity data we employ the first-order semiclassical kinetic theory results of Wang Chang and Uhlenbeck[93] corrected to allow for quantum-mechanical, spin-polarization effects.[94] The thermal conductivity has two contributions

$$\lambda^0(T) = \lambda_{tr}^0 + \lambda_{int}^0 \tag{8}$$

and

$$\lambda_{tr}^0 = \frac{5k^2 T}{2m\langle v\rangle_0}\left[\frac{\mathfrak{S}(1001) + r\mathfrak{S}(^{1010}_{1001})}{\mathfrak{S}(1010)\mathfrak{S}(1001) - \mathfrak{S}^2(^{1010}_{1001})}\right], \tag{9}$$

$$\lambda_{int}^0 = \frac{5k^2 T}{2m\langle v\rangle_0}\left[\frac{r\mathfrak{S}(^{1010}_{1001}) + r^2\mathfrak{S}(1010)}{\mathfrak{S}(1010)\mathfrak{S}(1001) - \mathfrak{S}^2(^{1010}_{1001})}\right] S. \tag{10}$$

The quantities $\mathfrak{S}(^{pqrs}_{p'q'r's'})$ are effective cross sections that include all the dynamical information about binary collisions in the gas and hence the intermolecular pair potential. In addition,

$$\langle v\rangle_0 = 4\left(\frac{kT}{\pi m}\right)^{1/2}, \tag{11}$$

$$r = \left(\frac{2c_{int}}{5k}\right)^{1/2}, \tag{12}$$

and

$$S \simeq 1 - \frac{5}{3}\left(1 + \frac{\lambda_{tr}^0}{\lambda_{int}^0}\right)\left(\frac{\Delta\lambda_{\|}}{\lambda}\right)_{sat}. \tag{13}$$

Here, c_{int} is the internal isochoric heat capacity of the molecule and $(\Delta\lambda_{\|}/\lambda)_{sat}$ is the asymptotic value of the relative change in the thermal conductivity of the gas parallel to a magnetic field at saturation. It is the factor S that introduces the spin-polarization corrections.

In the form set out above the equations are not directly useful for examining the thermal-conductivity data because none of the effective cross sections can be obtained theoretically. However, we make use of relationships among the effective cross sections:

$$\mathfrak{S}(^{1010}_{1001}) = \tfrac{5}{6}r\mathfrak{S}(0001), \tag{14}$$

$$\mathfrak{S}(1010) = \tfrac{2}{3}\mathfrak{S}(2000) + \tfrac{25}{18}r^2\mathfrak{S}(0001), \tag{15}$$

$$\mathfrak{S}(0010) = \tfrac{5}{3}r^2\mathfrak{S}(0001), \tag{16}$$

and other measurable macroscopic quantities. (The effective cross section $\mathfrak{S}(2000)$ differs from $\mathfrak{S}_\eta$ introduced in Eq. (3) because the latter includes correction factors to the first-order kinetic theory. The difference is of the order of 1% and is unimportant for the present analysis). In addition, by using

$$\eta^0(T) = \frac{kT}{\langle v\rangle_0\mathfrak{S}(2000)}, \tag{17}$$

and the collision number for internal energy relaxation:

$$\zeta_{coll} = \frac{4kT}{\pi\eta^0\langle v\rangle_0\mathfrak{S}(0001)}, \tag{18}$$

we can evaluate a consistent set of all the effective cross sections $\mathfrak{S}(^{pqrs}_{p'q'r's'})$ from experimental data on the thermal conductivity, viscosity, the collision number ζ_{coll}, the internal heat capacity and $(\Delta\lambda_{\|}/\lambda)_{sat}$. This process has been described in detail elsewhere.[12] Here, it is therefore sufficient to report the sources of information for the analysis. We have taken c_{int} from work by Ely et al.[95] For the viscosity we have, of course, used the correlation of the previous section. The collision number, ζ_{coll}, contains contributions from both rotational and vibrational relaxation and can be written as

$$\frac{c_{int}}{\zeta_{coll}} = \frac{c_{rot}}{\zeta_{rot}} + \frac{c_{vib}}{\zeta_{vib}}. \tag{19}$$

The quantity ζ_{vib} has been measured by a number of workers[96–98] over the temperature range 240 K$<T<$770 K and a correlation of the results yields[12]

$$\frac{1}{\zeta_{vib}} = 4.52234\times10^{-4}\exp(-948.148/T). \tag{20}$$

Over the temperature range of interest here $\zeta_{vib} \gg \zeta_{rot}$ and $c_{vib} \gg c_{rot}$ so that the contribution of ζ_{vib} to ζ_{coll} in Eq. (19) is rather small. Thus one can safely extrapolate Eq. (20) to temperature regions outside of the experimental range and still retain an adequate estimate of ζ_{coll}.

There are no reliable measurements of ζ_{rot} over a range of temperature but there is one measurement at 300 K ($\zeta_{rot} = 1.95$) made by Millat et al.[99] It can be used as a basis for an estimation of ζ_{rot} over a wide temperature range. For this purpose we use a formula provided by Brau and Jonkman.[100] There is considerable evidence[99] that this formula provides an adequate estimate of the temperature dependence of ζ_{rot} for linear molecules. Thus we have used the value of ζ_{rot} from Millat et al.[99] and the formula[100]

$$\zeta_{rot} = \zeta_{rot}^\infty\left[1 + \frac{\pi^{1/2}}{2}\left(\frac{1}{T^*}\right)^{1/2} + \left(2 + \frac{\pi^2}{4}\right)\left(\frac{1}{T^*}\right)\right.$$
$$\left. + \pi^{3/2}\left(\frac{1}{T^*}\right)^{3/2}\right]^{-1}, \tag{21}$$

from which we have determined

$$\zeta_{rot}^\infty = 22.53. \tag{22}$$

Finally, Heemskerk et al.[101] have reported an almost temperature-independent value for $(\Delta\lambda_{\|}/\lambda)_{sat}$ for a number of gases in the temperature range 85 K$<T<$300 K. We have therefore adopted the value[101]

$$(\Delta\lambda_{\|})/\lambda)_{sat} = -0.0075, \tag{23}$$

measured at 300 K for all temperatures. Because the effect of the entire correction term S of Eq. (10) has an effect of less than 1% on the total thermal conductivity, the effect of ignoring the temperature dependence is negligible.

Using the preliminary, primary thermal-conductivity data defined above, we have evaluated all of the effective cross sections as well as various combinations of them.[12] Of particular interest for the present work is the evaluation of the ratio

$$D_{int}/D = \frac{5}{6}\frac{kT}{\langle v\rangle_0\eta^0 A^*}\left[\mathfrak{S}(1001) - \frac{1}{2}\mathfrak{S}(0001)\right]^{-1}, \tag{24}$$
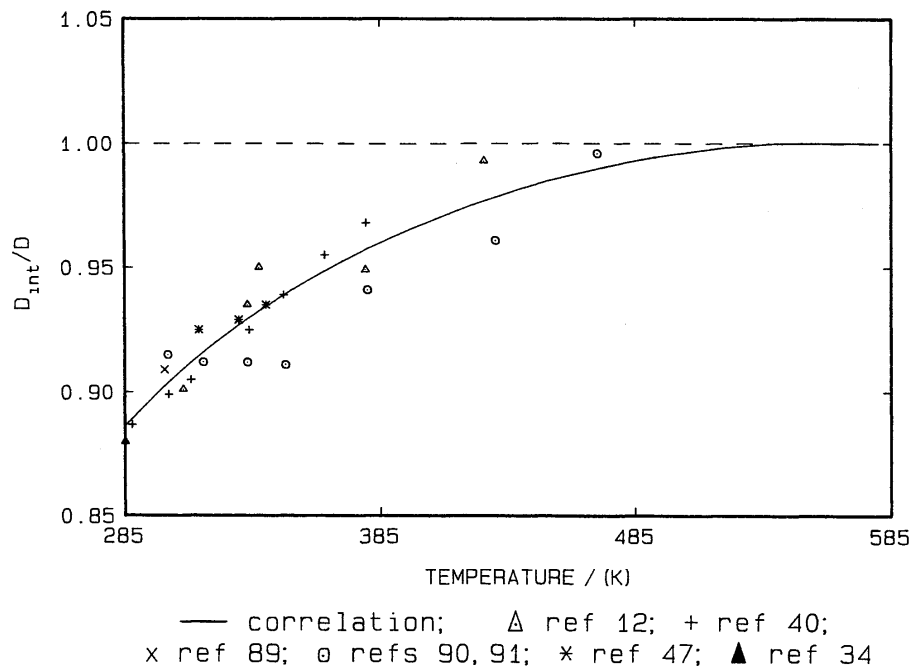
FIG. 3. The ratio D_{int}/D, Eq. (24), as a function of temperature obtained from the primary experimental data.

for which it is necessary to employ a value for the effective cross-section ratio A *, a quantity not accessible to measurement.[102] Recent quantum-mechanical calculations[103] indicate that A * may be quite reliably estimated (within a few percent) by a method based entirely on calculations for spherically symmetric, structureless molecules. Thus we employ here values of A * given by a corresponding states analysis.[102]

Figure 3 shows the experimental values of D_{int}/D for carbon dioxide based upon the preliminary, primary thermal-conductivity data only. Although the scatter in the original thermal-conductivity data is magnified by this analysis, there is a clear upward trend of the results towards unity as the temperature is increased. This observation is entirely consistent with an analysis[12] of the theoretical results of Moraal, McCourt and Snider[104,105] which shows that for linear molecules, D_{int}/D approaches unity from below in the high-temperature limit.

As we shall show, the available thermal-conductivity data for carbon dioxide at temperatures above those studied using the transient hot-wire technique are completely and systematically inconsistent with this behavior. Accordingly, we cannot extend our primary database upwards in temperature using experimental results and we have therefore been forced to adopt a different approach. Given the consistency between the transient hot-wire results and theory we have decided to use the results of our kinetic theory analsis to predict thermal-conductivity data in the high-temperature range. For this purpose the experimental values of D_{int}/D shown in Fig. 3 have been represented by a function which is effectively asymptotic to unity at high temperatures. The function selected is chosen to be consistent with that for oth-

er effective cross sections and is

$$\ln\left(\frac{D_{int}}{D}\right)$$
$$= -0.17274 + 0.47676(\ln T^*) - 0.56838 (\ln T^*)^2$$
$$+ 0.53368(\ln T^*)^3 - 0.28734(\ln T^*)^4,$$
$$285 \text{ K} < T \leqslant 530 \text{ K}$$

and

$$\frac{D_{int}}{D} = 1, \quad T > 530 \text{ K}. \tag{25}$$

This function is shown as the solid line in Fig. 3.

Together with the equations and data sources quoted earlier, Eq. (25) permits the evaluation of the thermal conductivity of carbon dioxide within the temperature range from 285 to 1500 K, the limit of the viscosity correlation.

Figure 4 contains the deviations of a selection of zero-density thermal-conductivity data, taken from the sources in Appendix I, from the values predicted on the foregoing theoretical basis. Because the preceding theory can make no definitive statement about the behavior of D_{int}/D below 285 K, the comparison is confined to temperatures above that. It can be seen that there are marked systematic differences that approach 8% at the highest temperatures. Among the experimental data that deviate from the prediction it is possible to discern two different types of behavior. In the first type we include the data,[44,49,50,58,59,73,82,84,85] exemplified in Fig. 4 by the results of Ref. 73, for which the ratio D_{int}/D has a theoretically inexplicable temperature dependence such that the ratio never approaches unity. Because such a behavior cannot be reconciled with the theoretical analysis, it is excluded

+ref 12;　xref 90, 91;　⊖ref 89;　■ref 34;　△ref 47;　▽ref 40
▲ref 71;　*ref 73;　□ ref 78;　◇ref 61;　▼ ref 54;　◁ ref 88
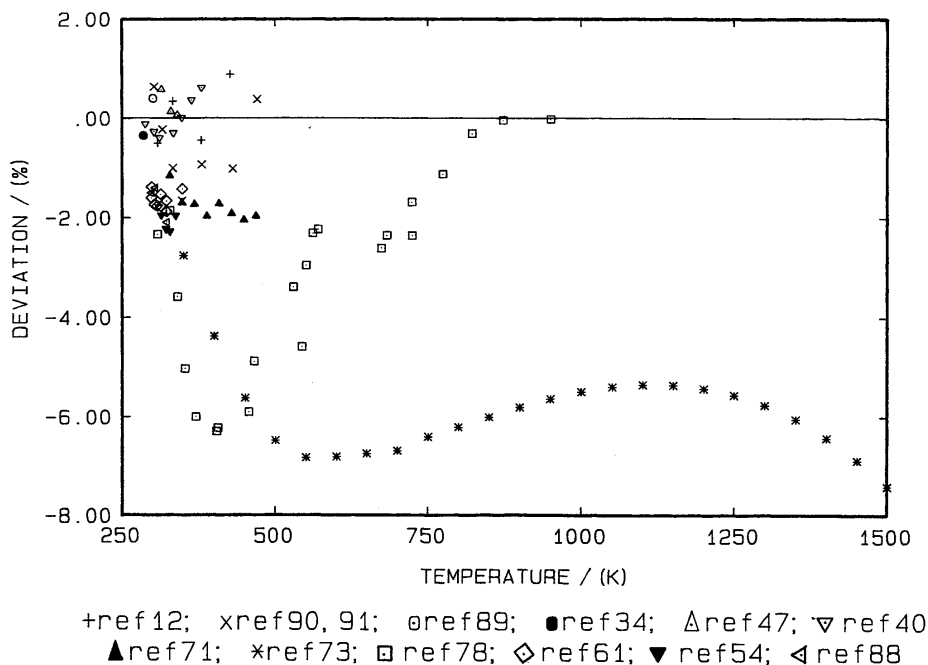
FIG. 4. Deviations of selected experimental zero-density thermal-conductivity data from semitheoretical calculations.

from further consideration in developing the correlation. On the other hand, there are data[36,39,42,45,47,54,61,71,77,78,88] represented in Fig. 4 by the data of Ref. 78 that confirm the theoretical behavior of D_{int}/D but show systematic deviations from the data obtained with the transient hot-wire technique. These data have also been excluded from further analyses.

3.2.b. Primary Data

The experimental high-temperature thermal-conductivity data are therefore not included in the primary set used to develop a representation of the zero-density thermal conductivity of carbon dioxide. Indeed, in the temperature range above 500 K it is preferable to use the thermal conductivity predicted by the procedure outlined above. However owing to the excitation of vibrational levels, the extrapolation of D_{int}/D to very high temperatures is less securely founded on theory. Therefore, it has been decided to limit the thermal-conductivity correlation to 1000 K. Hence, we have generated 28 data points for thermal conductivity, according to the procedure outlined above, equally spaced within the temperature range 285 K $\leqslant T \leqslant$ 1000 K, as indicated in Table 2. In view of the accuracy of the thermal conductivity data on which the theoretical prediction is based for 285 K $\leqslant T \leqslant$ 470 K, and our confidence in the extrapolation procedure, it is estimated that the uncertainty in the generated thermal conductivity data is one of $\pm$ 0.5% in the lower temperature range, rising to $\pm$ 2% at the upper temperature extreme.

The remaining temperature range in which thermal conductivity data are required is that below 285 K. In that range there is no theoretical guidance as to the temperature dependence of any of the effective cross sections or their

ratios. Consequently, it is necessary to rely entirely upon experiment. There are four independent reports of thermal-conductivity measurements in the gas phase of carbon dioxide below 285 K,[40,48,53,84] and they are included in Table 2. None of the data has the accuracy associated with the results of the transient hot-wire method. However, the data of Keyes,[53] Johnston and Grilly,[40] and Bakulin et al.[84] cover a wide temperature range. The measurements of Keyes[53] were performed in a concentric-cylinder apparatus, whereas those of Johnston and Grilly[40] and of Bakulin et al.[84] were made in a steady-state hot-wire instrument. For none of these instruments is it clear that the effects of convection were completely absent. Thus, whereas it is necessary to include the data in the primary data set because they cover the low-temperature range, the uncertainty ascribed to them must reflect these doubts. Accordingly, we assign an uncertainty of $\pm$ 5% to these data uniformly because it is not possible to distinguish them and because they are mutually consistent within this band.

The primary data for the zero-density thermal conductivity are completed by inclusion of the single temperature measurement at 197 K of Franck,[48] performed in a steady-state hot-wire instrument.

3.2.c. Representation

In principle, the zero-density thermal conductivity of carbon dioxide could be represented in the manner used above for the prediction of high-temperature data. However, the method is cumbersome because it consists of a relatively large number of separate representational equations for individual quantities. A different approach is therefore adopted which retains the advantage that it is securely based in theory but has the additional benefit that it is simpler. This ap-

proach derives from the work of Thijsse *et al.*[106] on an alternative formulation of the kinetic theory of polyatomic gases. In this formulation, to a first-order approximation, the thermal conductivity is written

$$\lambda^0 = \frac{5k^2T}{2m\langle v\rangle_0}\frac{(1+r^2)}{\mathfrak{S}(10E)}\left[1 - \frac{\mathfrak{S}^2\!\left(\genfrac{}{}{0pt}{}{10E}{10D}\right)}{\mathfrak{S}(10E)\mathfrak{S}(10D)}\right]^{-1},$$

(26)

in which $\mathfrak{S}(10E)$, $\mathfrak{S}\left(\genfrac{}{}{0pt}{}{10E}{10D}\right)$, and $\mathfrak{S}(10D)$ are further effective cross sections, related to those introduced earlier. But it transpires that for all gases examined so far, and for carbon dioxide in particular, the factor in braces departs from unity by no more than $\pm 0.4\%$.[13] Consequently, for representational purposes we may employ the equation

$$\lambda^0 = \frac{5k^2T}{2m\langle v\rangle_0}\frac{(1+r^2)}{\mathfrak{S}_\lambda(T)},$$

(27)

in which $\mathfrak{S}_\lambda(T)$ is approximately equal to $\mathfrak{S}(10E)$. Then if we introduce a reduced form of $\mathfrak{S}_\lambda$:

$$\mathfrak{S}_\lambda^* = \mathfrak{S}_\lambda/\pi\sigma^2,$$

(28)

where σ is given in Eq. (6), as well as values for the molecular and fundamental constants, we can write

$$\lambda^0 = \frac{0.475598(T)^{1/2}(1+r^2)}{\mathfrak{S}_\lambda^*(T^*)},$$

(29)

in which λ^0 is given in mW m^{-1} K^{-1} and the temperature in K.

The primary data permit the evaluation of $\mathfrak{S}_\lambda^*$ for each temperature according to Eq. (29), using the correlation of the ideal-gas heat capacities given by Ely *et al.*[95] Subsequently the entire set of data for $\mathfrak{S}_\lambda^*$ has been represented by the equation

$$\mathfrak{S}_\lambda^* = \sum_{i=0}^{7} b_i/T^{*i}.$$

(30)

The representation of the data using this equation has been carried out with the SEEQ algorithm.[107] Appropriate statistical weights for the data have been determined from the estimated uncertainty in the measurements. The optimum values of the coefficients b_i are included in Table 1. For completeness, the same table includes the coefficients c_i in the representation of the ideal-gas heat capacity of carbon dioxide,[95] which has the form

$$\frac{c_{\text{int}}}{k} = 1.0 + \exp(-183.5/T)\sum_{i=1}^{5} c_i(T/100)^{2-i}.$$

(31)

Figure 5 shows the deviations of the entire set of data of Table 2 from the representation given by Eqs. (29) and (31). The experimental data from Millat *et al.*[12] deviate at most by 0.8% from the correlation while those of Johns *et al.*[90,91] have a standard deviation of $\pm 1\%$, which is consistent with their estimated uncertainty, although one point deviates by as much as 1.6%. The standard deviation taken over all of the experimental data in the temperature range 285 K$\leqslant T\leqslant$470 K is one of $\pm 0.6\%$ so that we can safely ascribe an uncertainty of $\pm 1\%$ to the correlation in this region. For temperatures below 285 K there is some evidence of a systematic departure of some of the experimental data from the correlation although the average absolute deviation from the fit is only $\pm 0.5\%$. In view of the accuracy assigned to the later set of data the inaccuracy of the correlation may be as much as $\pm 5\%$ at the lowest temperature, although it must be much less near 285 K.

+ ref12; × ref90, 91; * ref89; ⊙ ref34; △ ref40
▲ ref47; □ ref53; ◇ ref48; ● ref 84;
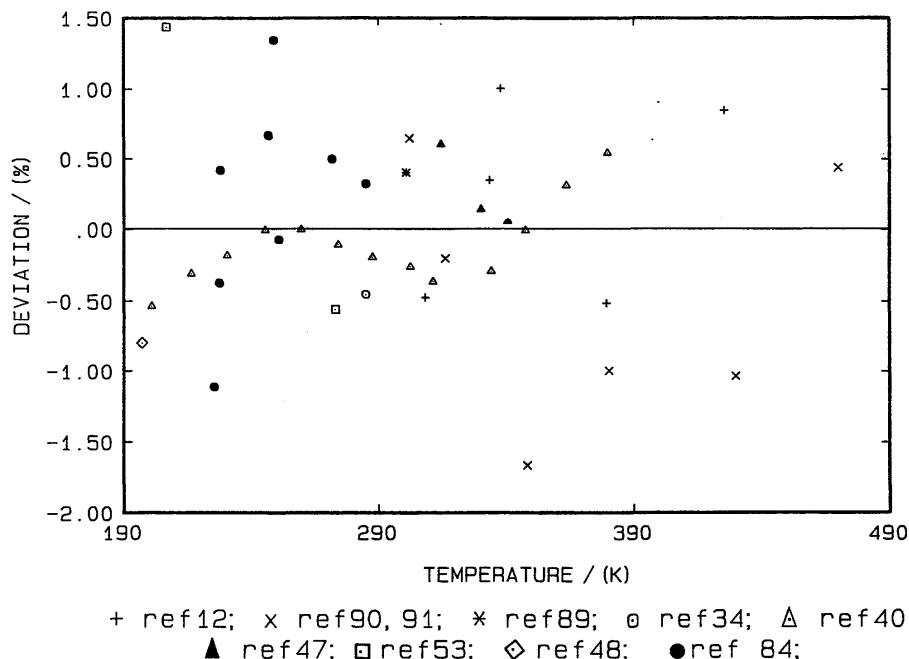
FIG. 5. Deviations of the primary zero-density thermal conductivity from the final correlation.

In the region of high temperature for which the primary data have been predicted ($T > 470$ K) the fit of the correlation to the calculated values is good, the standard deviation being $\pm 0.07\%$. It is naturally difficult to assign an uncertainty to the predicted thermal conductivity, but given the theoretical basis of the prediction, an estimate of $\pm 2\%$ does not seem unreasonable.

4. The Critical Region

4.1 Equations for the Transport Properties in the Critical Region

The thermal conductivity and viscosity of a fluid diverge at the critical point.[108] The critical enhancement of the thermal conductivity is strong and is observed in a large range of temperatures and densities around the critical point. The critical enhancement in the viscosity is much weaker and restricted to a very small region around the critical point. To describe the behavior of the transport properties in the critical region we write the thermal conductivity and the viscosity as

$$\lambda(\rho,T) = \bar{\lambda}(\rho,T) + \Delta_c\lambda(\rho,T) , \tag{32}$$

$$\eta(\rho,T) = \bar{\eta}(\rho,T) + \Delta_c\eta(\rho,T) , \tag{33}$$

where $\Delta_c\lambda$ and $\Delta_c\eta$ represent the critical enhancements, while $\bar{\lambda}$ and $\bar{\eta}$ are the background contributions defined in accordance with Eq. (2). The critical thermal-conductivity enhancement $\Delta_c\lambda$ is related to the critical part $\Delta_c D_T$ of the thermal diffusivity $D_T = \lambda/\rho c_p$ by

$$\Delta_c D_T = \frac{\Delta_c\lambda}{\rho c_p} , \tag{34}$$

where c_p is the specific heat at constant pressure. The theory of dynamic critical phenomena predicts for the asymptotic critical behavior of the transport properties[109]:

$$\Delta_c D_T = \frac{\Delta_c\lambda}{\rho c_p} = \frac{RkT}{6\pi\eta\xi} , \tag{35}$$

$$\eta = \Delta_c\eta + \bar{\eta} = \bar{\eta}(Q\xi)^z , \tag{36}$$

where k is Boltzmann's constant, ξ the correlation length of the density fluctuations which diverges at the critical point, and Q is a system-dependent amplitude. The amplitude R in Eq. (35) and the exponent z in Eq. (36) are universal quantities, i.e., they have the same value for all fluids. In this paper we adopt the values

$$R = 1.01, \quad z = 0.06 , \tag{37}$$

in good agreement with current theory and experiments.[108] The viscosity η exhibits a multiplicative anomaly in the critical region; that is, the critical viscosity enhancement is proportional to the background viscosity $\bar{\eta}$.

A problem is that few, if any, experimental thermal conductivity and viscosity data are available so close to the critical point that the asymptotic Eqs. (35) and (36) are sufficient. To represent the observed critical enhancements of the transport properties we need equations that incorporate the crossover from the singular behavior of the transport properties asymptotically close to the critical point to the nonsingular background behavior of these properties far away from the critical point. Such crossover equations have recently

been proposed by Olchowy and Sengers[4,110] and we adopt their equations in this paper. The equations are based on the mode-coupling formulae for the critical enhancements of the transport properties[109,111,112] which arise from long-range critical fluctuations with wave numbers up to a maximum cutoff wave number q_D. Specifically, $\Delta_c D_T$ and η are represented by [4,110]

$$\Delta_c D_T = \frac{\Delta_c\lambda}{\rho c_p} = \frac{RkT}{6\pi\eta\xi} (\Omega - \Omega_0) , \tag{38}$$

$$\eta = \bar{\eta} \exp(zH) , \tag{39}$$

where Ω, Ω_0, and H are functions of density and temperature as specified in Tables 3 and 4. Near the critical point $\xi \to \infty$, and one recovers from Eqs. (38) and (39) the predicted asymptotic behavior given by Eqs. (35) and (36). Far from

TABLE 3. Crossover function for the thermal conductivity

I. Parameters

$y_D = \mathrm{arctg}(q_D\,\xi)$

$y_\delta = \{\mathrm{arctg}[q_D\,\xi/(1 + q_D^2\,\xi^2)^{1/2}] - y_D\}/(1 + q_D^2\xi^2)^{1/2}$

$y_\alpha = \rho kT/8\pi\bar{\eta}^2\xi$

$y_\beta = \bar{\lambda}/\bar{\eta}(c_p - c_v)$

$y_\gamma = c_v/(c_p - c_v)$

II. Crossover function

$\dfrac{\Delta\lambda}{\rho c_p} = \dfrac{RkT}{6\pi\bar{\eta}\xi} [\Omega(\{y_i\}) - \Omega_0]$

$\Omega(\{y_i\}) = \dfrac{2}{\pi}\dfrac{1}{1 + y_\gamma}\left[y_D - \sum_{i=1}^{4} Y_i\,F(z_i, y_D) \right]$

$\Omega_0 = \dfrac{(1 - \exp\{- 1/[1/q_D\xi + (q_D\,\xi\rho_c/\rho)^2/3]\})}{[1 + y_\alpha(y_D + y_\delta) + y_\beta(1 + y_\gamma)^{-1}]\pi/2}$

$F(r,s) = \dfrac{1}{(1 - r^2)^{1/2}} \log\left[\dfrac{1 + r + (1 - r^2)^{1/2}\tan(s/2)}{1 + r - (1 - r^2)^{1/2}\tan(s/2)}\right]$

$\mathbf{y} = \begin{pmatrix} Y_1 \\ Y_2 \\ Y_3 \\ Y_4 \end{pmatrix};$

$\mathbf{y} = \mathbf{W}^{-1}\mathbf{x}; \quad \mathbf{x} = \begin{pmatrix} y_D\,y_\alpha \\ y_\beta - y_\gamma + y_\alpha\,y_\delta \\ y_\gamma\,y_\alpha\,y_D \\ y_\gamma\,y_\alpha\,y_\delta - y_\gamma^2 \end{pmatrix}$

III. Matrix $\mathbf{W} = [W_{ij}]$

$W_{1i} = 1$

$W_{2i} = \sum_{j=1}^{4} z_j(1 - \delta_{ij})$

$W_{3i} = -z_i\,W_{2i} + \dfrac{1}{2}\sum_{j,k=1}^{4} z_j z_k(1 - \delta_{jk})$

$W_{4i} = \left(\prod_{j=1}^{4} z_j\right)\Big/z_i$

IV. Roots of the quartic equation: z_i

$\prod_{i=1}^{4} (z + z_i) = z^4 + a_3 z^3 + a_2 z^2 + a_1 z + a_0 = 0$

$a_3 = y_D y_\alpha; \quad a_2 = y_\gamma + y_\beta + y_\alpha y_\delta; \quad a_1 = y_\gamma y_\alpha y_D; \quad a_0 = y_\gamma y_\alpha y_\delta$

TABLE 4. Crossover function for the viscosity

I. Parameters

$y_D = \text{arctg}(q_D \, \xi)$

$y_\delta = \{\text{arctg}[q_D \, \xi/(1 + q_D^2 \, \xi^2)^{1/2}] - y_D\}/(1 + q_D^2\xi^2)^{1/2}$

$y_\alpha = \rho k T/8\pi\bar\eta^2\xi$

$y_\beta = \bar\lambda/\bar\eta(c_p - c_v)$

$y_\gamma = c_v/(c_p - c_v)$

$y_\eta = (y_\delta + y_\beta/y_\alpha)/y_D$

$y_v = y_\gamma y_\delta/y_D$

II. Crossover function

$\eta = \bar\eta \exp(zH(\{y_i\}))$

$H(\{y_i\}) = h(\{y_i\}) + \sum_{i=1}^{3} N_i \, F(v_i, y_D)$

$h(\{y_i\}) = (3y_\gamma y_\eta + 3y_\eta/2 - y_\eta^3 - y_v)y_D$

$\qquad + (y_\eta^2 - 2y_\gamma - 5/4)\sin y_D - y_\eta(\sin 2y_D)/4 + (\sin 3y_D)/12$

$\qquad + \dfrac{(y_\gamma(1+y_\gamma))^{3/2}}{(y_v - y_\gamma y_\eta)} \text{arctg}([y_\gamma/(1 + y_\gamma)]^{1/2}\tan y_D)$

$F(r,s) = \dfrac{1}{(1 - r^2)^{1/2}} \log\left(\dfrac{1 + r + (1 - r^2)^{1/2}\tan(s/2)}{1 + r - (1 - r^2)^{1/2}\tan(s/2)}\right)$

$n = \begin{pmatrix} N_1 \\ N_2 \\ N_3 \end{pmatrix}; \quad n = M^{-1}p;$

$p = \begin{pmatrix} y_\eta^4 - 4y_\eta^2 y_\gamma - 2y_\eta^2 + 2y_\eta y_v + 3y_\gamma^2 + 4y_\gamma + 1 \\ (y_\eta y_\gamma - y_v)(y_\eta^2 - 3y_\gamma - 2) + y_\gamma^2(1 + y_\gamma)^2/(y_\eta y_\gamma - y_v) \\ y_\eta y_v(y_\eta^2 - 3y_\gamma - 2) + y_v^2 + y_v y_\gamma(1 + y_\gamma)^2/(y_\eta y_\gamma - y_v) \end{pmatrix}$

III. Matrix $M = [M_{ij}]$

$M_{1i} = 1$

$M_{2i} = -v_i + \sum_{j=1}^{3} v_j$

$M_{3i} = \left(\prod_{i=1}^{3} v_j\right)/v_i$

IV. Roots of the cubic equation: v_i

$\prod_{i=1}^{3} (v + v_i) = v^3 + y_\eta v^2 + y_\gamma v + y_v = 0$

the critical point $\xi \to 0$, $\Omega \simeq \Omega_0$, and $H \to 0$, so that $\Delta_c D_T$ vanishes while $\eta \to \bar\eta$.

4.2 Thermodynamic Properties and Correlation Length

The functions Ω, Ω_0, and H in Eqs. (38) and (39) not only depend on the density ρ and the temperature T explicitly, but also implicitly through the isochoric and isobaric specific heats c_v and c_p, the background transport properties $\bar\lambda$ and $\bar\eta$ and the correlation length ξ. Hence, Eqs. (38) and (39) need to be supplemented with a procedure for calculating the correlation length ξ as a function of density and temperature. This is accomplished by relating ξ to a reduced

symmetrized compressibility $\bar\chi$ defined as[112]

$$\bar\chi = (\, P_c/\rho_c^2 T_c)\, \rho T\left(\dfrac{\partial\rho}{\partial P}\right)_T . \tag{40}$$

Along the critical isochore $\rho = \rho_c$, ξ and $\bar\chi$ asymptotically diverge as[112,113]

$$\xi(\,\rho_c, T \geqslant T_c) = \xi_0(\Delta\tilde T)^{-\nu}, \tag{41}$$

$$\bar\chi(\,\rho_c, T \geqslant T_c) = \Gamma(\Delta\tilde T)^{-\gamma}, \tag{42}$$

where[112]

$$\nu = 0.630, \quad \gamma = 1.2415, \tag{43}$$

are universal exponents, while ξ_0 and Γ are system-dependent amplitudes which, for CO_2, assume the values[112]

$$\xi_0 = 1.5 \times 10^{-10} \text{ m}, \quad \Gamma = 0.052. \tag{44}$$

From Eqs. (41) and (42) we note that

$$\xi(\,\rho_c, T \geqslant T_c) = \xi_0(\bar\chi/\Gamma)^{\nu/\gamma}. \tag{45}$$

To calculate the correlation length ξ at arbitrary densities and temperature, Eq. (45) is generalized to[113]

$$\xi(\rho, T) = \xi_0(\Delta\bar\chi/\Gamma)^{\nu/\gamma}, \tag{46}$$

with

$$\Delta\bar\chi = \bar\chi(\,\rho, T) - \bar\chi(\,\rho, T_r)T_r/T, \tag{47}$$

where T_r is a reference temperature far above the critical temperature which is chosen as

$$T_r = 1.5 \, T_c \simeq 450 \text{ K}. \tag{48}$$

In Eq. (47) a background term has been subtracted from $\bar\chi(\rho, T)$ to ensure that ξ becomes vanishingly small far away from the critical point. It turns out that at temperatures close to the reference temperature T_r, Eq. (46) causes ξ to go to zero a bit too rapidly in a range of about ± 5 K around T_r. To alleviate this problem the correlation length ξ is calculated for $T \geqslant 445$ K as

$$\xi(\rho, T) = \xi(\,\rho, T = 445 \text{ K})\exp\left[-\left(\dfrac{T/K - 445}{10}\right)\right]. \tag{49}$$

Having related ξ to the compressibility, we need to specify a fundamental equation for calculating the various thermodynamic properties. In the near-critical region, i.e., in a range of temperatures and densities bounded by

$$301.15 \text{ K} \leqslant T \leqslant 323 \text{ K and } 290 \text{ kg m}^{-3} \leqslant \rho \leqslant 595 \text{ kg m}^{-3}, \tag{50}$$

we use the scaled fundamental equation proposed by Albright *et al.*[112] with the critical parameters

$$T_c = 304.107 \text{ K}, \quad \rho_c = 467.69 \text{ kg m}^{-3}, \text{ and } P_c = 7.3721 \text{ MPa}. \tag{51}$$

Outside the region defined by Eq. (50) we use an analytic equation proposed by Ely *et al.*[95]

The values of the various parameters that enter into the equations for the transport properties in the critical region are summarized in Table 5.

4.3 Thermal Conductivity in the Critical Region

Two primary sets of experimental data are available that give detailed information on the behavior of the thermal

TABLE 5. Constants in the equations for the transport properties in the critical region

Critical parameters

$T_c = 304.107$ K

$\rho_c = 467.69$ kg m^{-3}

$P_c = 7.3721$ MPa

Critical exponents

$z = 0.06$

$\nu = 0.630$

$\gamma = 1.2415$

Critical amplitudes

$R = 1.01$

$\xi_0 = 1.50 \times 10^{-10}$ m

$\Gamma = 0.052$

Cutoff wavenumber

$q_D^{-1} = 2.3 \times 10^{-10}$ m

$(\bar{q}_D^{-1} = 4.0 \times 10^{-10}$ m$)^a$

---

[a] For simplified thermal-conductivity equation.

conductivity in the critical region. Michels, Sengers, and van der Gulik[61] have measured the thermal conductivity of carbon dioxide in the critical region with a parallel-plate apparatus.[114] They were able to eliminate convection,[115] a problem usually encountered near the critical point, and their measurements definitely established the existence of a critical enhancement in the thermal conductivity.[61,116] Subsequently, Becker, and Grigull[86] were able to determine the thermal diffusivity of carbon dioxide in the critical region by using a transient method in which the time dependence of a temperature gradient below a heated horizontal plate was measured with optical holography.[117,118] An intercomparison between the thermal conductivity data of Michels et al.[61] and the thermal diffusivity data of Becker and Grigull[86] requires an accurate equation for the isobaric specific heat c_p. Within the accuracy to which the intercomparison can be made, the two data sets are judged to be consistent except at the isotherm 304.35 K closest to the critical temperature of 304.107 K, where the thermal conductivity data of Michels et al.[61] tend to pass through a larger maximum at the critical density than those deduced from the thermal diffusivity data of Becker and Grigull. However, it becomes extremely difficult to measure the thermal conductivity with the aid of a macroscopic stationary temperature gradient very close to the critical temperature; so we have excluded the thermal conductivity data at $T = 304.35$ K and with $|(\rho - \rho_c)/\rho_c|$ ≤ 0.2 from the primary data set.

It is also possible to determine the thermal diffusivity close to the critical point by measuring the decay rate of the entropy fluctuations from light-scattering measurements. For carbon dioxide such measurements have been reported by Swinney and Henry[119] and confirmed by Marcabee and White[120] and by Garrabos et al.[121] and by Reile et al.[122] The results of these light-scattering measurements are also consistent with the two primary data sets mentioned above.[122,123] Supplementary experimental evidence for the

critical enhancement of the thermal conductivity of carbon dioxide has been provided by Le Neindre et al.[78]

Our representative Eq. (38) for the thermal diffusivity and thermal conductivity in the critical region contains the background thermal conductivity and viscosity, $\bar{\lambda}$ and $\bar{\eta}$, and the parameter q_D. The background contributions $\bar{\lambda}$ and $\bar{\eta}$ are represented by equations of the form

$$\bar{\lambda}(\rho,T) = \lambda^0(T) + \Delta\lambda(\rho), \qquad (52)$$

$$\bar{\eta}(\rho,T) = \eta^0(T) + \Delta\eta(\rho), \qquad (53)$$

where $\Delta\lambda(\rho)$ and $\Delta\eta(\rho)$ are treated as functions of the density alone as further discussed in Secs. 5.1 and 5.2. In practice, we started with a preliminary estimate for the excess functions $\Delta\lambda(\rho)$ and $\Delta\eta(\rho)$ deduced from the thermal conductivity data for Le Neindre et al.[78] and from viscosity data of Kestin et al.[20] and Iwasaki and Takahashi.[30] The parameter $q_D^{-1} = 0.23$ nm was then determined by fitting Eq. (38) to the thermal conductivity data of Michels et al.[110] Improved equations for $\Delta\lambda(\rho)$ and $\Delta\eta(\rho)$ were then obtained as described in Sec. 5 and the comparison with the experimental data for the critical enhancement of the thermal conductivity was reconsidered. This process converged very rapidly, the value of q_D in fact did not change, and we present here a comparison with the experimental data using the final Eqs. (63) and (67) for $\Delta\lambda(\rho)$ and $\Delta\eta(\rho)$.

In Fig. 6 we show a comparison of Eq. (38) with the thermal diffusivity data of Becker and Grigull.[86] In the same figure we have also included the thermal diffusivities deduced from the thermal conductivity data of Michels et al.[61] A direct comparison with the thermal conductivity of Michels et al.[61] is presented in Fig. 7. For reasons mentioned earlier the thermal conductivity data at $T - T_c = 0.25$ K have not been included in the figure, although they were included in Fig. 6. Except for the latter temperature, the equations represent the thermal conductivity data of Mi-
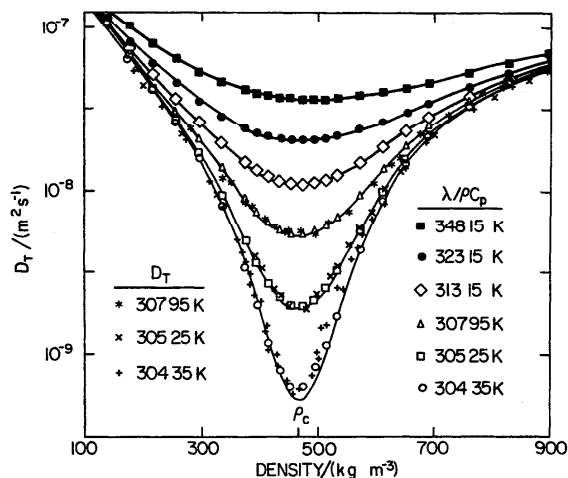
FIG. 6. The thermal diffusivity of carbon dioxide in the critical region as a function of density at various temperatures. The experimental data for D_T are those measured by Becker and Grigull[86] and for λ those measured by Michels et al.[61] The solid curves represent the values calculated from Eqs. (32) and (38).
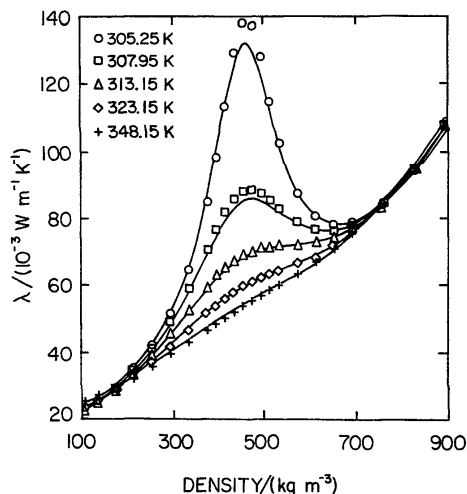
FIG. 7. The thermal conductivity of carbon dioxide in the critical region as a function of density at various temperatures. The experimental data are those of Michels *et al.*[61]. The solid curves represent the values calculated from Eqs. (32) and (38).

chels *et al.* with a standard deviation of about 1.5%.

Our Eq. (38) was constructed to account for the crossover of the asymptotic divergent behavior of the thermal conductivity near the critical point to the regular background behavior of the thermal conductivity far away from the critical point. Figure 8 shows the critical thermal conductivity enhancement[61] at 20 and 45 K above the critical temperature. From the information presented in Figs. 6–8 we conclude that our equation yields a satisfactory representation of the primary data at all densities and temperatures where a critical thermal conductivity enhancement has been observed.

In Fig. 9 we present a comparison with the thermal conductivity data of Le Neindre and co-workers.[78] The thermal-conductivity data of Le Neindre *et al.* are somewhat less accurate than those of Michels *et al.*,[61] but they have the advantage of extending to much higher temperatures. In preparing this comparison we have substituted for the dilute
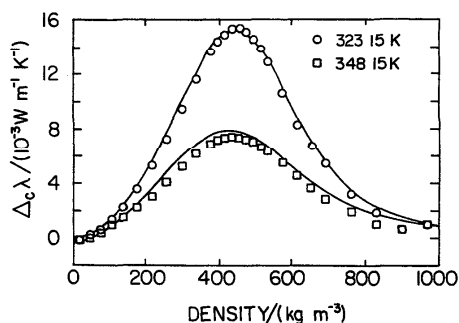
FIG. 9. The thermal conductivity of carbon dioxide as measured by Le Neindre and co-workers.[78] The solid curves represent the values calculated from Eq. (38).

gas limit $\lambda^0(T)$ in Eq. (52) the values extrapolated from the data of Le Neindre *et al.* As discussed in Sec. 5.1 there exists a discrepancy between $\lambda^0(T)$ deduced from the data of Le Neindre *et al.* and other available data judged to be more reliable at low densities. It is assumed that this can be accounted for by a shift independent of the density. The equation with $\lambda^0(T)$ adjusted represents the thermal conductivity data of Le Neindre *et al.* with an average standard deviation of about 1%.

In Fig. 10 a comparison is presented of the representative equation with the thermal conductivity data of Snel *et al.*[88] obtained with a stationary hot-wire instrument. Again in this comparison $\lambda^0(T)$ has been adjusted to the values extrapolated to low density which differs by about 1.5% from the correlating equation presented in Sec. 3 for $\lambda^0(T)$; the equation then reproduces the thermal conductivity data of Snel *et al.*[88] with a standard deviation of about 0.3%.

Scott *et al.*[90] have tried to measure the thermal conductivity of carbon dioxide in the supercritical region with a transient hot-wire instrument. A comparison with the thermal conductivity data of Scott *et al.*[90] is presented in Fig. 11. Excellent agreement is obtained at 45 K above the critical temperature as well as at lower densities at all temperatures, where the equation agrees with the data with a standard deviation of 1.4%. However, our analysis indicates that clos-

FIG. 8. The thermal conductivity enhancement $\Delta_c\lambda$ at 20 K and 45 K above the critical temperature as deduced from the measurement of Michels *et al.*[61] The solid curve represents the values calculated from Eq. (38).
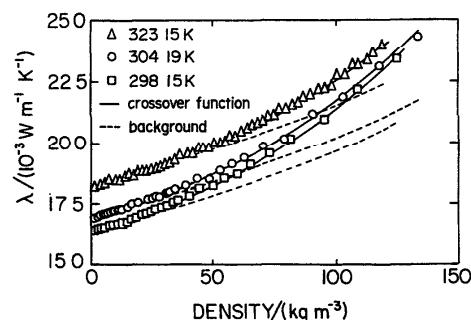
FIG. 10. The thermal conductivity of carbon dioxide as measured by Snel *et al.*[88] The solid curves represent the values calculated from Eqs. (32) and (38). The dashed curves represent the background thermal conductivity λ calculated from Eq. (52).
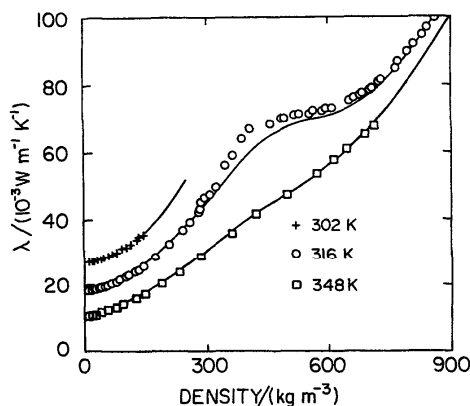
FIG. 11. The thermal conductivity of carbon dioxide as measured by Scott et al.[90] The solid curves represent the values calculated from Eqs. (32) and (38). The vertical scale corresponds to the thermal conductivity isotherm at 316 K. To separate the other isotherms, the values of $\lambda \times 10^3$ at 302 and 348 K have been displaced by $+10$ and -10 W m^{-1} K^{-1}, respectively.

FIG. 12. The viscosity of carbon dioxide at the critical density $\rho = \rho_c$ as a function of temperature as measured by Iwasaki and Takahashi[30] and by Bruschi and Torzo.[129] The solid curves represent the viscosity calculated from Eqs. (33) and (39) with Eq. (55) for $\Delta\eta(\rho)$.

cr to the critical point their instrument yields an apparent critical thermal-conductivity enhancement which becomes too large, presumably because convection becomes significant.

It should be emphasized that a critical enhancement of the thermal conductivity is present over a very large range of densities and temperatures around the critical point. The relative critical thermal-conductivity enhancement $\Delta_c\lambda/\lambda$ is smaller than 1% at densities and temperatures *outside* a range bounded approximately by

$$240 \text{ K} < T < 450 \text{ K, and } 25 \text{ kg m}^{-3} < \rho < 1000 \text{ kg m}^{-3} \, .$$

$$(54)$$

4.4 Viscosity in the Critical Region

Unlike the thermal conductivity, the viscosity exhibits a weak critical enhancement restricted to a rather small range of densities and temperatures around the critical point.[108] For some time uncertainty existed whether the viscosity of fluids would exhibit any enhancement near the gas–liquid critical point at all.[125] Michels, Botzen, and Schuurman[126] had reported an apparent strong viscosity enhancement for carbon dioxide in the critical region which in retrospect must be attributed to a failure of the validity of the working equations for their capillary-flow viscometer.[127] Subsequent measurements obtained by Kestin, Whitelaw, and Zien[128] with an oscillating-disk viscometer indicated the possible existence of only a small viscosity enhancement close to the critical point. The accuracy obtainable with their instrument close to the critical point was insufficient to make a quantitative assessment of the critical viscosity enhancement.

Detailed experimental studies of the behavior of the viscosity of carbon dioxide in the critical region have been reported by Iwasaki and Takahashi[30] and by Bruschi and Torzo.[129] Unfortunately, the two sets of data are mutually inconsistent as illustrated in Fig. 12 where the data obtained by the two groups at $\rho = \rho_c$ are shown. The data of Iwasaki
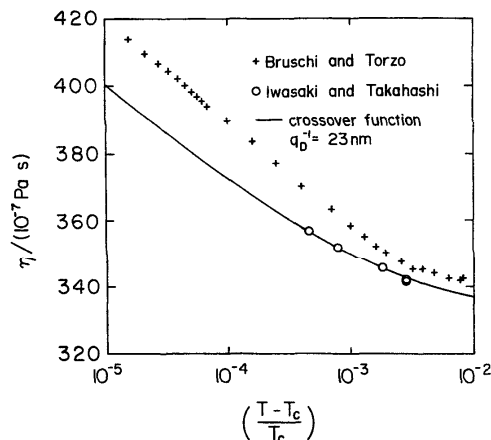
and Takahashi were obtained with an oscillating-disk method; at lower densities the data of Iwasaki and Takahashi are in good agreement with viscosity measurements obtained independently by Kestin, Korfali, and Sengers.[20] Bruschi and Torzo obtained their viscosity data with a novel rotating-disk viscometer[130] whose working equations have not yet been fully validated. We have accepted the data of Iwasaki and Takahashi as the more reliable.

Iwasaki and Takahashi measured both the viscosity and the density. We have accepted their experimental densities which differ from the densities we would calculate with the scaled equation of Albright et al.[112] from the experimental pressures quoted by Iwasaki and Takahashi.

We encountered serious problems in determining a suitable equation for the background viscosity $\bar{\eta}$ to analyse the critical viscosity enhancement for carbon dioxide. First, since the critical viscosity enhancement is small we need accurate values for $\bar{\eta}$ to make a quantitative analysis of the critical enhancement. Aggravated by possible systematic differences it w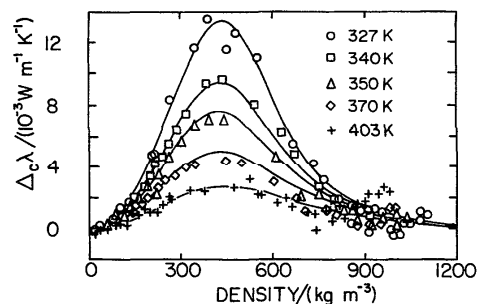as impossible to obtain acceptable values for $\bar{\eta}$ near the critical point from other experimental data far away from the critical point as will be further discussed in Sec. 5.2. Furthermore, the data of Iwasaki and Takahashi seem to imply a slight temperature dependence of the excess viscosity $\Delta\eta(\rho)$, a trend not confirmed by the data of Haepp[131] at higher temperatures.

In this section we use a local equation for a smoothly varying background excess viscosity $\Delta\eta(\rho)$, so that an adequate representation is obtained of the data of Iwasaki and Takahashi[30] and of Kestin et al.[20] at the temperatures close to the critical temperature where a critical viscosity enhancement has been observed. Hence, for the analysis of the critical viscosity enhancement in terms of Eq. (38) we continue to use the Eq. (63) for the excess thermal conductivity $\Delta\lambda(\rho)$, but for the excess viscosity $\Delta\eta(\rho)$ we use

$$\Delta\eta(\rho) = \sum_{i=1}^{4} e'_i \rho^i \, ,$$

$$(55)$$

TABLE 6. Coefficients in Eq. (55) for the excess viscosity near the critical temperature (ρ in kg m^{-3}; η in μPa s)

i	e_i'
1	5.5934×10^{-3}
2	6.1757×10^{-5}
3	0.0
4	2.6430×10^{-11}

with coefficients e_i' earlier determined by Olchowy and Sengers.[4,110] The coefficients e_i' are given in Table 6 with ρ expressed in kg m^{-3} and η in μPa s. Equation (55) reproduces the experimental background viscosity data to within 0.5% at 298 K$\leqslant T \leqslant$305 K and within 2% at 298 K$\leqslant T \leqslant$325 K. The equation to be adopted for the final global background excess viscosity $\Delta\eta(\rho)$ will be discussed in Sec. 5.2 [see Eq. (67) and Table 8].

The complete set of viscosity data of Iwasaki and Takahashi is shown in Fig. 13. This figure confirms that the critical viscosity enhancement is weak and restricted to the close vicinity of the critical point. A detailed comparison of Eq. (36) with the values for the critical viscosity enhancement deduced from the data of Iwasaki and Takahashi is shown in Fig. 14. Equation (36) does give a good representation of the variation of the critical viscosity enhancement with temperature and density. The equation represents the viscosity data at the near-critical temperatures (298.15 K$<T<$304.95 K) with a standard deviation of 0.25%. However, at $T = 308.15$ K and $T = 323.15$ K the average standard deviation becomes 1% with actual deviations up to 2%; this is a consequence of an apparent temperature dependence of the excess background viscosity implied by the measurements of Iwasaki and Takahashi. As further discussed in Sec. 5.2, it is

FIG. 14. The critical viscosity enhancement $\Delta_c\eta$ of carbon dioxide deduced from the data of Iwasaki and Takahashi.[30] The solid curves represent the values calculated from Eq. (39) as discussed in the text.

impossible to determine the background viscosity $\bar{\eta}$ with an accuracy better than 2% near the critical density and beyond.

A comparison of the viscosity data of Kestin, Korfali, and Sengers[20] with our equation is presented in Fig. 15. Our equation reproduces the data of Kestin *et al.*[20] to within 0.5%. It is interesting to note that our analysis also indicates the presence of a small viscosity enhancement in the data of Kestin *et al.* at densities beyond 200 kg m^{-3}.

From our equation we conclude that the relative critical viscosity enhancement $\Delta_c\eta/\eta$ is smaller than 1% at densities and temperatures outside a range bounded approximately by

$$300 \text{ K} < T < 310 \text{ K}, \quad 300 \text{ kg m}^{-3} < \rho < 600 \text{ kg m}^{-3}.$$

$$(56)$$

FIG. 13. The viscosity of carbon dioxide as a function of density at various temperatures as measured by Iwasaki and Takahashi.[30] The solid curves represent the values calculated from Eqs. (33) and (39) with Eq. (55) for $\Delta\eta(\rho)$. The vertical scale corresponds to the viscosity isotherm at 304.25 K. To separate the other isotherms, the values of $\eta \times 10^7$ at 298.15, 304.35, 304.65, 304.95, 308.15, and 323.15 K have been displaced by $+30$, -30, -60, -120 and -150 Pa s, respectively.

FIG. 15. The viscosity of carbon dioxide as measured by Kestin *et al.*[20] The dashed curve represents the background viscosity as given by Eq. (53) with (55) for $\Delta\eta(\rho)$. The solid curve represents the values calculated for the total viscosity $\eta + \Delta_c\eta$ from Eqs. (33) and (39) with Eq. (55) for $\Delta\eta(\rho)$.

4.5 A Simplified Equation for the Thermal Conductivity in the Critical Region

Equation (38), though readily programmable, is a somewhat complicated equation. In addition, we therefore propose a simplified version of this equation which will be adequate for many applications. This simplification is based on the observation that the critical viscosity enhancement is weak and noticeable only very close to the critical point. Hence, this critical viscosity enhancement is often neglected in engineering applications.[132] Neglecting the critical viscosity enhancement means identifying the actual viscosity η with the background viscosity $\bar{\eta}$ at all temperatures and densities including those near the critical point:

$$\eta(\rho,T) = \bar{\eta}(\rho,T) . \tag{57}$$

Introducing some additional approximations Olchowy and Sengers[133] have proposed the following alternative simplified equation for the critical enhancement of the thermal conductivity:

$$\frac{\Delta\lambda}{\rho c_p} = \frac{RkT}{6\pi\bar{\eta}\xi} (\tilde{\Omega} - \tilde{\Omega}_0) , \tag{58}$$

with

$$\tilde{\Omega} = \frac{2}{\pi} \left[\left(\frac{c_p - c_v}{c_p} \right) \arctan(\tilde{q}_D\xi) + \frac{c_v}{c_p} \tilde{q}_D\xi \right] , \tag{59}$$

and

$$\tilde{\Omega}_0 = \frac{2}{\pi} \left\{ 1 - \exp\left[-\frac{1}{(\tilde{q}_D\xi)^{-1} + \frac{1}{3} (\tilde{q}_D\xi\rho_c/\rho)^2} \right] \right\} \tag{60}$$

and where $\tilde{q}_D \neq q_D$ is now a modified effective cutoff parameter. For carbon dioxide

$$\tilde{q}_D^{-1} = 4.0 \times 10^{-10} \text{ m} , \tag{61}$$

as determined from a fit of Eq. (58) to the thermal conductivity data of Michels et al.[61] The correlation length ξ is still to be calculated as described in Sec. 4.2.

A comparison of the simplified Eq. (58) with the thermal diffusivity data is presented in Fig. 16 and with the ther-
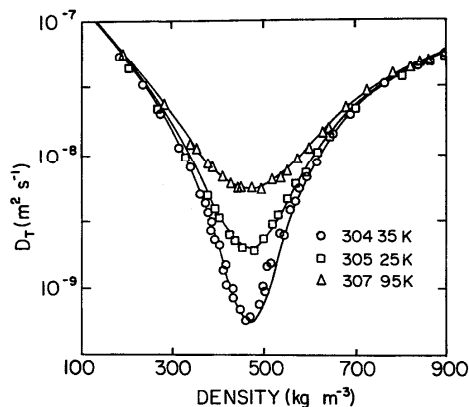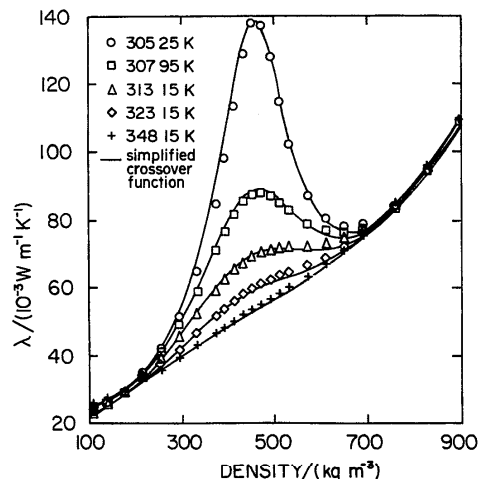
FIG. 17. The thermal conductivity of carbon dioxide in the critical region as a function of density at various temperatures. The experimental data are those of Michels et al.[61] The solid curves represent the values calculated with the aid of the simplified Eq. (58).

mal conductivity data in Fig. 17. In this comparison we have again represented $\bar{\lambda}$ and $\bar{\eta}$ by Eqs. (52) and (53) with the excess functions $\Delta\lambda(\rho)$ and $\Delta\eta(\rho)$ represented by Eqs. (63) and (67). The simplified Eq. (58) represents the thermal conductivity data of Michels et al. with a standard deviation of 2.7%, compared with a standard deviation of 1.5% obtained with the more detailed Eq. (38).

5. The Background Properties

The background transport property of a fluid $\bar{X}(\rho,T)$ is defined as that part of the property which does not arise from phenomena directly associated with the critical point. However, as the preceding discussion has shown, it is rather less straightforward to separate the critical enhancement and the background contributions from a given set of experimental data which, in principle, always contains both contributions. The iterative process whereby this separation has been achieved, described above, makes it clear that throughout the procedure our correlations of the background contributions to both the thermal conductivity and viscosity are continually refined. In general, the detailed results of the various stages of iteration are not important, so that it is the overall purpose of this section to set out the final representation of the background properties together with the rationale for the selection of the experimental data on which they are based. For this reason, the treatment given here assumes that the critical enhancements of both thermal conductivity and viscosity are given independently by the analysis of the preceding section. In exceptional circumstances the process of iteration reveals behavior that causes the set of primary data used to be adjusted. In such cases, the interim results leading to such adjustments are germane to the overall discussion and are therefore described. The discussion of the background properties is begun with the thermal conductivity because it is the critical enhancement of this property which is used to fix the one adjustable parameter, (q_D or $\tilde{q}_D$) in the equations for the transport properties in the critical region.

FIG. 16. The thermal diffusivity of carbon dioxide in the critical region as a function of density at various temperatures. The experimental data for D_T are those measured by Becker and Grigull.[86] The solid curves represent the values calculated with the aid of the simplified Eq. (58).

5.1 Thermal Conductivity

5.1.a Primary Data

Among the gas-phase measurements, following the argument in treating the zero-density contribution, the three groups of measurements carried out with the transient hot-wire technique[12,89-91] enjoy a high level of confidence and are therefore categorized as primary data. The measurements cover the temperature range 300 K$\leq T \leq$470 K and pressures up to 30 MPa. However, the data along the isotherm at 316 K reported in Ref. 90 reveal a density dependence of the thermal conductivity not present along any other isotherm. Thus, results for this isotherm are excluded from the primary data.

Snel et al.[88] have reported measurements of the thermal conductivity of carbon dioxide performed in a steady-state hot-wire instrument for which a complete theory was developed. The zero-density values derived from those measurements are consistent with the correlation given earlier within $\pm$ 1.5% over the limited temperature range studied. The data are therefore included in the primary data although the uncertainty claimed by the authors is increased to reflect the discrepancy in the zero-density data. Finally, we include in our set of primary data the results of Le Neindre et al.,[66,70,77,78] made with a concentric-cylinder apparatus, because they are one of the few sets of results that cover an extensive range of temperatures, 296 K$\leq T \leq$724 K and pressures, $P \leq$100 MPa. However, we note that these measurements provided rather poor values for the zero-density thermal conductivity, with deviations amounting to $\pm$ 5%. It would therefore be unreasonable to assign to these data an accuracy which is better than $\pm$ 5%, although the precision with which the density dependence is determined may be better.

Another set of information that could be considered for inclusion as primary data for the dense gaseous region comprises the results of Michels et al.[61] Because most of these measurements were carried out very near the critical temperature, the contribution of the critical enhancement to the measured value is large and frequently dominates the background contribution. It is therefore inappropriate to use these data to establish the background behavior. Similar comments apply to the work of Becker and Grigull.[86] Neither of these sets of data are employed in the primary data set for the background thermal conductivity. Table 7 identifies the selected primary data sets indicating their indi-

vidual pressure and temperature ranges and the assigned accuracy; there is a total of 676 data points.

There are eleven references[36,60,63,66,69,70,75,78,80,81,86] that contain data on the thermal conductivity of carbon dioxide in the liquid phase (as can be seen from Appendix I). Among these there are eight independent sets of measurements. The measurements that cover the greatest temperature range are those of Tarzimanov et al.[75,81] made with a steady-state hot-wire instrument. The 22 data points cover only the pressure range 7-9 MPa. The experimental technique is described only briefly and there is no strong evidence for the elimination of convection although it is discussed. Shingarev[69] has reported data, obtained by the same method, over a similar temperature range at one pressure for each temperature. In addition, Amirkhanov and Adamov[63] have used both parallel-plate and concentric-cylinder instruments to determine ten points along the saturation line in the liquid phase within the temperature range 293-304 K. There also seem to have been earlier measurements[81] although the literature is unavailable. However, it is noted in Ref. 81 that there are discrepancies of 30%-40% between various earlier sources and, in a more recent paper,[8] it is stated that further measurements have been made in the liquid phase but no data are reported.

In 1934 Sellschopp[36] reported measurements of the thermal conductivity of liquid carbon dioxide in the temperature range 284-304 K at pressures from 5 to 9 MPa. However, these measurements were influenced by convection, as was pointed out by Borovik.[43] Indeed, Borovik attempted to correct the original data for this effect. With our current understanding of convection in thermal conductivity instruments, it can be asserted that such a correction is extremely unlikely to lead to accurate experimental data. In view of doubts about most of these data and the narrow range of states covered by the measurements, it has been decided that none of these results fulfil the requirements for primary data.

The remaining data for the liquid phase cover the temperature range 273-298 K although all but four data points were taken within 2 K of 298 K. Notwithstanding the fact that some of these measurements are of high accuracy, the total number of data points is 41 and their distribution in density-temperature space is so narrow as to make them of virtually no value in developing a correlation. For these reasons it has been concluded that it is impossible to base a representation of the thermal conductivity of liquid carbon

TABLE 7. Set of primary data used for correlating the background thermal conductivity

Authors	Temperatures (K)	P range	No. of points	Ascribed uncertainty
1. Millat et al.[12]	308; 333; 380	0-7 MPa	79	$\pm$ 0.5%
2. Scott et al.[90]	302; 348	0-25 MPa	36	$\pm$ 0.5%
3. Johns et al.[91]	333; 380; 430; 470	0-30 MPa	78	$\pm$ 0.5%
4. Clifford et al.[89]	301	0-6 MPa	22	$\pm$ 0.5%
5. Snel et al.[88]	298; 304; 323	0-5 MPa	133	$\pm$ 1.5%
6. Le Neindre et al.[66,70,77,78]	296-724	0-100 MPa	328	$\pm$ 5%

dioxide on available experimental data. Instead the thermal conductivity of the liquid has been predicted by extrapolation of the gas-phase correlation and the available experimental data used as a check. Comparisons of this type will be presented later.

5.1.b. Analysis

The first stage of the analysis of the primary data set has been the correction of all data to isotherms. This has been accomplished, where necessary, by the application of a linear temperature correction using a temperature derivative deduced from the zero-density correlation. Because the correction applied was always less that $\pm 0.2\%$ of the thermal conductivity, the error introduced into the thermal conductivity by this procedure is negligible. In addition, the density for each data point was recalculated from the experimental temperature and pressure using consistently the most recent equations of state for carbon dioxide developed by Ely[95] and Albright et al.[112]

In the next step of the analysis, it is recognized that the precision of measurements is superior to their accuracy and that we have already established a reliable correlation for the zero-density thermal conductivity. Thus, the excess thermal conductivity, defined by the equation

$$\Delta\lambda(\rho,T) = \lambda(\rho,T) - \lambda^0(T) - \Delta_c\lambda(\rho,T), \qquad (62)$$

allows us to examine the behavior of $\Delta\lambda(\rho,T)$ free from constant, systematic errors in individual measurements of $\lambda(\rho,T)$, if for $\lambda^0(T)$ we use the values reported by individual authors. Subsequently, having represented $\Delta\lambda(\rho,T)$, the correlated values of $\lambda^0(T)$ can be added to it to produce the final background thermal conductivity.

It should be recalled here that the exact values of $\Delta_c\lambda(\rho,T)$ employed in Eq. (62) change throughout the iterative process described in Sec. 4, but in this case these changes caused no need for alteration of the data included in the primary data set. The results presented below therefore refer to the use of the final form of $\Delta_c\lambda(\rho,T)$ as given by Eq. (38) with the constants listed in Table 5.

Large-scale graphs of $\Delta\lambda(\rho,T)$, defined by Eq. (62), as a function of density along isotherms, as well as a series of simple fits to the data, were used to examine the temperature dependence of $\Delta\lambda(\rho,T)$. Figure 18 contains a plot of the excess thermal conductivity as a function of density along most of the isotherms listed in Table 7 so that the data cover the temperature range 296–724 K. No attempt is made to distinguish between the results of various authors although the results in different temperature ranges are distinguished, because the essential result to be derived from this figure is that there is no systematic temperature dependence of $\Delta\lambda(\rho,T)$. The spread of the results amounts to $\pm 0.8\%$ of the total thermal conductivity at low densities whereas at higher densities, it amounts to only $\pm 0.3\%$. These figures are commensurate with the uncertainty in the experimental data. If the experimental data from a single laboratory are examined, it is possible in just one case[90] to discern a systematic trend in $\Delta\lambda(\rho,T)$ with temperature, but when results from several laboratories are combined, this trend is lost. On this basis, it is concluded that, within the attainable experi-
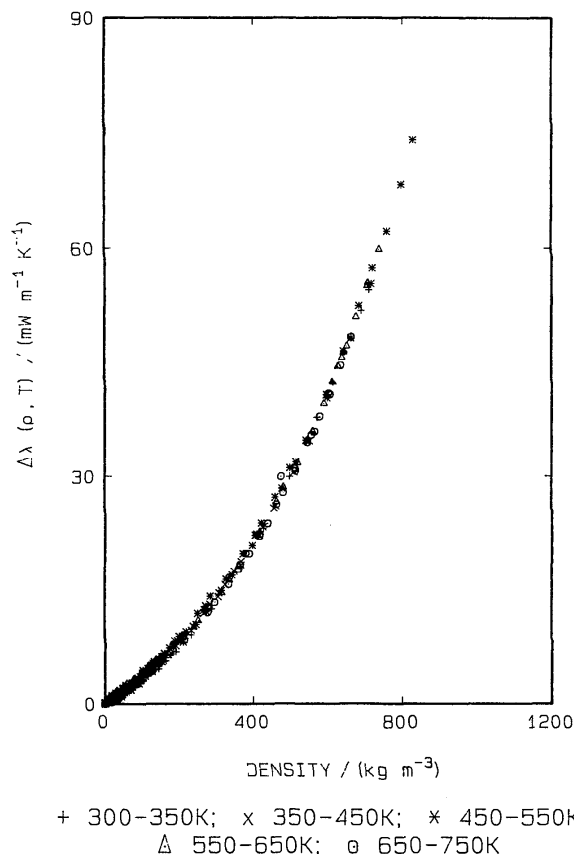
FIG. 18. The excess thermal conductivity as a function of density deduced from references listed in Table 7.

mental accuracy, there is no justification for including any temperature dependence within the excess thermal conductivity so that $\Delta\lambda(\rho,T) = \Delta\lambda(\rho)$ only. This should not be taken to imply that there is no temperature dependence but merely that it is so small as to be within experimental error.

5.1.c. Representation

In order to represent the density dependence of $\Delta\lambda$ we have selected a simple polynomial:

$$\Delta\lambda(\rho) = \sum_{i=1}^{4} d_i \, \rho^i, \qquad (63)$$

and determined the appropriate terms and the optimum values of their coefficients d_i by means of the SEEQ algorithm,[107] in a weighted least squares fit. The relative weights of data in this fitting were obtained as described elsewhere,[11] using the ascribed uncertainties listed in Table 7. Table 8 includes the final values of d_i where the density ρ is expressed in kg m^{-3} and $\Delta\lambda$ in mW m^{-1} K^{-1}.

The results of this representation can now be used, *ex post facto*, to further justify the use of a temperature-independent correlation by means of deviation plots, which display the deviations of particular authors' data for $\Delta\lambda(\rho,T)$ from the correlation. In these figures the deviation

TABLE 8. Coefficients of the correlation of the excess transport properties of carbon dioxide (ρ in kg m^{-3}; λ in mW m^{-1} K^{-1}; η in μPa s)

i	d_i	e_i
1	2.447164×10^{-2}	$\cdot\ 3.6350734 \times 10^{-3}$
2	8.705605×10^{-5}	7.209997×10^{-5}
3	-6.547950×10^{-8}	0.0
4	6.594919×10^{-11}	0.0
5	–	0.0
6	–	0.0
7	–	3.00306×10^{-20}

shown is

$$\epsilon' = [\ (\lambda_{\exp}(\rho,T) - \lambda_{\mathrm{calc}}(\rho,T))/\lambda_{\mathrm{calc}}(\rho,T)\ ] \times 100\%,$$
(64)

where

$$\lambda_{\mathrm{calc}} = \Delta\lambda_{\mathrm{corr}}(\rho) + \lambda^{0}(T) + \Delta\lambda_c(\rho,T),$$
(65)

with $\lambda^{0}(T)$ taken from the experimental results of individual authors. By this mechanism we avoid the generation of deviations arising solely from differences between the experimental and correlated zero-density thermal conductivity or the even larger deviations that result if the fractional error in $\Delta\lambda(\rho)$ itself is plotted.

Figure 19 contains the deviations of the data of Millat *et al.*[12] and Snel *et al.*[88] and Clifford *et al.*[89] from the correlation. The deviations approach 2% for some isolated points, but the standard deviation for the three sets of data is $\pm 0.6\%$, which is commensurate with their estimated uncertainty. Within the data reported by a single author, it is just possible to discern a systematic trend with temperature.

However, when the results of several authors are combined, this trend is lost and we conclude there is no evidence of an overall trend with temperature beyond the limits of the estimated uncertainty. Figure 20 contains the deviations for the two sets of measurements reported by Johns *et al.*[90,91] The standard deviation is slightly worse than for the other set of data but is again broadly consistent with the estimated error and it is not possible to discern a systematic temperature dependence within the scatter. Finally, in Fig. 21, the deviations of the data of Le Neindre *et al.*[66,70,77,78] from the correlation are shown. Here the scatter of the data is somewhat greater reflecting the lower accuracy. In addition, there is some evidence that the initial density dependence reported by Le Neindre *et al.*[66,70,77,78] is greater than that found in the transient hot-wire experiments. This is revealed by the systematically positive deviations from the correlation in the region of 150 kg m^{-3} for the data of Le Neindre *et al.*, which lie in a region where the fit is weighted to represent the transient hot-wire data. However, neither in this region, nor at higher densities where the fit to the data of Le Neindre *et al.* is better, is there any evidence of a systematic temperature dependence in $\Delta\lambda$.

5.1.d. Extensions

The correlation for $\Delta\lambda(\rho)$ has been developed on the basis of information on the gas-phase thermal conductivity in the temperature range 296–724 K. However, the temperature independence of $\Delta\lambda$ within this range suggests that even outside of this range, for the gaseous phase at least, it is possible to predict the thermal conductivity of the dense fluid simply by using the correlation for $\Delta\lambda(\rho)$ of Eq. (63) in
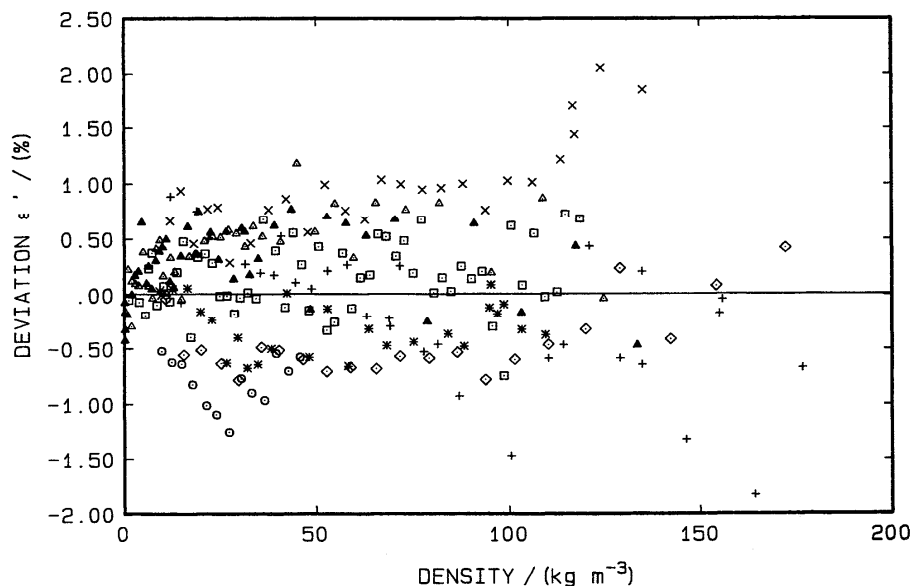
FIG. 19. Deviations ϵ' (Eq. 64) of data of Millat *et al.*,[12] Snel *et al.*,[88] and Clifford *et al.*[89] from the correlation.
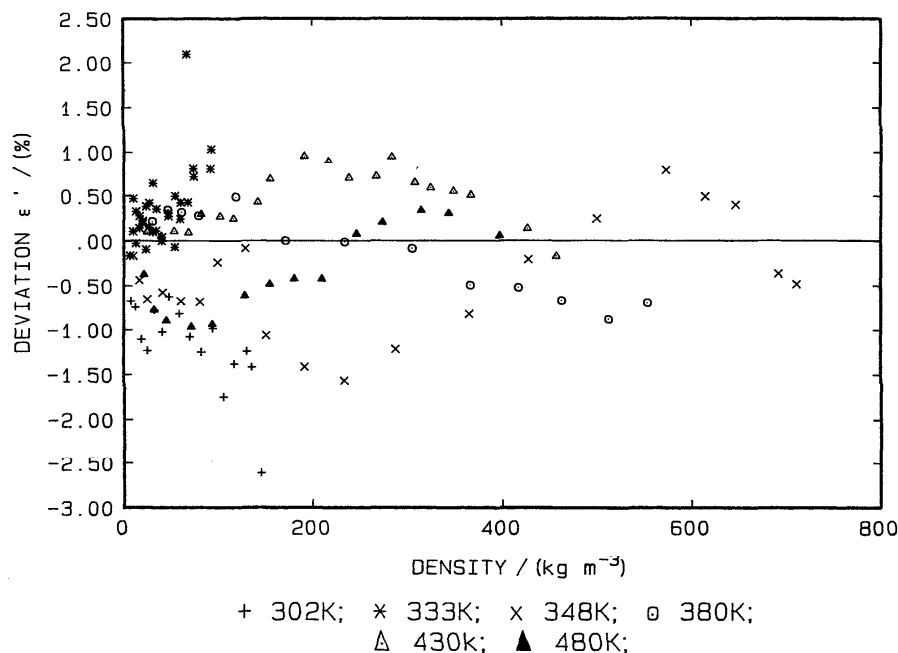
FIG. 20. Deviations ϵ' (Eq. 64) of data of Johns et al.[90,91] from the correlation.

conjunction with the correlations for $\lambda^0(T)$ and $\Delta\lambda_c(\rho,T)$. Of course, it is circumspect to increase the uncertainty of the thermal conductivity in the extended region to reflect the fact that the data are extrapolated. Nevertheless, the basis of the extrapolation seems rather secure given the evidence in the preceding discussion.

So far as the liquid phase is concerned, there is some evidence for other fluids that the near temperature independence of $\Delta\lambda(\rho)$ characteristic of the gas phase extends to the liquid phase. In the case of carbon dioxide, the experimental data are inadequate to examine the hypothesis directly. The alternative approach adopted here is to use the same hypoth-
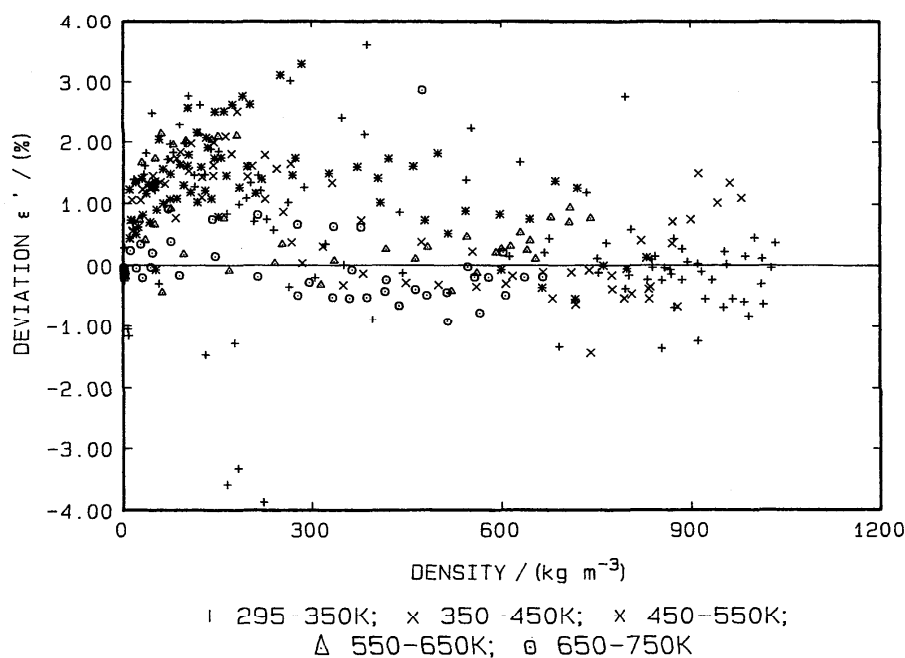
FIG. 21. Deviations ϵ' (Eq. 64) of data of Le Neindre et al.[66,70,77,78] from the correlation.

esis to calculate the total thermal conductivity in the liquid phase and to compare it with experiment. The results of such a calculation are best discussed when considering the performance of the overall representation of the thermal conductivity so that we postpone it until Sec. 6.1.

5.2 The Viscosity

5.2.a. Primary Data for the Gas Phase

Appendix II lists the entire set of literature sources available on the viscosity of carbon dioxide as a function of pressure or density in both gaseous and liquid phases.[20,22,23,27–30,126,128–131,134–148]

The most important sets of measurements in the dense gaseous state are those of Michels *et al.*[126] performed with a capillary viscometer, several sets of measurements by Kestin and his collaborators[20,22,23,27–29,128,135] with oscillating-disk instruments, the measurements of Haepp,[131] as well as Iwasaki and Takahashi[30] with a similar instrument, and finally the work of Golubev and his co-workers[136,140,141] at combined high temperatures and high pressures. All of these measurements have been carried out in instruments in which a high precision is *possible* and for which complete working equations are *available*. It is for these reasons that they have been selected for consideration from the entire data set.

Following the pattern established for the thermal conductivity we first construct the excess viscosity for each data set according to the equation

$$\Delta\eta(\rho,T) = \eta(\rho,T) - \eta^0(T) - \Delta_c\eta(\rho,T), \qquad (66)$$

using the critical enhancement term calculated from Eq. (39). In the process, we have also recalculated the density for each datum using the reported pressures and temperatures, except for the data of Iwasaki and Takahashi[30] as noted earlier. These excess viscosities were then plotted on large-scale graphs in order to examine the temperature dependence of the excess and the internal consistency of the results.

Figure 22 shows one such plot containing the excess viscosity derived from the results of Kestin and his collaborators,[20,22,23,27–29,128,135] for which the claimed uncertainty in the data is $\pm$ 0.1–0.2%. All except one set of measurements[135] were performed in the same oscillating disk viscometer near room temperature, with various suspension assemblies. The exceptional set was obtained with a different instrument of the same type in which a new mechanism was employed to compensate for the effects of thermal expansion on the alignment of the system at elevated temperatures. It can be seen from Fig. 22 that this one set of measurements reveals quite a different density dependence of the viscosity from the others and that there appears to be a strong temperature dependence of the excess viscosity, not shown by the measurements in the temperature range 293–304 K carried out independently.[20,22,23,27–29,128]

Figure 23 shows a similar plot for the data reported by Golubev *et al.*[136,140,141] for the gas phase for the moderate density region over the temperature range 293–733 K. These data have a rather greater claimed uncertainty than those of Kestin and his group amounting to $\pm$ 2% but, within that limit, there is no discernible trend of the excess viscosity with
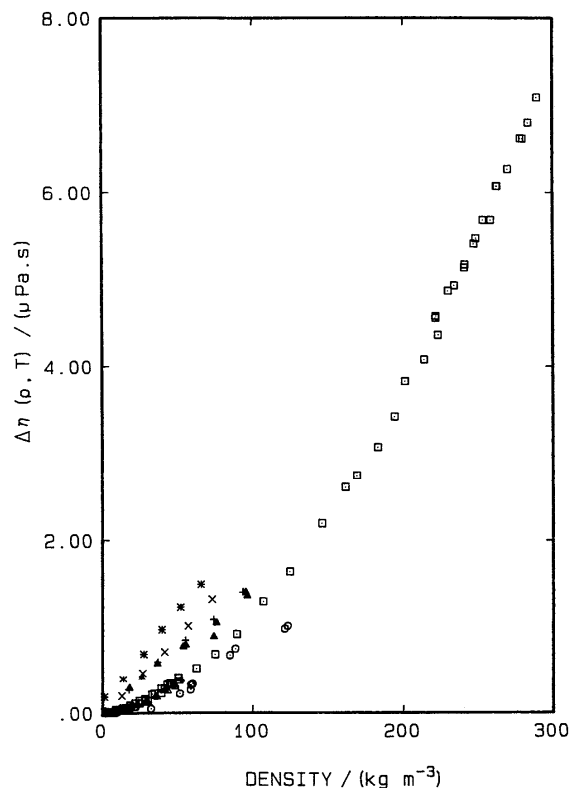
(□ 296K, ▲ 373K, + 426K, × 470K, ✳ 525k)[135]
△ 293K; ▣ 303–304K;

FIG. 22. The excess viscosity in the gas phase deduced from the results of Kestin and his collaborators.[20,22,23,27–29,128,135]

temperature, even over the extended temperature range. The conflicting behavior of one set of results[135] with respect to the others, cannot be reconciled without independent information. Fortunately, there are a number of indirect pieces of evidence which together point in just one direction. First, the zero-density viscosity data derived from the results of Kestin and Whitelaw[135] reveal a temperature dependence that is systematically different from that obtained in the earlier correlation.[11] This may indicate some unaccounted systematic error. Second, it has been confirmed by Kestin[149] that some difficulties surrounded the use of the thermal expansion compensation technique in the instrument employed in Ref. 135. Finally, there is a substantial body of evidence for other gases that $\Delta\eta$ is largely independent of temperature.[150,151] For these reasons we conclude that the data of Kestin and Whitelaw[135] are burdened with an unknown error and eliminate them from the primary data set.

We next consider the data of Michels *et al.*[126] In the region of the critical point the working equation employed for the analysis of the experimental results for the capillary viscometer was inappropriate.[127] Consequently it is necessary to omit some of the data from this source. The region of data omitted is bounded by 200 kg m^{-3} $\leqslant\rho\leqslant$ 700 kg m^{-3} and 298 K $\leqslant T\leqslant$ 313 K.

Figure 24 shows the collected excess viscosities
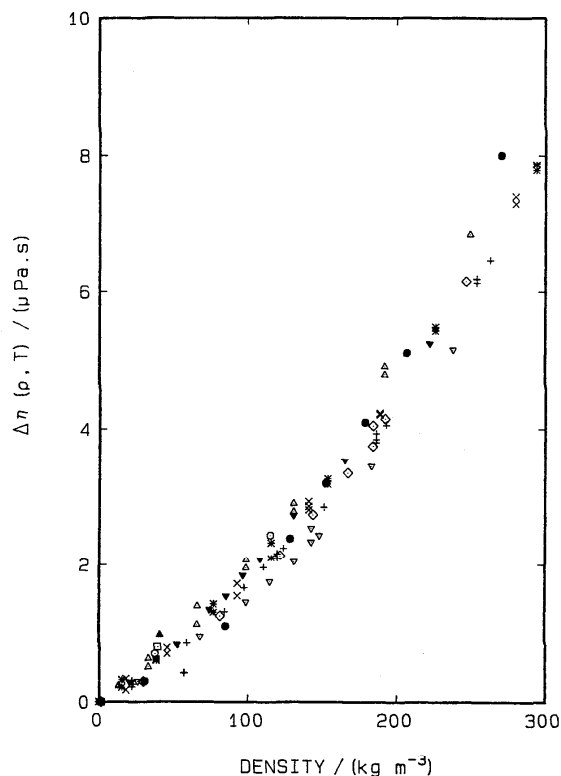
FIG. 23. The excess viscosity in the gas phase deduced from the results of Golubev and co-workers.[136,140,141]
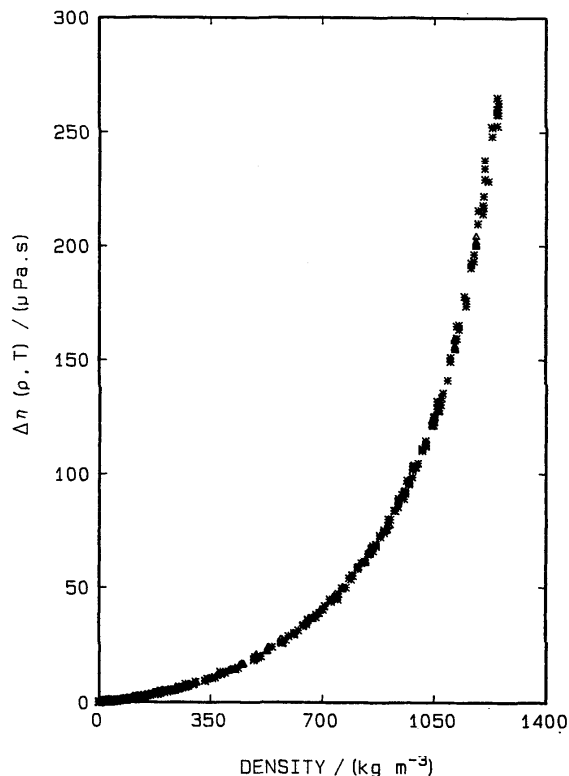
FIG. 24. The excess viscosity in the gas phase deduced form the results of Kestin et al.,[20,22,23,27–29,128] Michels et al.[126] and Golubev et al.[136,140,141]

deduced from the work of Kestin and his collaborators,[20,22,23,27–29,128] Michels et al.[126] and Golubev et al.[136,140,141] in which different temperatures are not distinguished. Over a wide range of densities the data sets are broadly consistent with each other within ± 4% of the total viscosity. This spread is more a reflection of the differences between different authors than any convincing evidence for a systematic temperature dependence of the excess viscosity.

The results of Haepp[131] have a claimed uncertainty of between 1%–1.6% and cover the temperature range 298–473 K at pressures up to 15 MPa, and therefore must be considered as candidates for inclusion in the set of primary data. However, as Fig. 25 shows, the excess viscosity of Haepp at low densities shows a different character from that observed by Kestin and his collaborators. In this figure the high-density excess-viscosity points of Haepp have been made coincident (by means of a vertical shift on the $\Delta\eta$ axis of -0.5 μPa s) with those of Kestin and his group[20,22,23,27–29,128]. In this region the two sets of data show a high degree of agreement. However, below a density of 20 kg m^{-3} the data of Haepp do not show the flattening as the zero-density limit is approached that is revealed in the other data. Because of the high precision of Kestin's data and the fact that the same behavior has been reported as a result of several independent studies, we conclude the data of Haepp

must suffer an unaccounted error at low densities. A corollary of this conclusion is that the zero-density data reported by Haepp[131] must be in error. We have redetermined the zero-density viscosity from his data following omission of the low-density points and used this value in constructing his data for the excess viscosity $\Delta\eta$.

The measurements of Iwasaki and Takahashi[30] were principally conducted to investigate the behavior in the region of the critical point. Because the extent of the critical enhancement of viscosity is small, the measurements were conducted along isotherms at 298.15, 304.25, 304.35, 304.65, 304.95, 308.15, and 323.15 K at pressures up to 14.5 MPa. In the initial stages of this work we took the view that those measurements in which the critical enhancement, predicted in the manner described in Sec. 4, was significant should be eliminated from the primary data used to determine the background representation. Thus, we excluded from the primary data all of the data of Iwasaki falling within a zone bounded by 304 K $\leqslant T \leqslant$ 305 K, 300 kg m^{-3} $\leqslant \rho \leqslant$ 600 kg m^{-3}. Of course, this implies that no data for the excess viscosity in the neighborhood of the critical point are included in the primary data used to determine its representation. However, if the evidence adduced earlier that the excess viscosity is temperature independent is correct, then this omis-
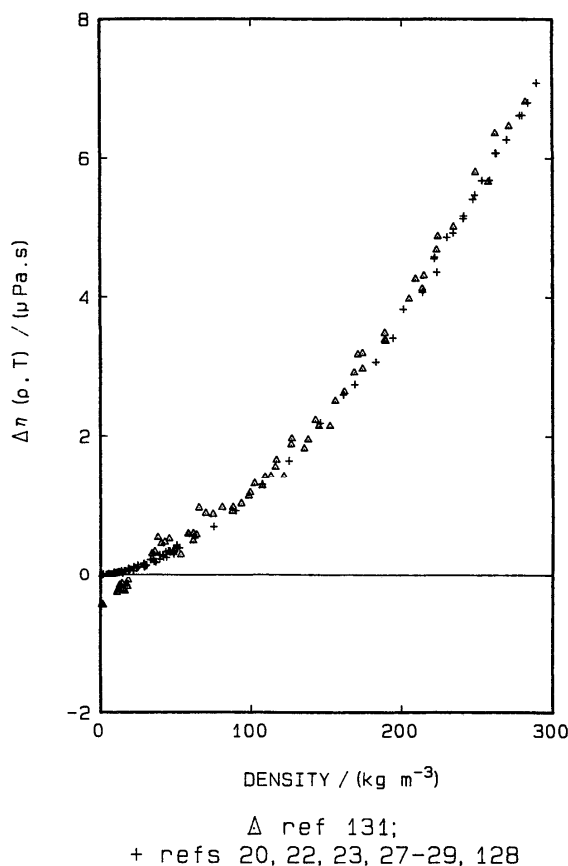
FIG. 25. The excess viscosity in the gas phase deduced from the results of Haepp,[131] superimposed on those of Kestin *et al.*[20,22,23,27–29,128] at moderate densities.

sion seems, superficially, to be of small significance because the *density* range of interest is covered by data at temperatures above the critical temperature. Accordingly, in the first determination of the excess viscosity we employ the set of primary data listed in Table 9 with the exclusions mentioned in the text. In each case, our estimate of the uncertainty in the total viscosity is also listed which was used as a basis for the assignment of statistical weights in the fitting.

In principle, it would now be possible to discuss the liquid-phase viscosity of carbon dioxide in order to provide a complete set of primary data for use in the development of a

global correlation. However, as will be shown later, there is considerable doubt about the liquid-phase viscosity data. Consequently, we prefer to treat the two phases separately.

5.2.b. Analysis and Representation of the Gas-Phase Data

In order to represent the excess viscosity of carbon dioxide in the gas, we have adopted a polynomial form in density which, following the earlier discussion, we presume to be temperature independent

$$\Delta \eta_g = \Delta \eta(\rho) = \sum_{i=1}^{n} e_i \rho^i . \qquad (67)$$

The weighted fitting of the preliminary primary data to this function was accomplished with the SEEQ algorithm[107] and it was found that four terms ($i = 1, 2, 6$ and 8) provided the best fit to the data.

In Figs. 26 to 29 we display the deviations of the data from this preliminary representation. In this case the deviations shown are those in the total viscosity:

$$\eta(\rho,T) = \eta^0(T) + \Delta \eta(\rho) + \Delta_c \eta(\rho,T), \qquad (68)$$

in which the correlations for $\eta^0(T)$ and the prediction for $\Delta_c \eta(\rho,T)$ have been employed. This is done in order to reveal simultaneously the extent to which the density-dependent viscosity data are consistent with the zero-density correlation for which they were not employed. Figure 26 contains the deviations of the data of Golubev *et al.*[136,140,141] for the entire temperature range 293–773 K. In the limit of zero density most of the data are ~2% below the correlation, which is essentially identical with their claimed accuracy. At higher densities the spread of data about the correlation is ± 4% except for a few isolated points, but there is no evidence of any systematic temperature dependence (see also Fig. A3.7), which supports the earlier discussion. Figure 27 contains a similar plot for the primary data of Kestin and his group.[20,22,23,27–29,128] The zero-density data are consistent with the correlation to within ± 0.2% and the density dependence of all of the data is represented within ± 0.5%. Although this figure exceeds the accuracy claimed for the measurements, it is consistent with the scatter between independent determinations. Figure 28 contains a deviation plot for the data of Haepp[131] and Michels *et al.*[126] Here the deviations are somewhat larger, and the defect in the low density data of Haepp is apparent, but elsewhere the data are consistent with the correlation.

TABLE 9. Set of primary data used for correlating the excess viscosity in the gas phase

Authors	T range	P range	No. of points	Ascribed uncertainty
1. Kestin *et al.*[22,23,27–29,128]	292–303 K	0–2.5 MPa	65	± 0.1%
2. Kestin *et al.*[20]	304 K	0–7 MPa	49	± 0.1%
3. Michels *et al.*[126,a]	273–348 K	0–210 MPa	123	± 0.5%
4. Haepp *et al.*[131,b]	298–473 K	3–15 MPa	62	± 3.0%
5. Golubev *et al.*[136,140,141]	293–773 K	0–350 MPa	274	± 3.0%
6. Iwasaki *et al.*[30]	298–323 K	0–15 MPa	248	± 0.2%

[a] Data in the region 200 kg m^3 < ρ < 700 kg/m^3, 298 K < T < 313 K have not been used as primary data.
[b] Data below 20 kg/m^3 have not been used.
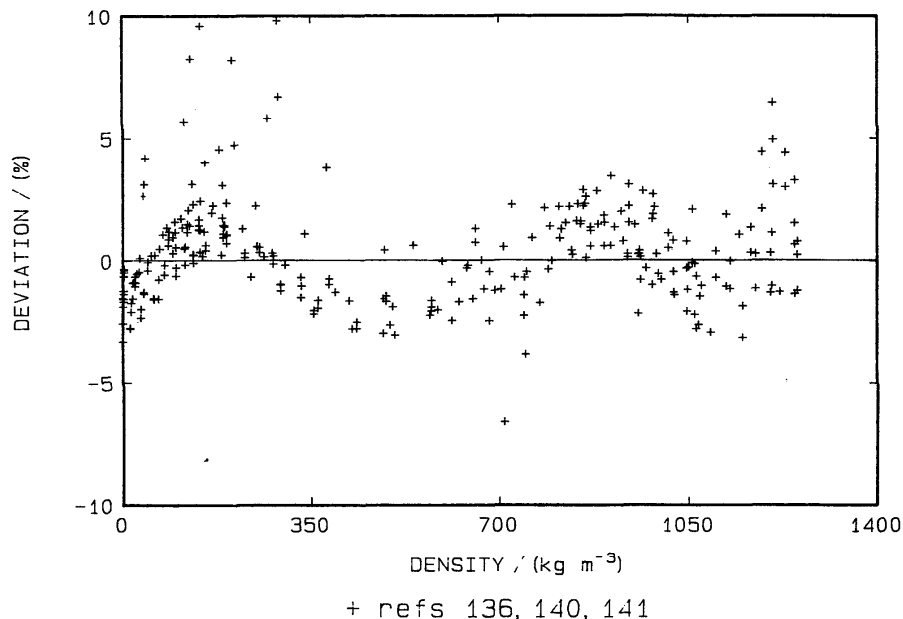
+ refs 136, 140, 141

FIG. 26. The deviations of the gas-phase viscosity data of Golubev *et al.*[136,140,141] from the preliminary representation.

In contrast, Fig. 29 contains a plot of the deviations for the entire set of viscosity data reported by Iwasaki and Takahashi[30] including the points in the critical region. It can be seen that while the low-density and high-density data are well represented at most temperatures, there is a rather significant ($\sim 2\%$) negative deviation at a density of about 400 kg m^{-3} for the isotherms 304.25 to 304.95 K which is reduced for the isotherm at 308.15 K, whereas the isotherm at 323 K show a distinctly different pattern.

This figure reveals a difficulty because the data of Iwasaki and Takahashi[30] are undoubtedly the most precise and accurate ($\simeq \pm 0.2\%$) in the critical region and, in particular, near the critical density, for *any* temperature. The failure to obtain a satisfactory fit to these data can be due to one or

+ refs 20, 22, 23, 27-29, 128
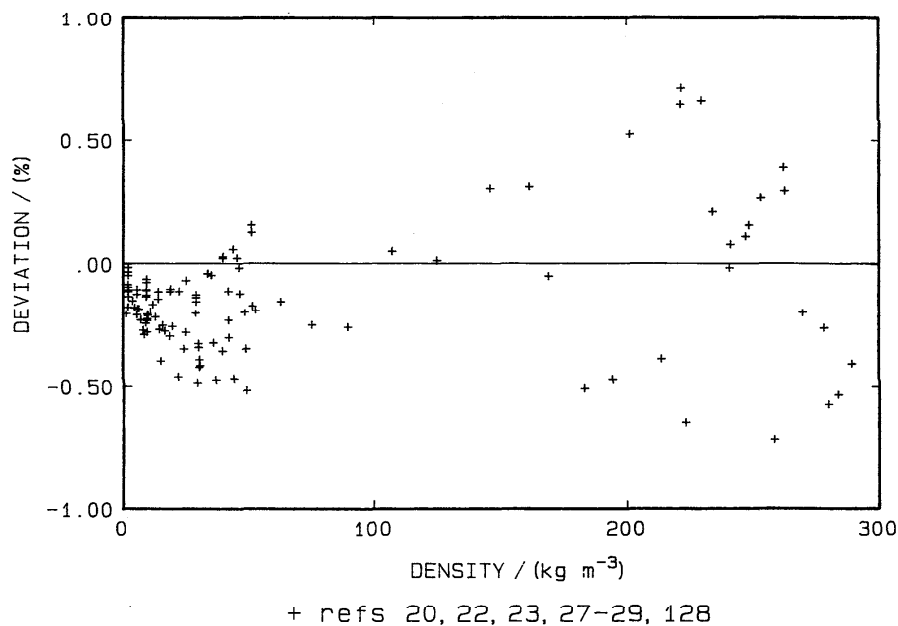
FIG. 27. The deviations of the gas-phase viscosity data of Kestin and his co-workers[20,22,23,27-29,128] from the preliminary representation.
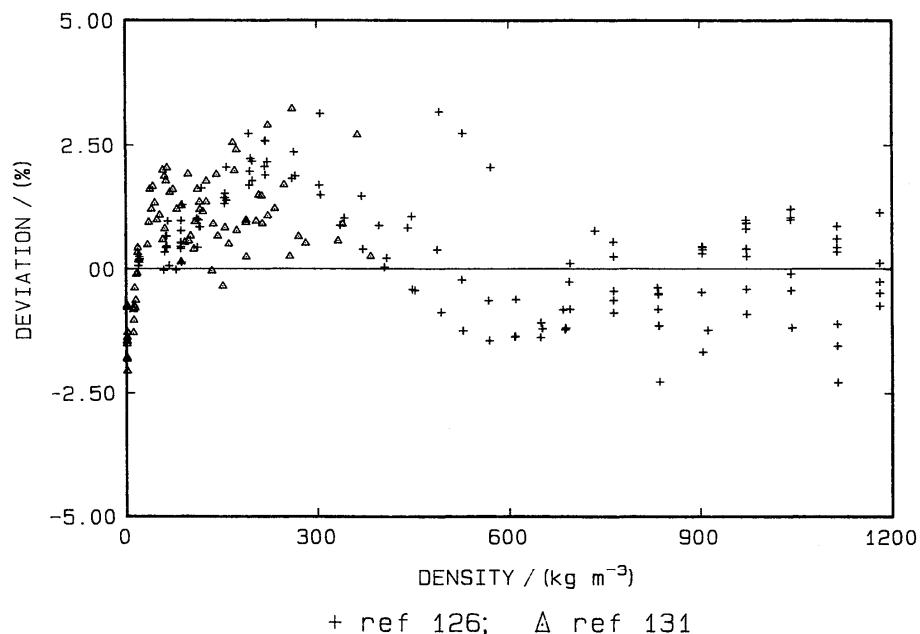
Fiu. 28. The deviations of the gas-phase viscosity data of Michels *et al.*[126] and Haepp[131] from the preliminary representation.

both of the following causes: (i) The background viscosity we employ near the critical density at each temperature is derived from data of poorer accuracy than that of Iwasaki and Takahashi.[30] Thus, the background viscosity may be in error. (ii) The predicted critical enhancement may be in error.

The second of these possibilities implies a failure of the theory of the critical enhancement of the viscosity *and* thermal conductivity described in Sec. 4. In view of its pedigree and the good representation of the enhancements of the thermal conductivity and viscosity with a single adjustable parameter, this proposition is unlikely. Consequently, we must
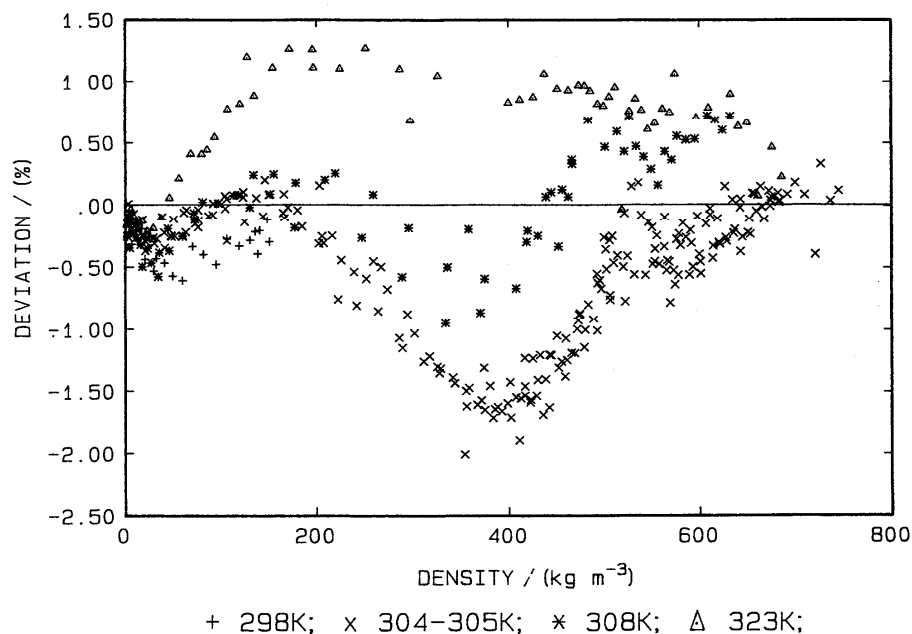
FIG. 29. The deviations of the gas-phase viscosity data of Iwasaki and Takahashi[30] from the preliminary representation.

(+ 298K x 304-305K * 308K △ 323K) [30]
▲ refs 20, 22, 23, 27-29, 128
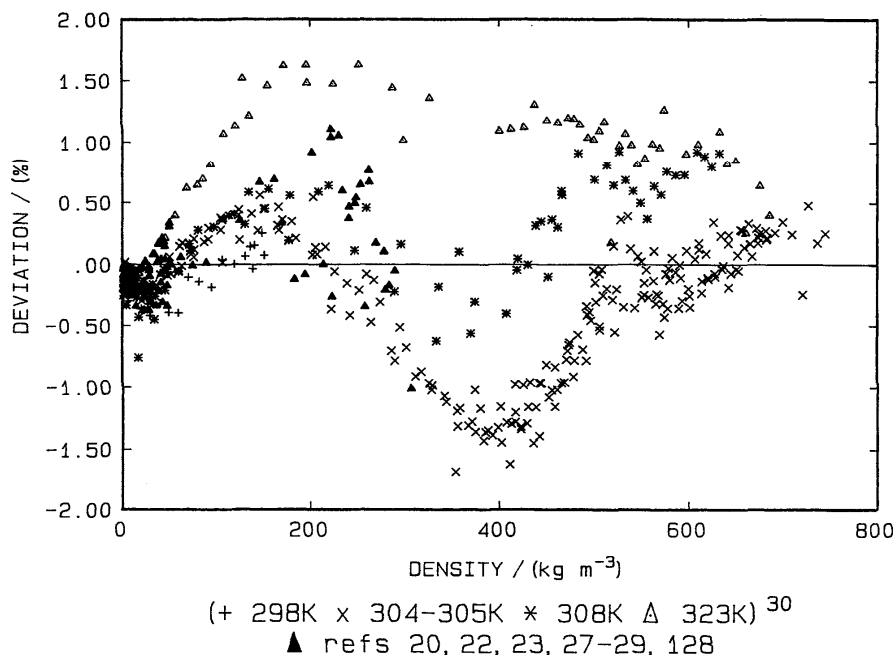
FIG. 30. The deviations of the gas-phase viscosity data of Kestin and his collaborators,[20,22,23,27-29,128] and Iwasaki and Takahashi[30] from a fit to *all* the primary viscosity data.

examine the first possibility in detail.

First, we consider the internal consistency of the data of Iwasaki and Takahashi alone. From Fig. 29 it is evident that the excess viscosity calculated from their data[30] is temperature dependent and strongly so. From studies of other fluids it is expected that any temperature dependence of the excess viscosity should be strongest at lower temperatures, in the liquid phase, and should decrease as the temperature is increased. The behavior revealed by the data of Iwasaki and Takahashi is inconsistent with this observation because the isotherm at 323 K reveals a qualitatively different behavior than is shown by the temperature-independent excess, being 1% above it on average. Conversely, two other isotherms show a marked negative dip with respect to the temperature-independent excess which is not revealed by other isotherms or other authors. These findings are given further support if the predicted critical enhancement, $\Delta_c \eta$, is subtracted from *all* of the data listed in Table 9, including those of Iwasaki and Takahashi in the critical region. The optimum, properly weighted, fit of a temperature-independent function of the form of Eq. (67) to these data was achieved with the SEEQ algorithm,[107] using just three terms with $i = 1, 2$, and 7. The deviations of the most precise data[20,22,23,27-30,128] from this correlation are shown in Fig. 30. It is clear that the negative deviations in the data of Iwasaki and Takahashi near a density of $\rho = 400$ kg m^{-3} persist in this plot although they are very slightly smaller in magnitude.

The nature of the inconsistency is revealed to some extent by selecting just the data of Kestin *et al.*[20,22,23,27-29,128] and Iwasaki and Takahashi,[30] and by fitting to them the background viscosity temperature-independent function $\Delta \eta(\rho)$ again. In this case an optimum fit was obtained with four terms with $i = 0, 1, 2$, and 4 and the deviations are shown in Fig. 31(a). Here it can be seen that the negative dip in the deviations of the data of Iwasaki and Takahashi[30] along the lower isotherms are rendered significantly smaller, while the positive deviations of the isotherm at 323 K are increased. Furthermore, the appearance of a term with $i = 0$ in the correlating equation indicates that the data then require a different zero-density viscosity not required by the entire primary data set. This adds a further doubt concerning at least some of the isotherms of the data of Iwasaki and Takahashi.[30]

From Fig. 31(a) it is also clear that the 323 K isotherm of Iwasaki and Takahashi[30] has quite a different character from that of the lower isotherms so the process described above was repeated following omission of the data for that isotherm. As a result, an optimum fit to the data was achieved with a $\Delta \eta(\rho)$ function containing six terms for $i = 1, 2, 4, 5, 6$, and 7 with alternating signs. Figure 31(b) shows the corresponding deviation plot which indicates that the negative dip in the deviations of the lowest isotherm has been removed at the expense of the growth of a positive deviation for the isotherm at 308 K and a much more complicated density function for $\Delta \eta(\rho)$ with an implausible structure.

On the basis of these tests we conclude that it is not possible to reconcile all of the experimental data, within their uncertainty, with a temperature-independent excess viscosity. Thus, we must either accept that it is not possible, with our present knowledge, to define the viscosity background of carbon dioxide to better than $\pm 2\%$ in the neighborhood of the critical point, or we must accept a totally different (and implausible) density function for the background near the critical temperature from that which per-
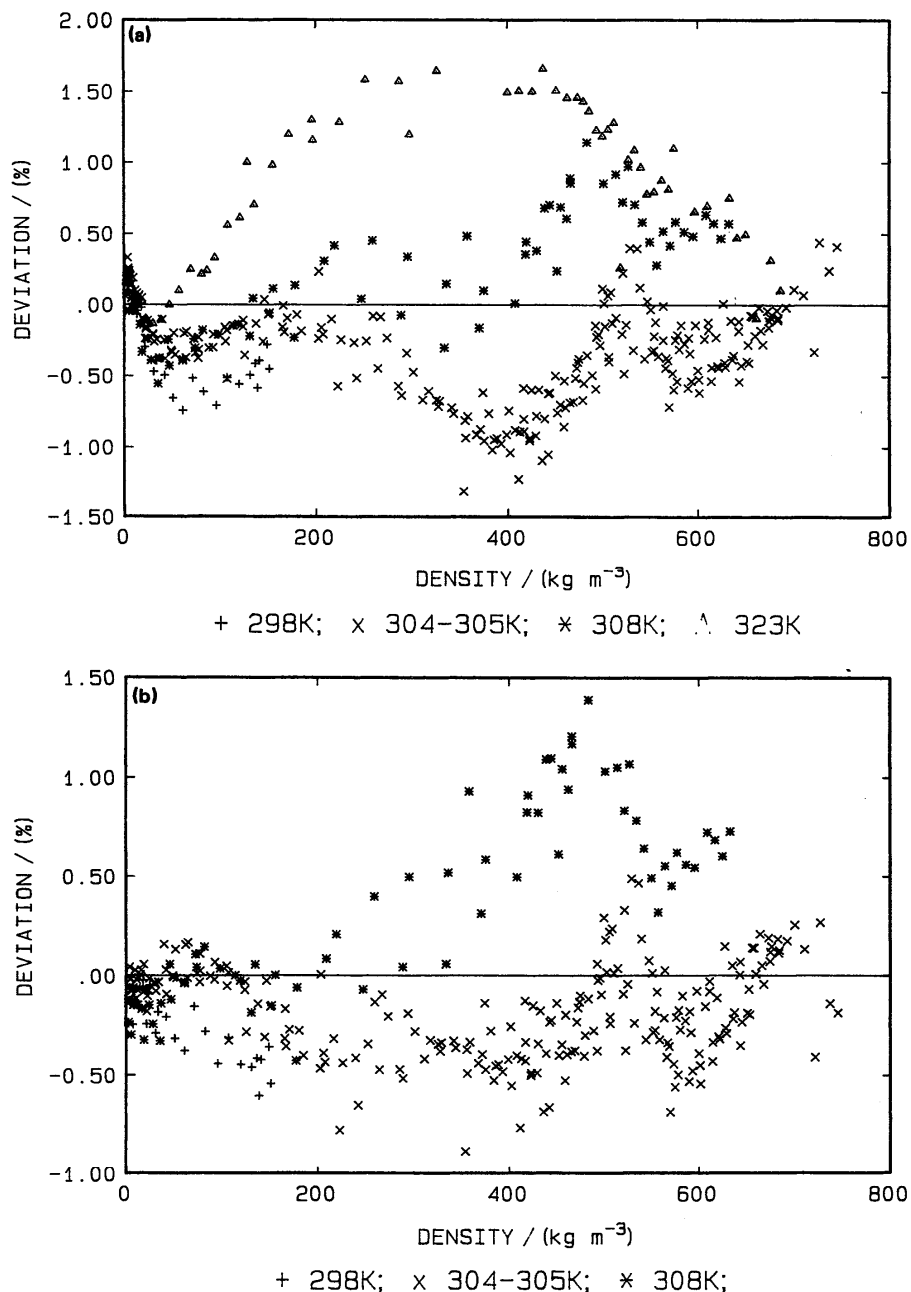
FIG. 31. (a) The deviations of the gas-phase viscosity data of Iwasaki and Takahashi from a fit to all of their background data and that of Kestin *et al.*[20,22,23,27-29,128] (b) Deviations for a fit to data from which the 323 K isotherm of Iwasaki and Takahashi[30] is omitted.

tains at all other temperatures including those only 15 K higher. We prefer to adopt the first alternative and its corollary that it will not prove possible to represent the most accurate data for the total viscosity of carbon dioxide to better than ± 2% near the critical temperature and density.

5.2.c. Final Representation

In view of the discussion above, the best representation of the excess viscosity of carbon dioxide is that derived from a weighted fit to all of the data listed in Table 9, including the

near-critical region data of Iwasaki and Takahashi.[30] The final coefficients e_i are listed in Table 8. A detailed comparison of the final representation with experimental data is given in Sec. 6.

5.2.d. Primary Data for the Liquid Phase

There are four extensive series of measurements of the viscosity of carbon dioxide in the liquid, as can be seen from Appendix II. The measurements of Golubev *et al.*,[139] which were carried out in a capillary viscometer, cover the tem-

perature range 243 K$\leqslant T \leqslant$293 K and the pressure range 5 MPa$\leqslant P \leqslant$50 MPa and have a claimed accuracy of $\pm$ 2%. A second set of measurements by Ulybin and Makarushkin[142-144] with the same type of instrument covers the temperature range 223 K$\leqslant T \leqslant$293 K and the pressure range 6 MPa$< P <$55 MPa, with a claimed accuracy of $\pm$ 1.7%. Diller and Ball[148] and Herreman et al.[137,138] have employed an oscillating quartz-crystal viscometer for measurements over a similar range of conditions and the accuracy claimed for the measurements of Diller and Ball[148] is $\pm$ 2%. Also, Michels et al.[126] have reported data along one isotherm in the liquid phase.

The data of Herreman et al.[137,138] are not useful for our purposes because the instrument and data analysis have been incompletely described and because although both the dynamic viscosity η and the kinematic viscosity η/ρ are quoted, the density itself is not.

In order to illustrate the situation for the remainder of the data, it is useful once more to examine the excess viscosity for the various data sets and this is shown in Fig. 32. The solid line shown in this figure is the temperature-independent excess function deduced from the final analysis of the gas phase data which is included for reference. The data of Golubev et al.[139] for the liquid phase are seen to lie very close

FIG. 32. The excess viscosity of liquid carbon dioxide for the data of Golubev et al.,[139] Ulybin and Makarushkin,[142-144] Diller and Ball[148] and predictions of the high-density gas correlation.

to this excess function and there is, within them, very little evidence of a temperature dependence in the liquid excess viscosity. The results of Ulybin and Makarushkin[142-144] lie significantly above those of Golubev et al. by as much as 14% at low temperatures and reveal a small temperature dependence in the excess. The most recent results of Diller and Ball[148] are even higher than the results of Ulybin and Makarushkin, by as much as 6%, and show a pronounced stratification of various isotherms.

Finally, it is noteworthy that the discrepancy among the various sets of data decreases as the temperature increases. Indeed, at a temperature of 300 K all the data sets[139,144,148] and the results of Michels et al.[126] are in agreement within their mutual uncertainty.

The differences among the various data sets for the viscosity of liquid carbon dioxide are therefore seen to be large. It is not normally desirable to incorporate all of these data into a correlation and, instead, some effort should be devoted to establishing a preferred set of data. The capillary viscometers used by Golubev et al.[139] and Ulybin and Makarushkin[142-144] have been given reasonably complete descriptions in the literature and the technique is capable of high accuracy when employed with a full working equation. Unfortunately, it is not possible to discern from the references whether a complete working equation has been employed. On the other hand, for the quartz-crystal viscometer employed by Diller and Ball,[148] no complete theory is available, the fluid motion takes place at high frequency ($\sim$35 kHz) and the possibility of secondary flow in the fluid cannot be discounted and has not been investigated. However, the instrument used by Diller and Ball has never produced results differing from data of the highest quality for other fluids[151] and its behavior during the measurements of carbon dioxide was in no way exceptional.[152]

However, the measurements performed in the compressed gas region along the isotherm at 320 K by Diller and Ball are, on average, some 4% above the data of Iwasaki et al.[30] and Michels et al.[126] It seems that on the basis of the published experimental work there is no strong evidence on which to form a judgement of a preferred data set.

Theories of transport properties in the liquid phase are still in a rudimentary stage although their semi-empirical extension is often useful.[153] Consequently, it is not possible to make use of such theories as an independent discriminant among the data. A different strategy is therefore necessary to provide such a discriminant. Through the aegis of the Subcommittee on Transport Properties of the International Union of Pure and Applied Chemistry, a new set of measurements of the viscosity of liquid carbon dioxide has been commissioned. Dr. P. S. van der Gulik of the van der Waals laboratory in Amsterdam has agreed to perform these measurements with the purpose of obtaining an accurate set of viscosity data for liquid carbon dioxide over a wide range of temperature. At present, measurements have been completed[9] along just two isotherms at 300 and 303 K and it is unlikely that the results of measurements at lower temperatures will be available for some time. The data along these two isotherms are consistent with all other measurements near room temperature, as is shown in Fig. 33. The figure
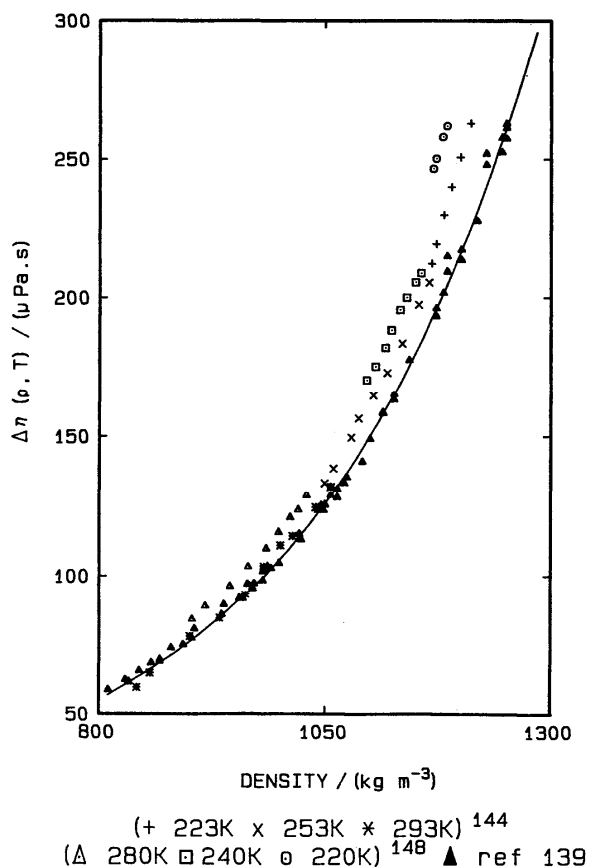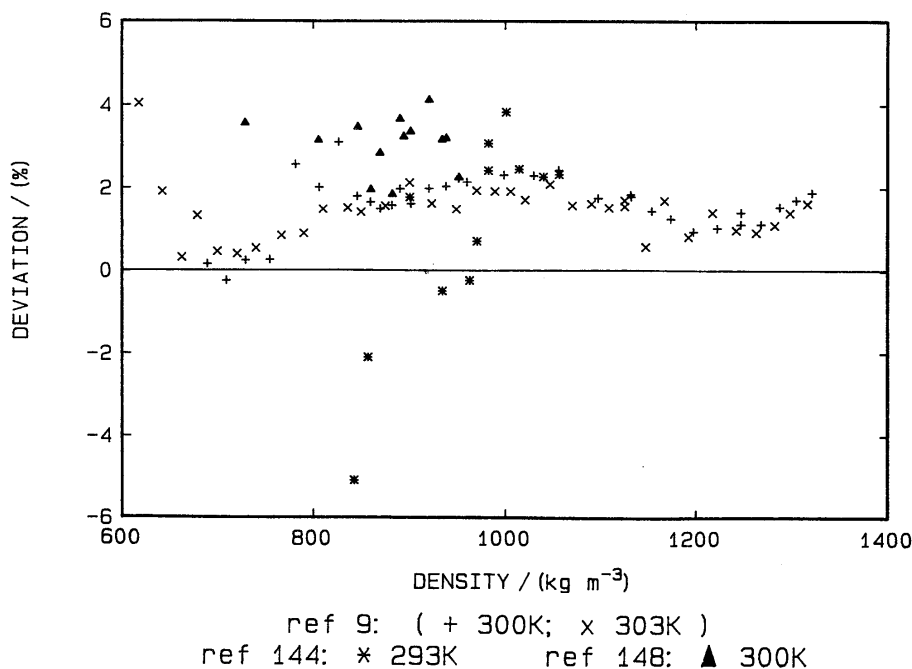
FIG. 33. The deviations of the liquid-phase viscosity data from the high-density gas-phase correlation for isotherms around 300 K.

contains the plot of the deviations of the experimental liquid-phase viscosity data[9,144,148] at around 300 K from the correlation of the gas phase data which provides a convenient reference. There is some evidence that the experimental data of Diller and Ball[148] are more consistent with those of van der Gulik[9] than are those of Ulybin and Makarushkin.[144] However, the evidence is not sufficiently strong that one can reject one set of data in favor of another. Consequently, until further experimental data are available, an objective selection of data is impossible.

In the face of this difficulty, there seems no alternative but to develop a representation of the viscosity for the liquid phase of carbon dioxide which incorporates all the available data in some way. Inevitably, this means that the uncertainty to be attached to the representation must be large, but this is deemed preferable to the complete omission of the liquid-phase viscosity from the representation. It is to be hoped that new experimental information will eventually become available that will permit an improvement in the accuracy with which the liquid-phase viscosity can be represented.

The representation of the liquid-phase viscosity is based upon an equation proposed by Hildebrand[154]:

$$\frac{1}{\eta_r(\rho,T)} = \frac{1}{\eta(\rho,T)} = B(T)[V - V_0(T)], \quad (69)$$

which is an empirical extension of a result derivable from the rigid-sphere theory of transport in liquids.[153] In Eq. (69) V is the volume of the fluid and $V_0(T)$ a weakly temperature-dependent characteristic volume. For many systems,[153–156] Eq. (69) provides a satisfactory representation of the data and both $B(T)$ and $V_0(T)$ are smooth functions of temperature.

For the present purposes we have slightly modified the fluidity Eq. (69) to account for the fact that we include the critical enhancement of the viscosity in our representation and write

$$\frac{1}{\eta_r(\rho,T) - \Delta_c\eta(\rho,T)} = B(T)\left[\frac{1}{\rho} - V_0(T)\right], \quad (70)$$

using the density in preference to the volume for consistency with earlier representations. In the case of every experimental isotherm, the critical enhancement is a very small fraction of the total viscosity in the liquid phase.

Equation (70) has been fitted to each individual isotherm for each of the data sets available for the viscosity of liquid carbon dioxide in order to determine $B(T)$ and $V_0(T)$ and the results for these two quantities are shown in Figs. 34 and 35. It has been found that the data for each individual isotherm can be adequately represented by Eq. (70) but Figs. 34 and 35 serve to emphasize the differences between the viscosity data from various sources at low temperatures. Furthermore, the scatter of both of the parameters $B(T)$ and $V_0(T)$ about a smooth function for even one author is quite large. We have therefore represented $B(T)$ and $V_0(T)$ as a function of temperature by simple linear functions chosen to pass through what are thought to be the most reliable results of van der Gulik[9] but otherwise representing the results of other authors equally. The discrepancies between the data mean that any more sophisticated methods of fitting are inappropriate.

The functions chosen are

$$B = 18.56 + 0.014\ T \quad (71)$$
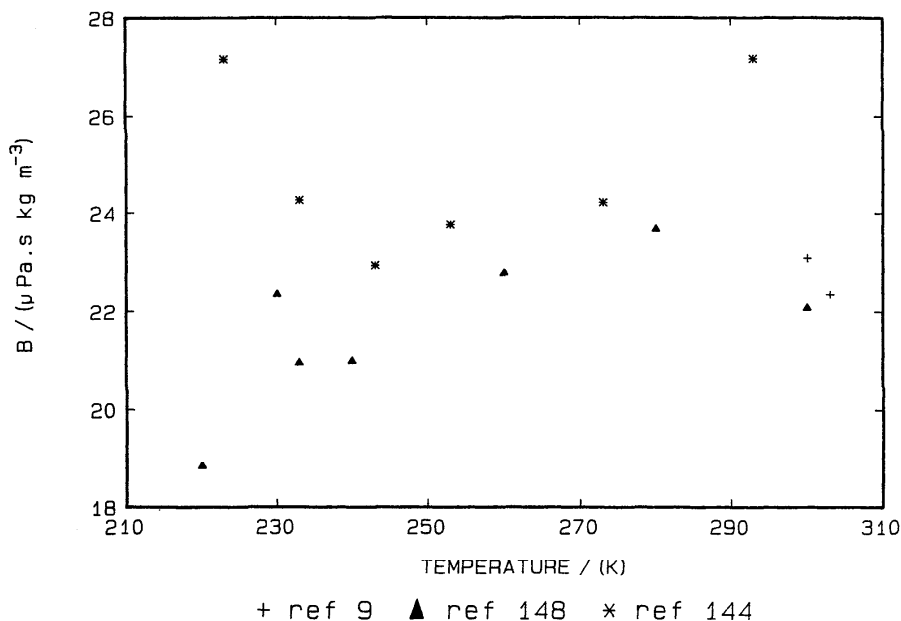
FIG. 34. The coefficient $B(T)$ for the liquid-phase viscosity correlation of Eq. (70) using the data of van der Gulik,[9] Ulybin and Makarushkin,[144] and Diller and Ball.[148]

and

$$V_0(T) = 7.41 \times 10^{-4} - 3.3 \times 10^{-7} T. \qquad (72)$$

Here B has the units of μPa kg m^{-3} and $V_0(T)$ the units of m^3 kg^{-1} with T in degrees kelvin.

Figure 36 contains a composite plot of the deviations of the results of van der Gulik,[9] Ulybin and Makarushkin[144] and Diller and Ball[148] from the representation given by Eqs. (70)–(72) without distinguishing temperatures. More detailed deviation plots are contained in Figs. A3.8 and A3.9. These plots show that the representation reproduces almost
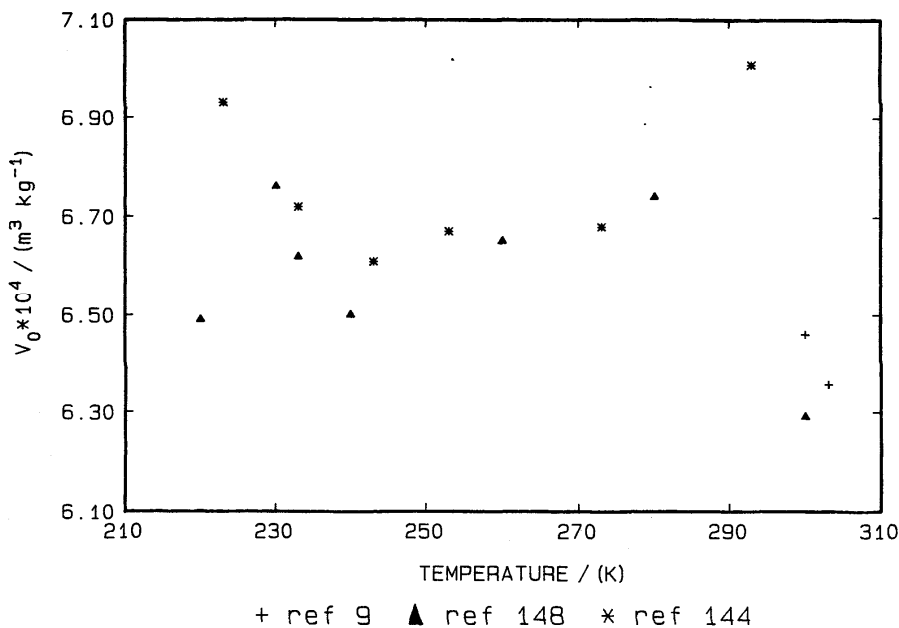
FIG. 35. The characteristic molar volume $V_0(T)$ for the liquid-phase viscosity correlation of Eq. (70).

FIG. 36. The deviations of the liquid-phase viscosity data of van der Gulik,[9] Ulybin and Makarushkin,[144] and Diller and Ball[148] from the liquid-phase correlation.

all of the available experimental data within $\pm$ 7%, which is commensurate with the discrepancies between the various sources of information. From Figs. 36 and A3.8 and A3.9, there is some evidence that the linearity of the fluidity with volume may not be preserved over the widest density range near to the critical temperature, because the data of van der Gulik[9] show a systematic curvature. However, the bulk of the experimental data do not warrant any further refinement and the representation of the data embodied in Eqs. (70)–(72) is deemed satisfactory.

5.2.e. The Blending Function

It is appropriate to represent the liquid-phase data by an equation separate from that for the gas phase and to join the two by means of a blending function.[150] This choice permits a rather more straigthforward improvement of the correlation when improved information becomes available.

Anticipating the future availability of this information, a suitable blending function for the excess viscosity is of the form

$$\Delta\eta = \frac{\Delta\eta_g}{1 + \exp[-Z(T-T_s)]} + \frac{\Delta\eta_g}{\{1 + \exp[Z(T-T_s)]\}[1 + \exp[Z(\rho-\rho_s)]]}$$

$$+ \frac{\eta_\ell - \eta^0}{\{1 + \exp[Z(T-T_s)]\}\{1 + \exp[-Z(\rho-\rho_s)]\}}. \tag{73}$$

It incorporates a switch between the excess gas-phase viscosity $\Delta\eta_g$ and the liquid viscosity η_ℓ. The switching is performed at both the switching temperature T_s and switching density ρ_s. By ensuring that T_s is a few degrees below the critical temperature T_c one can associate ρ_s with ρ_c and avoid any discontinuities when switching in density, since ρ_s would be in the two-phase region. A proper choice of an arbitrary parameter Z ensures a smooth change of viscosity at T_s and also recovers both the gas and liquid experimental viscosities within their uncertainty. In the present representation

$$\rho_s = 467.689 \text{ kg m}^{-3}, \quad T_s = 302 \text{ K} \tag{74}$$

and $Z = 1.0$.

6. The Overall Correlation

6.1 Thermal Conductivity

The final correlation for the thermal conductivity is written as

$$\lambda(\rho,T) = \lambda^0(T) + \Delta\lambda(\rho) + \Delta_c\lambda(\rho,T), \tag{75}$$

in which $\lambda^0(T)$ is given by Eq. (29) with the coefficients of Table 1, $\Delta\lambda(\rho)$ is given by Eq. (63) with the coefficients of Table 8 and $\Delta_c\lambda(\rho,T)$ is given by Eq. (38) with the coefficients of Table 5.

Figure 37(a) shows the behavior of the thermal conductivity of carbon dioxide along isobars over the range of thermodynamic states covered by the correlation. Figure
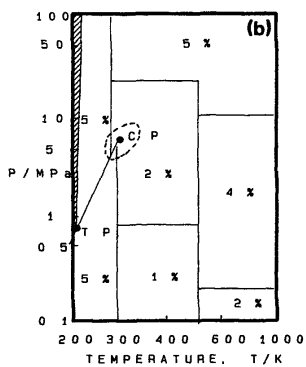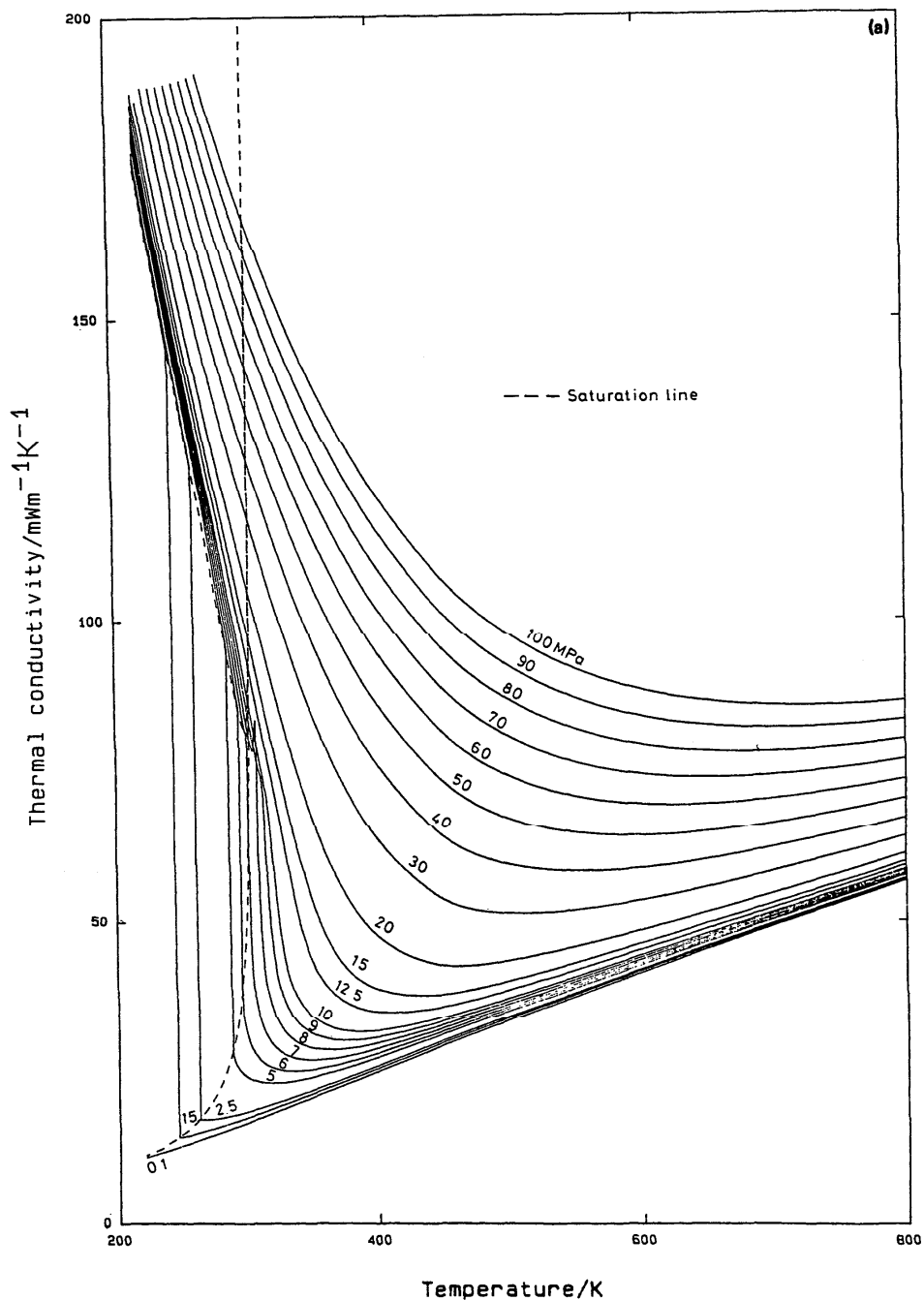
FIG. 37. (a) The thermal conductivity of carbon dioxide along isobars. (b) The extent of the thermal conductivity correlation and its estimated uncertainty. Temperature scale is in arbitrary units. No correlation available in the hatched region.
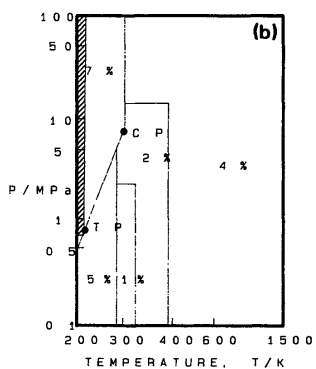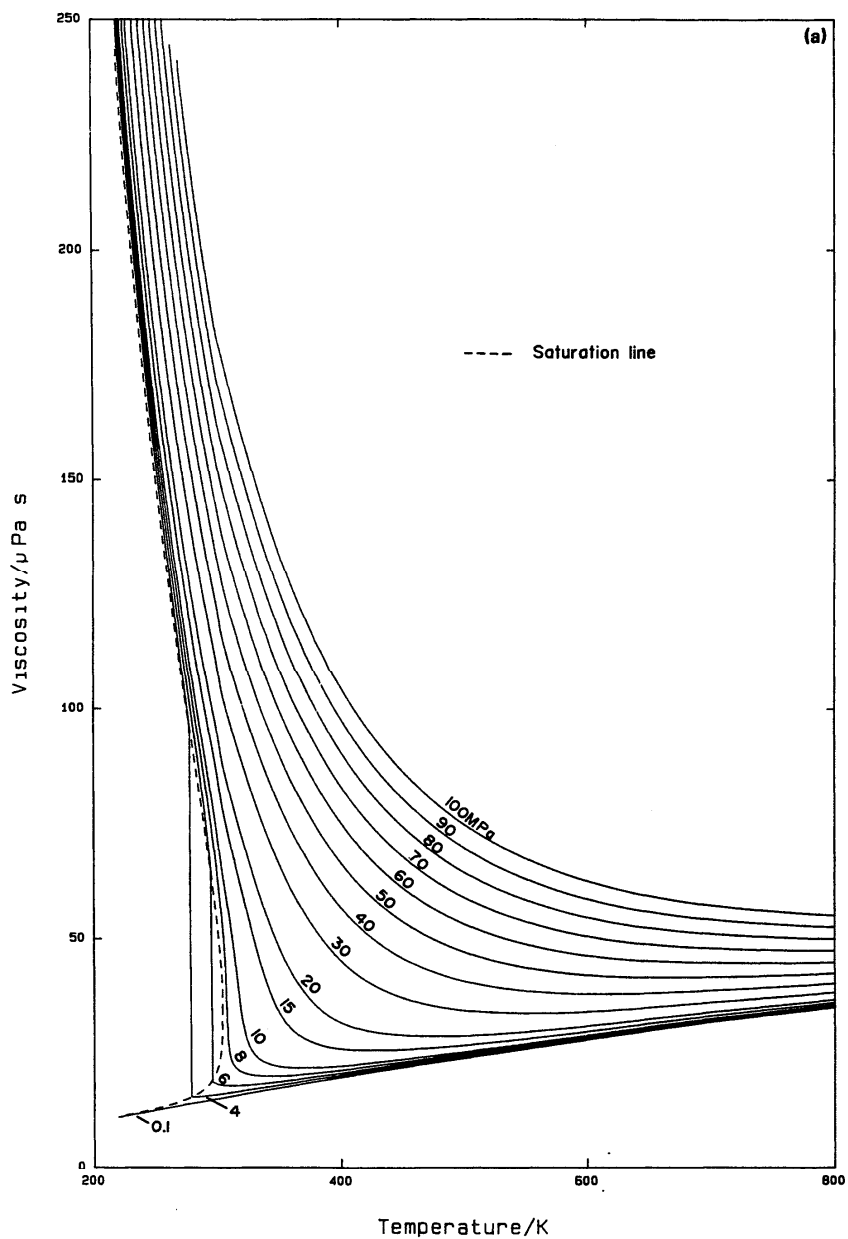
FIG. 38. (a) The viscosity of carbon dioxide along isobars. (b) The extent of the viscosity correlation and its estimated accuracy. Temperature scale is in arbitrary units. No correlation is available in the hatched region.

37(b) illustrates the range of applicability of the representation as well as the estimated uncertainty in various ranges of thermodynamic states. For the thermal conductivity the limits of the representation are 200 $K \leqslant T \leqslant 1000$ K; $\rho \leqslant 1200$ kg m^{-3}. The uncertainty estimates have largely been based on the errors in the experimental data in the various ranges except when the data have had to be predicted when the estimate is based on the arguments presented earlier.

Appendix III contains representative deviation plots of experimental data from the final thermal-conductivity correlation. In these plots we have not included every set of data but those which formed the primary data set and a selection of the secondary data. Figure A3.1 contains the deviations of the gas-phase data of Millat et al.,[12] Scott et al.,[90,91] Clifford et al.,[89] and Snel et al.[88] from the final correlation. The deviations are typically no more than $\pm$ 2.0% over most of the density range. Figure A3.2 contains a similar plot for the data of Le Neindre et al.[60,70,77,78] Here the deviations amount

to as much as 6%, a figure that arises principally from the zero-density value.

Figure A3.3 shows the deviations of the experimental data of Tarzimanov et al.[87] from the final correlation of the gas-phase thermal conductivity. These data were not included in the development of the representation but cover a wide range of conditions, and the deviations are seen to be less than $\pm$ 6% in all cases, and of the order of 3% within the range of the correlation.

Figure A3.4 contains the deviations of all the liquid-phase thermal conductivity data of carbon dioxide, including those along the saturation line,[63] from the final correlation, which in this case represents an extrapolation. None of the experimental data were used in constructing the final equation but the deviations do not exceed $\pm$ 5%. This establishes some confidence for the further extrapolation of the representative equation beyond the range of the experimental data.

6.2 Viscosity

The final correlation for the viscosity is written as

$$\eta = \eta^0(T) + \frac{\Delta\eta_g}{1 + \exp[-Z(T-T_s)]} + \frac{\Delta\eta_g}{\{1 + \exp[Z(T-T_s)]\}\{1 + \exp[Z(\rho-\rho_s)]\}}$$
$$+ \frac{\eta_\ell - \eta^0}{\{1 + \exp[Z(T-T_s)]\}\{1 + \exp[-Z(\rho-\rho_s)]\}} + \Delta_c\eta(\rho,T), \tag{76}$$

where $\eta^0(T)$ is given by Eq. (3) with the coefficients of Table 1, $\Delta\eta_g(\rho)$ is the excess viscosity for the gas phase given by Eq. (67) with the coefficients of Table 8, η_ℓ is the liquid phase viscosity given by Eqs. (70)–(72), and $\Delta_c\eta(\rho,T)$ is the critical enhancement of the viscosity, given by Eq. (38) with the coefficients of Table 5.

Figure 38(a) illustrates the behavior of the viscosity of carbon dioxide along isobars over the range of thermodynamic states covered by the correlation. Figure 38(b) illustrates the range of applicability, together with the estimated uncertainty in various regions. Once again these estimates have been based on errors in the experimental data. The representation may be employed in the ranges 200 $K \leqslant T \leqslant 1500$ K, $\rho \leqslant 1200$ kg m^{-3}.

The plots containing the deviations of the selection of experimental data from the final correlation are contained in Appendix III. Figure A3.5 shows the deviations of the data of Iwasaki and Takahashi[30] from the final correlation. For the reasons discussed earlier, the deviations amount to as much as 2% in certain density regions. Figure A3.6 contains the deviations of the data of Haepp,[131] Kestin and his collaborators[20,22,23,27–29,128] from the final correlation, whereas Fig. A3.7 contains those for the data of Golubev et al.[136,140,141] and Michels et al.[126] for the gas phase.

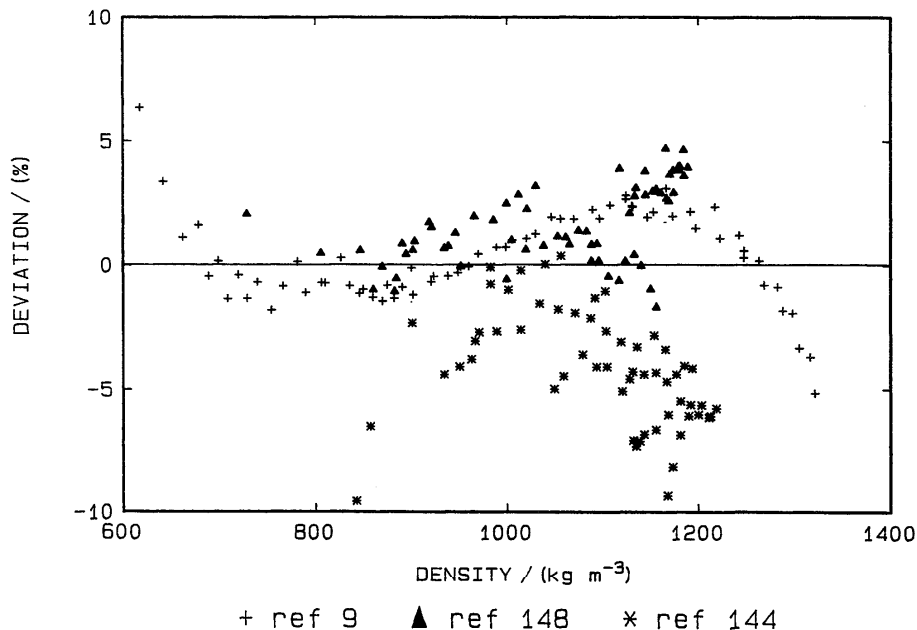Finally, Figs. A3.8 and A3.9 show the deviations of the liquid-phase viscosity data of van der Gulik,[9] Ulybin and Makarushkin[144] and Diller and Ball[148] from the final correlation.

7. Tabulations

We present, in Appendix IV, tabulations of the viscosity and thermal conductivity of carbon dioxide over the entire range of the correlation, including the saturation line. These tabulations have been generated directly from the correlation as functions of pressure and temperature using the equation of state.[95,112] The intervals in the tables are relatively large, but in the region of the critical point they are smaller in order to accommodate the more rapid change of the properties in this region. In order to assist those programming the representative equations with the checking of their coding we include a small table at the end of Appendix IV giving both viscosity and thermal conductivity as a function of temperature and density.

8. Conclusions

It is believed that the final representations of the viscosity and thermal conductivity of carbon dioxide developed in this work are the best that can be produced from the available data. However, it should be remembered that in the case of the zero-density thermal conductivity at high temperatures and the liquid-phase thermal conductivity, the experimental data available were not used either because of their demonstrably poor quality, or because of their small extent. Furthermore, in the liquid phase the viscosity data available differed significantly among themselves. Given the amount of research effort devoted to the measurement of these prop-

erties it is rather discouraging to have to report this situation. It would now seem that from both the theoretical and experimental points of view, our knowledge of the transport properties of fluids is best in the critical region where they are singular. It is to be hoped that the analysis described here will encourage new measurements to place the representation over the whole range of thermodynamic states on a more secure base. For many engineering purposes the present formulation will prove adequate but from a scientific point of view, there is considerable scope for improvement.

9. Acknowledgments

10. References

[1] *Chemical Engineering at Supercritical Fluid Conditions*, edited by M. F. Paulitis, J. M. L. Penninger, R. D. Gray, Jr., and P. Davidson (Ann Arbor Science, Michigan, 1983).

[2] *Nuclear Power Technology*, edited by W. Marshall (Clarendon Press, Oxford, 1983), Vol. 1.

[3] P. C. Albright, Z. Y. Chen, and J. V. Sengers, Phys. Rev. B **36**, 877 (1987).

[4] G. A. Olchowy and J. V. Sengers, Phys. Rev. Lett. **61**, 15 (1988).

[5] V. V. Altunin and M. A. Sakhabetdinov, Thermal Eng. **19**(8), 124 (1972).

[6] J. T. R. Watson, *The Dynamic Viscosity of Carbon Dioxide Gas and Liquid* (Engineering Sciences Data Unit, No. 76021, Technical Editing and Reproduction Ltd., London, 1976).

[7] J. T. R. Watson, *Thermal Conductivity of Carbon Dioxide Gas and Liquid* (Engineering Sciences Data Unit, No. 76030, Technical Editing and Reproduction Ltd., London, 1976).

[8] S. A. Ulybin and S. S. Bakulin, Thermal Eng. **24**(1), 68 (1978).

[9] P. S. van der Gulik *et al.* (to be published).

[10] W. A. Cole and W. A. Wakeham, J. Phys. Chem. Ref. Data **14**, 209 (1985).

[11] R. D. Trengove and W. A. Wakeham, J. Phys. Chem. Ref. Data **16**, 175 (1987).

[12] J. Millat, M. Mustafa, M. Ross, W. A. Wakeham, and M. Zalaf, Physica **145A**, 461 (1987).

[13] J. Millat, V. Vesovic, and W. A. Wakeham, Physica **148A**, 153 (1988).

[14] E. J. Harris, C. G. Hope, D. W. Gough, and E. B. Smith, J. Chem. Soc. Faraday Trans. I **75**, 892 (1979).

[15] G. C. Maitland and E. B. Smith, J. Chim. Phys. **67**, 631 (1970).

[16] B. J. Bailey, J. Phys. D **3**, 550 (1970).

[17] J. Kestin, S. T. Ro, and W. A. Wakeham, J. Chem. Phys. **56**, 4114 (1972).

[18] J. Kestin, H. E. Khalifa, and W. A. Wakeham, J. Chem. Phys. **67**, 4254 (1977).

[19] J. Kestin, H. E. Khalifa, S. T. Ro, and W. A. Wakeham, Physica **88A**, 242 (1977).

[20] J. Kestin, O. Korfali, and J. V. Sengers, Physica **100A**, 335 (1980).

[21] R. DiPippo and J. Kestin, Natl. Sci. Found. Res. Grant No. GK 1305 (1967).

[22] J. Kestin and W. Leidenfrost, Physica **25**, 1033 (1959).

[23] J. D. Breetveld, R. DiPippo, and J. Kestin, J. Chem. Phys. **45**, 124 (1966).

[24] J. Kestin, S. T. Ro, and W. A. Wakeham, Trans. Faraday Soc. **67**, 2308 (1971).

[25] J. Kestin, H. E. Khalifa, and W. A. Wakeham, J. Chem. Phys. **65**, 5186 (1976).

[26] Y. Abe, J. Kestin, H. E. Khalifa, and W. A. Wakeham, Ber. Bunsenges. Phys. Chem. **83**, 271 (1979).

[27] R. DiPippo, J. Kestin, and K. Oguchi, J. Chem. Phys. **46**, 4758 (1967).

[28] J. Kestin, Y. Kobayashi, and R. T. Wood, Physica **32**, 1065 (1966).

[29] J. Kestin and J. Yata, J. Chem. Phys. **49**, 4780 (1968).

[30] H. Iwasaki and M. Takahashi, J. Chem. Phys. **74**, 1930 (1981).

[31] E. Vogel and L. Barkow, Z. Phys. Chem. Leipzig **267**, 5 (1986).

[32] E. Vogel, Ber. Bunsenges. Phys. Chem. **83**, 997 (1984).

[33] M. Trautz, A. Zündel, Ann. Phys. **17**(41), 23 (1933).

[34] B. G. Dickins, Proc. Roy. Soc. Lond. **A143**, 517 (1934).

[35] W. G. Kannuluik and L. H. Martin, Proc. Roy. Soc. Lond. **A144**, 496 (1934).

[36] W. Sellschopp, Forsch. Gebiete des Ingenieurwesens **5**, 162 (1934).

[37] G. G. Sherratt and E. Griffiths, Phil. Mag. **27**, 68 (1939).

[38] A. Eucken, Forsch. Gebiete Ingenieurwesens **11**, 6 (1940).

[39] B. Koch and W. Fritz, Wärme und Kältetechnik **42**, 13 (1940).

[40] H. L. Johnston and E. R. Grilly, J. Chem. Phys. **14**, 233 (1946).

[41] N. B. Vargaftik and O. N. Oleshchuk, Izvest. Vses. Teplotekhn. Inst. **5**(6), 7 (1946).

[42] W. G. Kannuluik and P. G. Law, Proc. Roy. Soc. Victoria **58**, 142 (1947).

[43] E. Borovik, Zh. Eksp. Teor. Fiz. **19**(7), 561 (1949).

[44] F. G. Keyes, Office of Naval Research, Contract 78, Project Design No. NR-058-037, MIT, USA (1949).

[45] W. G. Kannuluik and H. B. Donald, Aust. J. Sci. Res. **3**, 417 (1950).

[46] E. A. Stolyarov, V. V. Ipatev, and V. N. Teodorovich, Zhur. Fiz. Khim. **24**, 166 (1950).

[47] J. M. Lenoir and E. W. Comings, Chem. Eng. Prog. **47**, 223 (1951).

[48] E. U. Franck, Z. für Elektrochemie **55**, 636 (1951).

[49] F. G. Keyes, Trans. ASME **73**, 597 (1951).

[50] F. G. Keyes, Trans. ASME **74**, 1303 (1952).

[51] J. M. Davidson and J. F. Music, U. S. Atomic Energy Comm. Rep. HW29021 (1953).

[52] A. J. Rothman, U. S. AEC UCRL-2339 (1954).

[53] F. G. Keyes, Trans. ASME **76**, 809 (1954).

[54] L. B. Thomas and R. C. Golike, J. Chem. Phys. **22**, 300 (1954).

[55] A. J. Rothman and L. A. Bromley, Ind. & Eng. Chem. **47**, 899 (1955).

[56] M. Salceanu and S. Bojin, Comp. Rend. **243**, 237 (1956).

[57] L. A. Guildner, Proc. Nat. Acad. Sci. **44**, 1149 (1958).

[58] R. G. Vines, Trans. ASME J. Heat Trans. **82**, 48 (1960).

[59] H. Geier and K. Schäfer, Allg. Wärmetechnik **10**, 70 (1961).

[60] L. A. Guildner, J. Res. Nat. Bureau of Standards, A Physics & Chem. **66A**, 341 (1962).

[61] A. Michels, J. V. Sengers, and P. S. van der Gulik, Physica **28**, 1216 (1962).

[62] A. A. Westenberg and N. de Haas, Phys. Fluids **5**, 266 (1962).

[63] K. I. Amirkhanov and A. P. Adamov, Teploenergetika **10**(7), 77 (1963).

[64] P. Mukhopadhyay, A. Gupta, and A. K. Barua, Brit. J. Appl. Phys. **18**, 1301 (1967).

[65] A. K. Barua, A. Manna, and P. Mukhopadhyay, J. Phys. Soc. Jpn. **25**, 862 (1968).

[66] B. Le Neindre, P. Bury, R. Tufeu, P. Johannin, and B. Vodar, in *7th Conference on Thermal Conductivity*, edited by D. R. Flynn and B. A. Peavy, NBS Special Publ. 302 (U.S. Gov't., Washington, DC, 1968), p. 579.

[67] R. L. Christensen, PhD Thesis, University of Oregon, Department of Chemistry (1968).

[68] W. van Dael and H. Cauwenbergh, Physica **40**, 165 (1968).

[69] M. P. Vukalovich and V. A. Altunin, *Thermophysical Properties of CO₂*

(Collets, London and Wellingborough, 1968), p. 433.

[70]B. Le Neindre, P. Bury, R. Tufeu, P. Johannin, and B. Vodar, *9th Conference on Thermal Conductivity,* edited by H. R. Shanks (U. S. Atomic Energy Commission, 1969), p. 69.

[71]J. W. Haarman, PhD Thesis, University of Delft (1969) & API Conf. Proc. **11**, 193 (1973).

[72]B. M. Rosenbaum and G. Thodos, J. Chem. Phys. **51**, 1361 (1969).

[73]G. P. Gupta and S. C. Saxena, Mol. Phys. **19**, 871 (1970).

[74]M. L. R. Murthy and H. A. Simon, Phys. Rev. A **2**, 1458 (1970).

[75]A. A. Tarzimanov, Trans. Kazan. Ch. Tech. Inst. **45**, 235 (1970).

[76]M. L. R. Murthy and H. A. Simon, *Proceedings of the 5th Symposium on Thermophysical Properties,* edited by C. F. Bonilla (American Society of Mechanical Engineers, New York, 1970), p. 214.

[77]B. Le Neindre, Int. J. Heat Mass Trans. **15**, 1 (1972).

[78]B. Le Neindre, R. Tufeu, P. Bury, and J. V. Sengers, Ber. Bunsenges. Phys. Chem. **77**, 262 (1973).

[79]M. L. Murthy, PhD Thesis, University of Illinois (1973).

[80]R. V. Paul, PhD Thesis, University of Calgary (1973).

[81]R. S. Salmanov and A. A. Tarzimanov, Trans. Kazan. Ch. Tech. Inst. **51**, 167 (1973).

[82]S. H. P. Chen, P. C. Jain, and S. C. Saxena, J. Phys. B **8**, 1962 (1975).

[83]A. G. Shashkov and F. P. Kamchatov, Vesti Ak. Nauka Belorusia **3**, 61 (1973).

[84]S. S. Bakulin, S. A. Ulybin, and E. P. Zherdev, Tr. Mosk. Energ. **234**, 96 (1975).

[85]S. S. Bakulin, S. A. Ulybin, and E. P. Zherdev, High Temp. **14**, 351 (1976).

[86]H. Becker and U. Grigull, Wärme—und Stoffübertragung **11**, 9 (1978).

[87]A. A. Tarzimanov and V. A. Arslanov, Teploni Mass. v Khim. Tekhnol. **6**, 13 (1978).

[88]J. A. A. Snel, N. J. Trappeniers, and A. Botzen, Proc. Koninlijke Nederlands e Akad. van Wetenschappen, Series B **82**, 303 (1979).

[89]A. A. Clifford, J. Kestin, and W. A. Wakeham, Physica **97A**, 287 (1979).

[90]A. C. Scott, A. I. Johns, J. T. R. Watson, and A. A. Clifford, J. Chem. Soc. Faraday Trans. I **79**, 733 (1983).

[91]A. I. Johns, S. Rashid, J. T. R. Watson, and A. A. Clifford, J. Chem. Soc. Faraday Trans. I **82**, 2235 (1986).

[92]J. Kestin and W. A. Wakeham, *Transport Properties of Fluids (Experimental Theory and Prediction)* (CINDAS, Hemisphere, 1988).

[93]C. S. Wang Chang, G. E. Uhlenbeck, and J. de Boer, *Studies in Statistical Mechanics,* edited by J. de Boer and G. E. Uhlenbeck (North-Holland, Amsterdam, 1964), Vol. 2, Part C.

[94]L. A. Viehland, E. A. Mason, and S. I. Sandler, J. Chem. Phys. **68**, 5277 (1978).

[95a]J. F. Ely, J. W. Magee, and W. M. Haynes, *Thermophysical Properties of Carbon Dioxide from 217 K to 1000 K with Pressures to 3000 bar.* (NIST Monograph, 1990).

[95b]J. F. Ely, J. W. Magee, and W. M. Haynes, *Thermophysical Properties for Special High CO_2 Content Mixtures,*—Research Report No. RR-110 (Gas Processors Association, Tulsa, OK, 1987).

[96]K. M. Merrill and R. C. Amme, J. Chem. Phys. **51**, 844 (1969).

[97]A. Eucken and R. Becker, Z. Phys. Chemie B **27**, 235 (1934); A. Eucken and E. Nümann, Z. Phys. Chemie B **36**, 163 (1937).

[98]L. Küchler, Z. Phys. Chemie B **41**, 192 (1938).

[99]J. Millat, A. Plantikow, D. Mathes, and H. Nimz, Z. Phys. Chemie (Leipzig) **269**, 865 (1988).

[100]C. A. Brau and M. Jonkman, J. Chem. Phys. **52**, 291 (1970).

[101]J. P. J. Heemskerk, F. G. van Kuik, H. F. P. Knaap, and J. J. M. Beenakker, Physica **71**, 484 (1974); B. Thijsse, PhD Thesis, University of Leiden, The Netherlands (1978).

[102]G. C. Maitland, M. R. Rigby, E. B. Smith, and W. A. Wakeham, *Intermolecular Forces* (Clarendon Press, Oxford, 1981).

[103]G. C. Maitland, M. Mustafa, W. A. Wakeham, and F. R. W. McCourt, Mol. Phys. **61**, 359 (1987).

[104]H. Moraal and R. F. Snider, Chem. Phys. Lett. **9**, 401 (1971).

[105]F. R. McCourt and H. Moraal, Phys. Rev. A **5**, 2000 (1972).

[106]B. J. Thijsse, G. W. 't. Hooft, D. A. Coombe, H. F. P. Knaap, and J. J. M. Beenakker, Physica **98A**, 307 (1979).

[107]K. M. de Reuck and B. Armstrong, Cryogenics, September, 505 (1979).

[108]J. V. Sengers, Int. J. Thermophys. **6**, 203 (1985).

[109]P. C. Hohenberg and B. I. Halperin, Rev. Mod. Phys. **49**, 435 (1977).

[110]G. A. Olchowy and J. V. Sengers, *Representative Equations for the*

Transport Properties of Carbon Dioxide in the Critical Region, Technical Report No. BN 1052 (Institute for Physical Science and Technology, University of Maryland, 1986).

[111]K. Kawasaki, in *Phase Transitions and Critical Phenomena,* edited by C. Domb and M. S. Green (Academic, New York, 1976), p. 165.

[112]P. C. Albright, T. J. Edwards, Z. Y. Chen, and J. V. Sengers, J. Chem. Phys. **87**, 1717 (1987).

[113]J. V. Sengers and J. M. H. Levelt Sengers, in *Progress in Liquid Physics,* edited by C. A. Croxton (Wiley, New York, 1978), p. 103.

[114]A. Michels, J. V. Sengers, and P. S. van der Gulik, Physica **28**, 1201 (1962).

[115]A. Michels and J. V. Sengers, Physica **28**, 1238 (1962).

[116]J. V. Sengers and A. Michels, in *Proceedings 2nd Symposium on Thermophysical Properties,* edited by J. F. Masi and D. H. Tsai (American Society of Mechanical Engineers, New York, 1962), p. 434.

[117]H. Becker and U. Grigull, Optik **35**, 223 (1972).

[118]H. Becker and U. Grigull, Maschinenmarkt **81**, 50 (1975).

[119]H. L. Swinney and D. L. Henry, Phys. Rev. A **8**, 2586 (1973).

[120]B. S. Maccabee and J. A. White, Phys. Lett. **35A**, 187 (1971).

[121]Y. Garrabos, R. Tufeu, B. Le Neindre, G. Zalczer, and D. Beysens, J. Chem. Phys. **72**, 4637 (1980).

[122]E. Reile, P. Jany, and J. Straub, Wärme—und Stoffübertragung **18**, 99 (1984).

[123]R. S. Basu and J. V. Sengers, in *Thermal Conductivity 16,* edited by D. C. Larsen (Plenum, New York, 1983), p. 591.

[124]J. V. Sengers, Ber. Bunsenges. Phys. Chemie **76**, 234 (1972).

[125]J. V. Sengers, in *Critical Phenomena,* edited by M. S. Green and J. V. Sengers, National Bureau of Standards Miscellaneous Publication 273 (U. S. Government Printing Office, Washington DC, 1966), p. 165.

[126]A. Michels, A. Botzen, and W. Schuurman, Physica **23**, 95 (1957).

[127]H. R. van den Berg (private communication).

[128]J. Kestin, J. H. Whitelaw, and T. F. Zien, Physica **30**, 161 (1964).

[129]L. Bruschi and G. Torzo, Phys. Lett. A **98**, 265 (1983).

[130]L. Bruschi, M. Santini, and G. Torzo, J. Phys. E **17**, 312 (1984).

[131]H. J. Haepp, Wärme—und Stoffübertragung **9**, 281 (1976).

[132]J. V. Sengers and J. T. R. Watson, J. Phys. Chem. Ref. Data **15**, 1291 (1986).

[133]G. A. Olchowy and J. V. Sengers, Int. J. Thermophys. **10**, 417 (1989).

[134]E. W. Comings and R. S. Egly, Ind. and Eng. Chem. **33**, 1224 (1941).

[135]J. Kestin and J. H. Whitelaw, Physica **29**, 355 (1963).

[136]I. F. Golubev, *Viscosity of Gases and Gas Mixtures* (Israel Programme for Scientific Translation, Jerusalem, 1970), p. 80.

[137]W. Herreman, W. Grevendonk, and A. De Bock, J. Chem. Phys. **53**, 185 (1970).

[138]W. Herreman, A. Lattenist, W. Grevendonk, and A. De Bock, Physica **52**, 489 (1971).

[139]I. F. Golubev and R. I. Shepeleva, Kimiya i teknologiya organicheska sinteza, ONTI, GIAP, part 8, 44–47 (1971).

[140]I. F. Golubev, N. E. Gnezdilov, and G. V. Brodskoya, Kimiya i teknologiya organicheska sinteza, ONTI, GIAP, part 8, 48–53 (1971).

[141]V. I. Kurin and I. F. Golubev, Thermal Engineering **21**(11), 125 (1974).

[142]W. I. Makarushkin and S. A. Ulybin, Tr. Mosk. Energ. In.-Ta **234**, 83 (1975).

[143]S. A. Ulybin and W. I. Makarushkin, Proc. 7th Symposium on Thermophysical Properties, edited by A. Cezairliyan (American Society of Mechanical Engineers, New York, 1977), p. 678.

[144]S. A. Ulybin and W. I. Makarushkin, Thermal Engineering **23**(6), 65 (1976).

[145]D. L. Timrot and S. A. Traktueva, Thermal Engineering **22**, 81 (1975).

[146]L. Bruschi and M. Santini, Physics Lett. A **73**, 395 (1979).

[147]L. Bruschi, Il Nuovo Cim. **1D**, 361 (1982).

[148]D. E. Diller and M. J. Ball, Int. J. Thermophys. **6**, 619 (1985).

[149]J. Kestin (private communication).

[150]J. C. Nieuwoudt, B. Le Neindre, R. Tufeu, and J. V. Sengers, J. Chem. Eng. Data **32**, 1 (1987).

[151]D. E. Diller and L. J. Van Poolen, Int. J. Thermophys. **6**, 43 (1985).

[152]D. E. Diller (private communication).

[153]J. H. Dymond, Chem. Soc. Rev. **43**, 317 (1985).

[154]J. H. Hildebrand, *Viscosity and Diffusivity* (Wiley, New York, 1977).

[155]J. H. Dymond, R. J. Young, and J. D. Isdale, Int. J. Thermophys. **1**, 345 (1980).

[156]J. H. Dymond, J. Robertson, and J. D. Isdale, Int. J. Thermophys. **2**, 223 (1981).

APPENDIX I: List of All Available Data from Measurements of the Thermal Conductivity of Carbon Dioxide

Methods	Code
CC-concentric cylinder	C-predominantly critical region data
I-interferometry	D-λ as a function of density
SSHW-steady-state hot wire	L-data available in liquid region
THW-transient hot wire	ZD-zero-density data
PP-parallel plate	

Ref. no.	Method	T/K range	P/MPA range	Code
33	SSHW	273	⋯	ZD
34	SSHW	285	⋯	ZD
35	SSHW	275	⋯	ZD
36	CC	284–323	5–9	ZD,D,L
37	SSHW	339–565	⋯	ZD
38	SSHW	200–600	⋯	ZD
39	SSHW	283–313	⋯	ZD
40	SSHW	186–380	⋯	ZD
41	SSHW	325–881	⋯	ZD
42	SSHW	200–373	⋯	ZD
43	Results of Ref. 36 corrected for convection	283–313	5–9	D,L
44	CC	300	⋯	ZD
45	CC	273	⋯	ZD
46	SSHW	280–473	0–20	ZD,D
47	CC	314–340	0–20	ZD,D
48	SSHW	197–600	⋯	ZD
49	CC	273–423	0–6	ZD,D
50	CC	273–623	⋯	ZD
51	CC	273	⋯	ZD
52	CC	376–774	⋯	ZD
53	CC	210–273	⋯	ZD
54	SSHW	313–337	⋯	ZD
55	CC	273–800	⋯	ZD
56	SSHW	303	⋯	ZD
57	CC	303–358	3–30	D
58	CC	540–1130	⋯	ZD
59	CC	273–1400	⋯	ZD
60	CC	276–348	0.2–30	D.L
61	PP	298–348	1–200	C
62	SSHW	300–1100	⋯	ZD
63	PP,CC	298–304	sat. line	D,L
64	SSHW	258–473	⋯	ZD
65	SSHW	273–473	⋯	ZD
66	CC	295–308	0–100	ZD,D,L
67	SSHW	308–378	⋯	ZD
68	SSHW	297	⋯	ZD
69	SSHW	230–307	0–20	ZD,D,L
70	CC	298–961	0–100	ZD,D,L
71	SSHW	323–468	⋯	ZD
72	CC	335–434	0–70	ZD,D
73	SSHW	373–1350	⋯	ZD
74	PP	302–308	0–8	ZD,D,C
75	SSHW	298–578	0–7	ZD,D,L
76	PP	305–309	7–8	C
77	CC	298–950	0–100	ZD,D,L
78	CC	298–950	0–100	ZD,D,L,C
79	PP	303–305	0–8	ZD,D,C
80	HW	298–313	0–30	ZD,D,L
81	HW	222–282	2–9	L
82	HW	350–2000	⋯	ZD
83	HW	314–403	⋯	ZD
84	SSHW	225–314	0.1–2	ZD,D

APPENDIX I: List of All Available Data from Measurements of the Thermal Conductivity of Carbon Dioxide (Continued)

Ref. no.	Method	T/K range	P/MPA range	Code
85	SSHW	400–1300	⋯	ZD
86	I	298–307	3–20	C,D,L
87	SSHW	294–573	0–150	ZD,D
88	SSHW	298–323	0–5	ZD,D
89	THW	301	0–6	ZD,D
90	THW	300–348	0–25	ZD,D
91	THW	380–470	0–30	ZD,D
12	THW	308–379	0–7	ZD,D

APPENDIX II: List of All Available Data from Measurements of Viscosity of Dense Carbon Dioxide

Methods	Code
C-capillary	C-predominantly critical region data
OD-oscillating disk	D-n as a function of density
T-transpiration method	L-liquid region
VC-vibrating crystal	
FC-falling cylinder	
RDV-rotating disk viscometer	

Ref. no.	Method	T/K range	P/MPA range	Code
134	C	313	0.1–14	D
126	T	273–348	0.1–210	D,L
22	OD	293	0.1–2	D
135	OD	293–543	0.1–15	D
128	OD	303–323	0.1–12	D
28	OD	293–313	0.1–2.5	D
23	OD	293–313	0.1–2.5	D
27	OD	293–313	0.1–2.5	D
29	OD	293–313	0.1–2.5	D
136	C	293–523	0.1–12	L,D
137	VC	219–303	3–20	L,D
138	VC	283–313	0.1–5	D
139	FC	243–293	5–50	L
140	C	473–773	0.1–50	D
141	C	293–423	0.1–350	D
142	C	223–293	6–55	L
143	C	223–293	6–55	L
144	C	223–293	6–55	L
145	OD	297–453	0.1–8	D
131	OD	298–473	0.1–15	D
20	OD	303–304	0.2–7	D,C
30	OD	298–323	0.1–15	C
146	VC	6 isochores around the critical isochore		C
147	VC			C
129	VC	298–313	$\sim P_c$	C
130	RDV	304.51	0.1–3	C
148	VC	220–320	0.1–30	L,D

APPENDIX III: Deviation Plots of the Experimental Data from the Correlation

+ ref 12; x ref 91; ⊙ ref 89;
Δ ref 88; * ref 90;
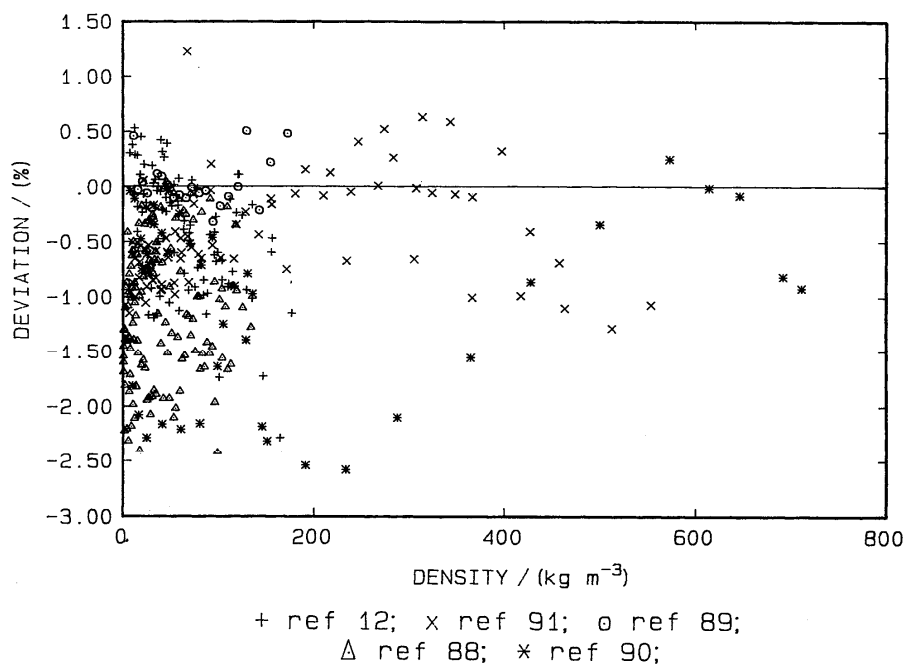
A3.1 Deviations of primary gas-phase thermal-conductivity data[12,88-91] from the final correlation.

+ 295-350K; x 350-450K; * 450-550K;
Δ 550-650K; ⊙ 650-750K;
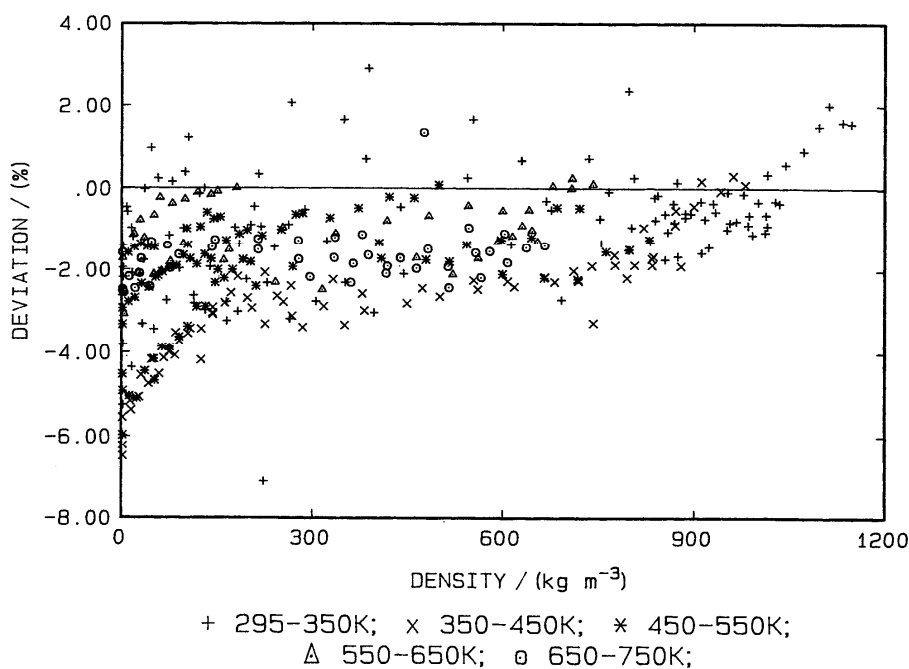
A3.2 Deviations of the gas-phase thermal-conductivity data of Le Neindre et al.[66,70,77,78] from the correlation.
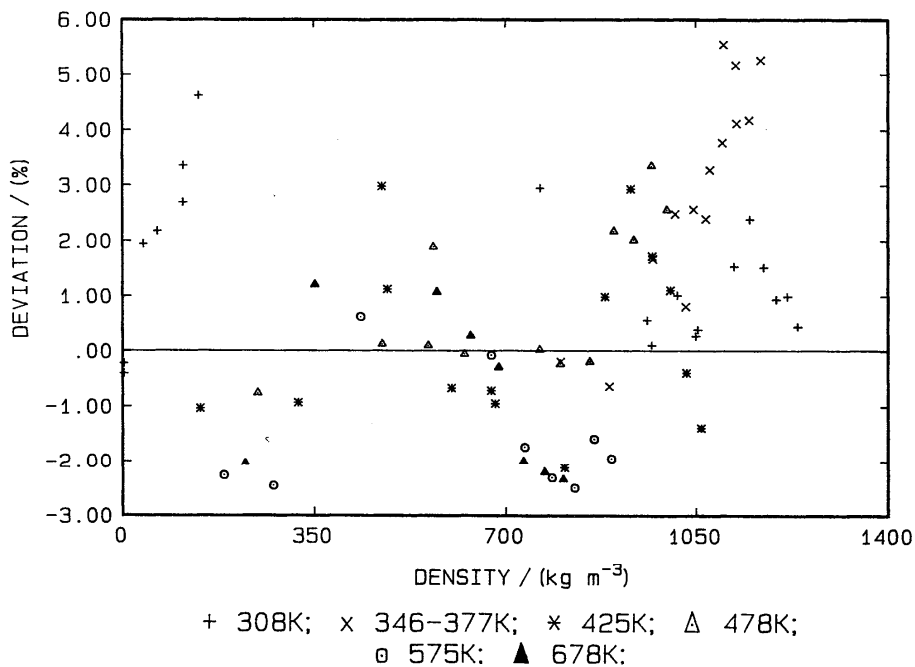
A3.3 Deviations of the gas-phase thermal conductivity of Tarzimanov *et al.*[87] from the final correlation.
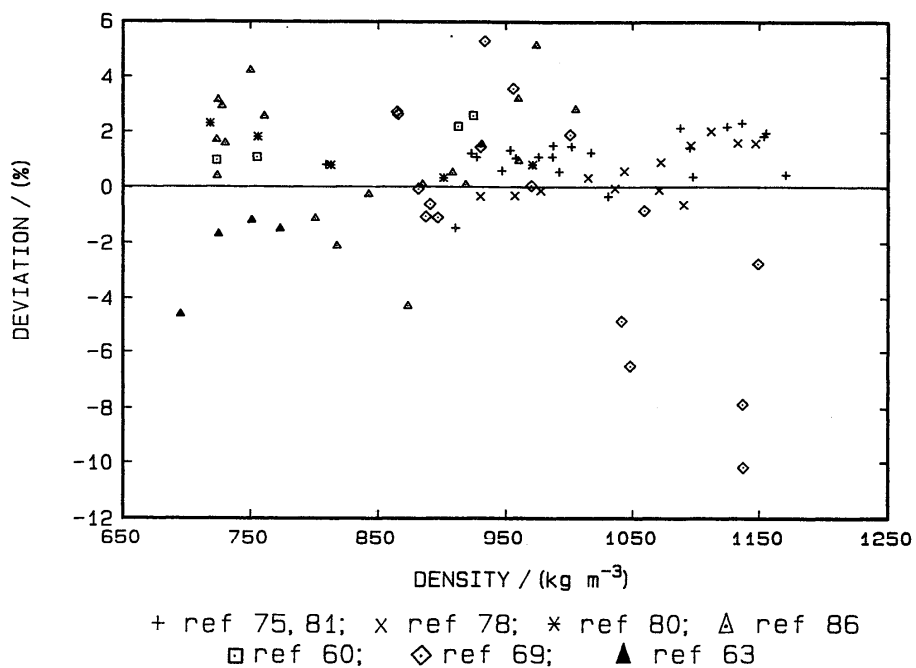
A3.4 Deviations of the liquid-phase thermal-conductivity data from the correlation.
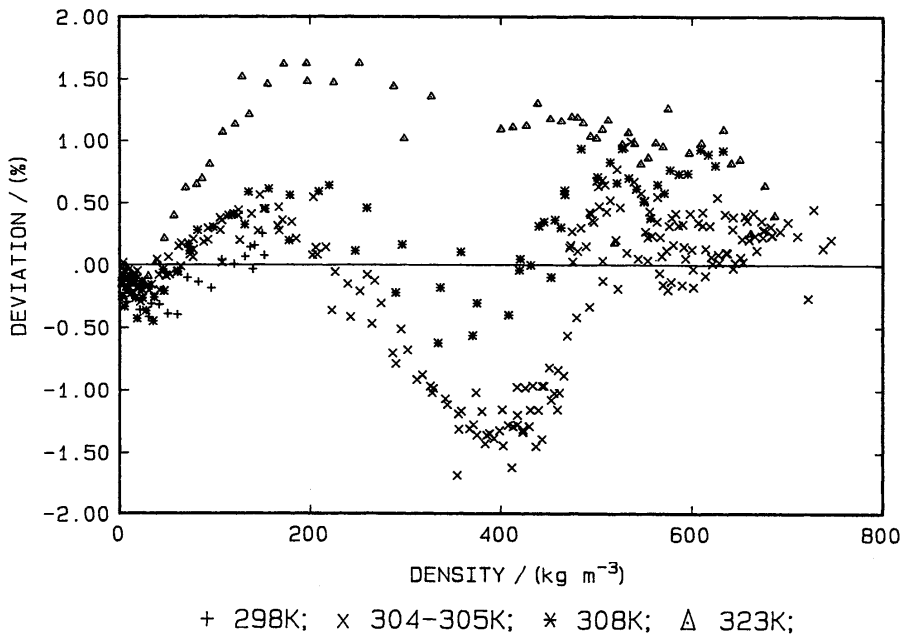
+ 298K; x 304-305K; * 308K; △ 323K;

A3.5 Deviations of the gas-phase viscosity data of Iwasaki and Takahashi[30] from the final correlation.

refs20, 22, 23, 27-29, 128: (+ 293K   x 303K); ref131:
(*300-353K △373-393K ⊖411-423K ▲452-473K)
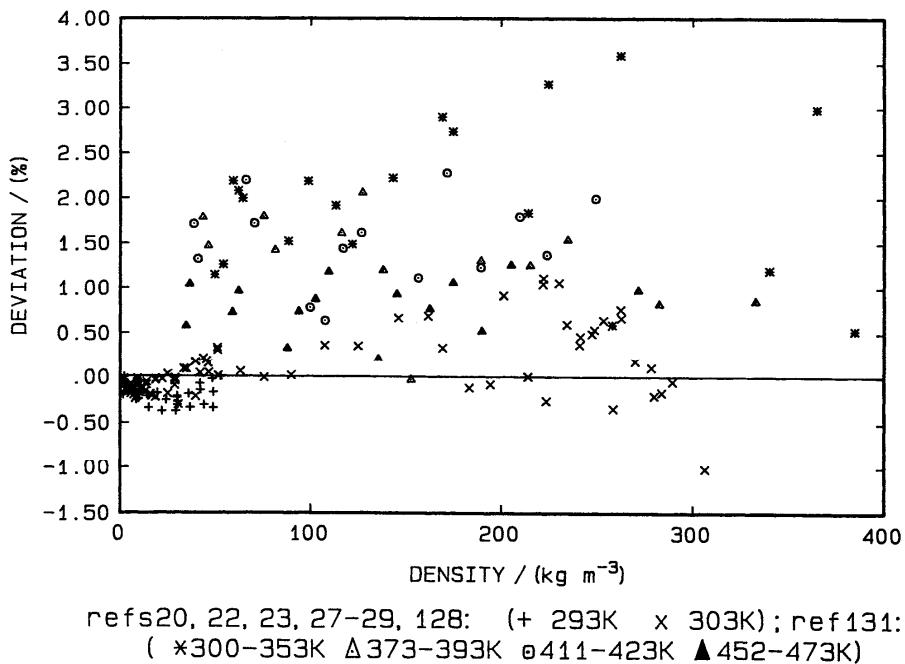
A3.6 Deviations of the gas-phase viscosity data[20,22,23,27-29,128,131] from the correlation.
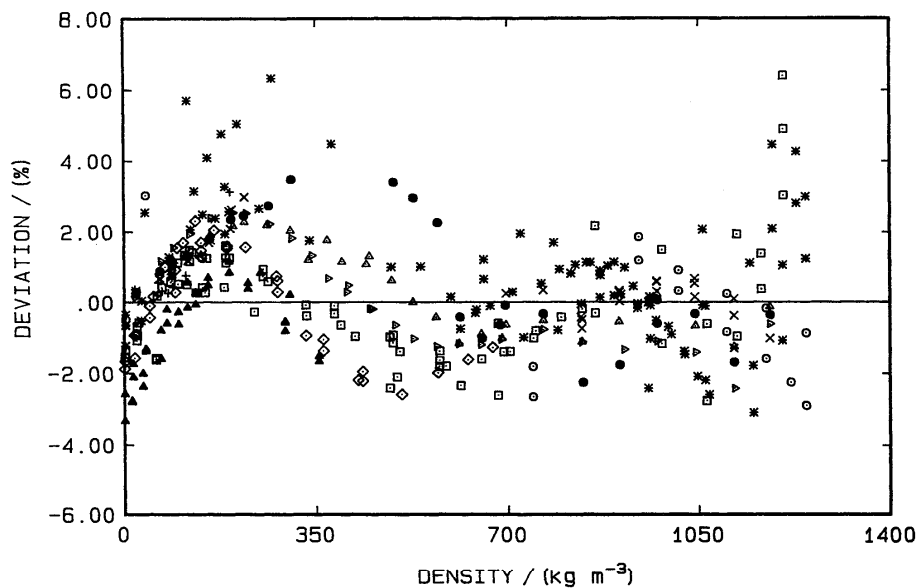
ref126: (+273-293K x304K ●313K △323K ▷348K); ref136
140, 141: (⊡453K ◇553K ▲ 723K ⊙ 300K * 353K)

A3.7 Deviations of the gas-phase viscosity data[126,136,140,141] from the correlation.
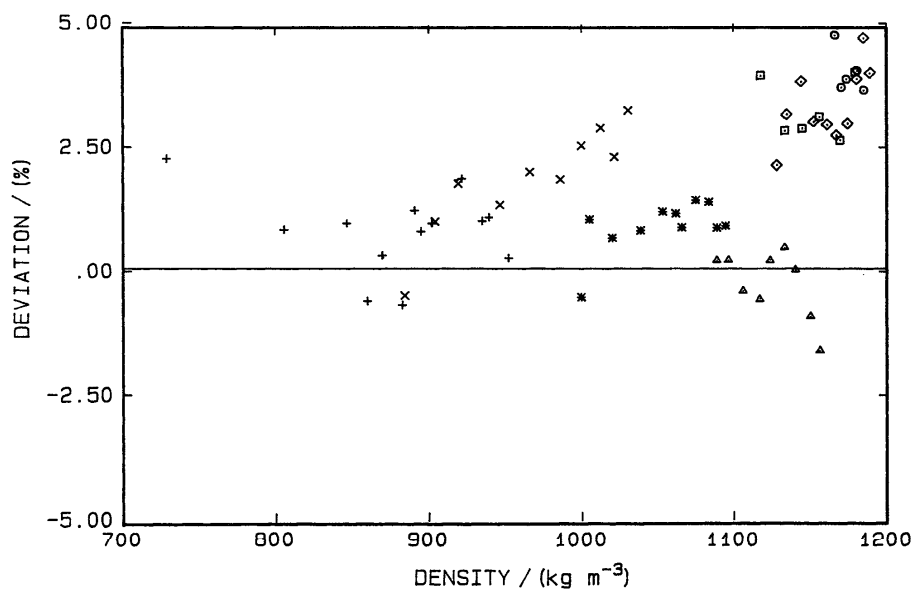
+ 300K; x 280K; * 260K; △ 240K; ⊡233K;
◇230K; ⊙ 220K;

A3.8 Deviations of the liquid-phase viscosity data[148] from the correlation.
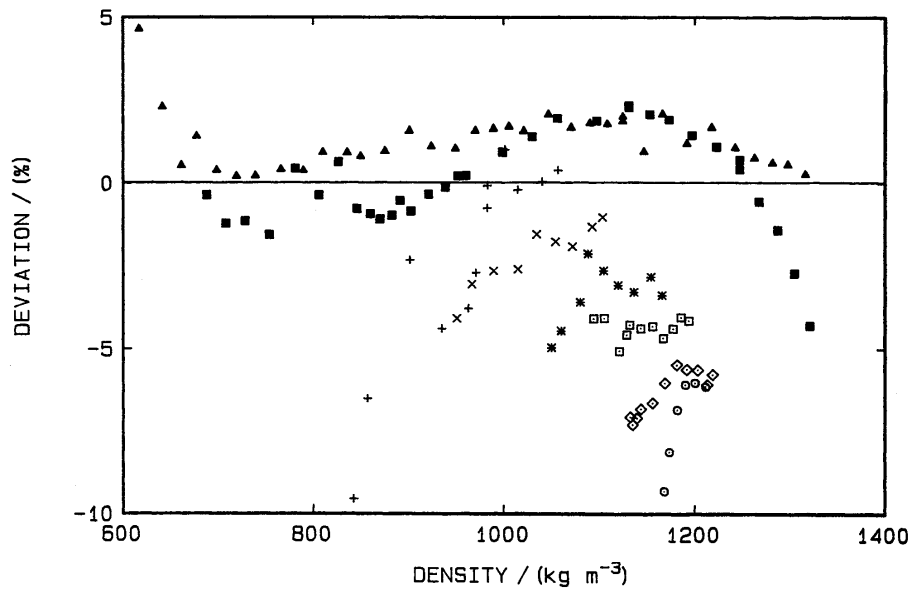
(+ 293K x 273K * 253K ▣ 243K ◇ 233K ⊙ 223K) [144]

(■ 300K ▲ 303K) [9]

A3.9 Deviations of the liquid-phase viscosity data[9,144] from the correlation.

APPENDIX IV: Tabulations of the Transport Properties of Carbon Dioxide

The viscosity of carbon dioxide (η/μPa s)

T/K P/MPa	200	240	260	280	300	320	340	360
0.1	10.05	12.07	13.06	14.05	15.02	15.98	16.93	17.87
0.5	···	12.11	13.10	14.08	15.05	16.01	16.96	17.89
1.0	···	12.19	13.17	14.14	15.11	16.06	17.00	17.93
2.5	···	179.82	130.52	14.48	15.39	16.30	17.21	18.12
5.0	···	184.49	135.60	94.82	16.67	17.19	17.91	18.70
7.5	···	189.04	140.34	101.30	61.00	19.69	19.41	19.80
10.0	···	193.50	144.81	106.82	72.44	32.40	22.70	21.75
12.5	···	197.88	149.07	111.72	79.74	50.96	29.95	25.07
15.0	···	202.20	153.17	116.20	85.55	60.04	40.06	30.14
17.5	···	206.47	157.14	120.37	90.53	66.54	48.33	36.31
20.0	···	210.70	161.01	124.30	94.96	71.88	54.77	42.33
22.5	···	214.90	164.78	128.04	99.03	76.53	60.10	47.68
25.0	···	219.06	168.47	131.64	102.81	80.72	64.71	52.40
27.5	···	223.21	172.10	135.10	106.38	84.57	68.84	56.62
30.0	···	227.33	175.67	138.47	109.76	88.18	72.62	60.46
35.0	···	235.55	182.68	144.94	116.13	94.87	79.44	67.29
40.0	···	243.75	189.55	151.15	122.08	101.03	85.58	73.36
45.0	···	251.95	196.32	157.16	127.73	106.82	91.27	78.92
50.0	···	260.17	203.02	163.02	133.15	112.33	96.63	84.09
55.0	···	···	209.66	168.75	138.38	117.63	101.73	89.00
60.0	···	···	216.27	174.40	143.47	122.75	106.64	93.69
65.0	···	···	222.87	179.97	148.45	127.73	111.39	98.21
70.0	···	···	229.46	185.49	153.32	132.60	116.01	102.59
75.0	···	···	236.07	190.97	158.12	137.36	120.53	106.86
80.0	···	···	242.69	196.41	162.86	142.05	124.95	111.03
85.0	···	···	249.34	201.84	167.54	146.66	129.30	115.12
90.0	···	···	···	207.25	172.18	151.20	133.58	119.15
95.0	···	···	···	212.66	176.78	155.70	137.80	123.11
100.0	···	···	···	218.08	181.36	160.14	141.97	127.02

The viscosity of carbon dioxide (η/μPa s)

T/K P/MPa	800	900	1000	1100	1300	1500
0.1	35.09	38.27	41.26	44.08	49.32	54.13
0.5	35.10	38.28	41.27	44.09	49.33	54.14
1.0	35.11	38.29	41.28	44.10	49.33	54.15
2.5	35.17	38.34	41.32	44.14	49.36	54.17
5.0	35.28	38.44	41.40	44.21	49.42	54.22
7.5	35.44	38.56	41.51	44.30	49.49	54.28
10.0	35.63	38.72	41.64	44.41	49.58	54.34
12.5	35.86	38.90	41.79	44.54	49.67	54.42
15.0	36.12	39.11	41.96	44.69	49.78	54.51
17.5	36.41	39.34	42.16	44.85	49.90	54.60
20.0	36.74	39.60	42.37	45.02	50.03	54.71
22.5	37.09	39.88	42.59	45.21	50.18	54.82
25.0	37.48	40.18	42.84	45.42	50.33	54.94
27.5	37.89	40.50	43.10	45.64	50.49	55.06
30.0	38.32	40.84	43.38	45.87	50.66	55.20
35.0	39.26	41.58	43.98	46.37	51.03	55.48
40.0	40.27	42.38	44.63	46.92	51.43	55.80
45.0	41.35	43.23	45.32	47.50	51.87	56.13
50.0	42.48	44.13	46.06	48.12	52.33	56.49
55.0	43.66	45.07	46.83	48.77	52.81	56.87
60.0	44.87	46.04	47.63	49.44	53.32	57.27
65.0	46.10	47.03	48.46	50.14	53.84	57.68
70.0	47.35	48.05	49.31	50.86	54.39	58.11
75.0	48.62	49.09	50.17	51.60	54.95	58.56
80.0	49.89	50.13	51.05	52.36	55.52	59.01
85.0	51.16	51.19	51.95	53.12	56.11	59.48
90.0	52.44	52.25	52.85	53.90	56.71	59.96
95.0	53.71	53.32	53.76	54.68	57.32	60.45
100.0	54.98	54.38	54.67	55.47	57.93	60.94

The viscosity of carbon dioxide (η/μPa s)

T/K P/MPa	380	400	450	500	550	600	650	700
0.1	18.79	19.70	21.90	24.02	26.05	28.00	29.87	31.68
0.5	18.81	19.72	21.92	24.03	26.06	28.01	29.89	31.69
1.0	18.85	19.75	21.95	24.06	26.09	28.03	29.90	31.70
2.5	19.01	19.90	22.07	24.16	26.18	28.11	29.97	31.77
5.0	19.51	20.34	22.40	24.43	26.40	28.30	30.14	31.91
7.5	20.38	21.06	22.91	24.82	26.71	28.57	30.37	32.11
10.0	21.79	22.16	23.63	25.35	27.13	28.91	30.65	32.36
12.5	23.92	23.73	24.57	26.01	27.64	29.32	31.00	32.65
15.0	26.93	25.83	25.75	26.83	28.26	29.81	31.40	33.00
17.5	30.78	28.48	27.17	27.78	28.97	30.37	31.87	33.39
20.0	35.14	31.57	28.82	28.87	29.77	31.00	32.38	33.82
22.5	39.57	34.93	30.67	30.09	30.66	31.70	32.95	34.30
25.0	43.81	38.37	32.67	31.41	31.63	32.46	33.56	34.81
27.5	47.75	41.76	34.77	32.83	32.67	33.27	34.22	35.36
30.0	51.40	45.02	36.94	34.32	33.77	34.13	34.92	35.95
35.0	57.99	51.09	41.31	37.44	36.12	35.97	36.42	37.21
40.0	63.86	56.60	45.60	40.65	38.58	37.93	38.04	38.56
45.0	69.20	61.66	49.72	43.86	41.11	39.98	39.73	40.00
50.0	74.17	66.37	53.65	47.02	43.67	42.07	41.48	41.49
55.0	78.85	70.81	57.40	50.11	46.21	44.19	43.27	43.03
60.0	83.31	75.03	61.00	53.12	48.72	46.31	45.08	44.59
65.0	87.60	79.08	64.46	56.05	51.19	48.41	46.89	46.17
70.0	91.74	82.99	67.81	58.90	53.62	50.50	48.71	47.75
75.0	95.77	86.78	71.07	61.68	56.01	52.57	50.51	49.34
80.0	99.70	90.48	74.24	64.40	58.36	54.61	52.30	50.93
85.0	103.55	94.10	77.33	67.06	60.66	56.62	54.07	52.51
90.0	107.33	97.65	80.37	69.67	62.93	58.61	55.83	54.07
95.0	111.05	101.15	83.36	72.24	65.16	60.57	57.57	55.63
100.0	114.72	104.59	86.29	74.77	67.36	62.51	59.30	57.18

The thermal conductivity of carbon dioxide ($\lambda/$mW m^{-1} K^{-1})

T/K P/MPa	200	240	260	280	300	320	340	360
0.1	9.63	12.23	13.67	15.19	16.77	18.41	20.07	21.76
0.5	···	12.52	13.91	15.40	16.97	18.58	20.24	21.91
1.0	···	13.05	14.32	15.73	17.25	18.84	20.47	22.12
2.5	···	152.12	126.92	17.46	18.54	19.87	21.34	22.89
5.0	···	154.60	130.32	104.61	24.03	23.20	23.75	24.78
7.5	···	156.96	133.43	109.54	82.70	31.71	28.28	27.85
10.0	···	159.24	136.32	113.72	89.80	60.94	36.82	32.66
12.5	···	161.44	139.03	117.40	95.54	73.17	50.41	39.58
15.0	···	163.56	141.60	120.73	100.28	80.06	61.44	47.84
17.5	···	165.62	144.03	123.80	104.37	85.69	68.69	55.49
20.0	···	167.63	146.39	126.66	108.02	90.45	74.56	61.76
22.5	···	169.59	148.64	129.34	111.34	94.60	79.55	67.12
25.0	···	171.50	150.82	131.89	114.39	98.30	83.91	71.84
27.5	···	173.36	152.92	134.31	117.25	101.67	87.80	76.06
30.0	···	175.19	154.96	136.63	119.93	104.78	91.33	79.88
35.0	···	178.74	158.87	141.02	124.89	110.40	97.59	86.61
40.0	···	182.16	162.60	145.12	129.43	115.42	103.07	92.44
45.0	···	185.47	166.16	148.99	133.65	120.00	108.00	97.63
50.0	···	188.68	169.59	152.67	137.61	124.25	112.51	102.34
55.0	···	···	172.89	156.19	141.36	128.23	116.69	106.69
60.0	···	···	176.09	159.57	144.93	131.99	120.62	110.74
65.0	···	···	179.20	162.83	148.35	135.56	124.33	114.55
70.0	···	···	182.21	165.98	151.64	138.97	127.85	118.15
75.0	···	···	185.15	169.03	154.81	142.25	131.22	121.59
80.0	···	···	188.02	172.00	157.87	145.41	134.45	124.88
85.0	···	···	190.82	174.89	160.85	148.46	137.56	128.03
90.0	···	···	···	177.70	163.73	151.41	140.57	131.07
95.0	···	···	···	180.45	166.55	154.28	143.48	134.01
100.0	···	···	···	183.14	169.29	157.07	146.31	136.86

The thermal conductivity of carbon dioxide (λ /mW m^{-1} K^{-1})

T/K P/MPa	380	400	450	500	550	600	650	700
0.1	23.46	25.15	29.38	33.54	37.61	41.59	45.49	49.29
0.5	23.60	25.29	29.50	33.64	37.71	41.68	45.57	49.36
1.0	23.79	25.47	29.65	33.78	37.83	41.80	45.67	49.46
2.5	24.48	26.10	30.17	34.23	38.23	42.16	46.00	49.76
5.0	26.06	27.46	31.21	35.10	38.99	42.83	46.61	50.32
7.5	28.37	29.33	32.48	36.13	39.86	43.59	47.28	50.93
10.0	31.66	31.80	34.00	37.31	40.84	44.43	48.02	51.59
12.5	36.06	34.96	35.79	38.64	41.93	45.35	48.83	52.30
15.0	41.43	38.76	37.84	40.12	43.11	46.35	49.68	53.05
17.5	47.24	43.03	40.12	41.73	44.38	47.40	50.59	53.85
20.0	52.87	47.49	42.61	43.46	45.74	48.52	51.54	54.68
22.5	57.99	51.90	45.25	45.28	47.16	49.69	52.53	55.55
25.0	62.62	56.10	47.99	47.19	48.64	50.90	53.56	56.44
27.5	66.83	60.05	50.76	49.16	50.17	52.15	54.62	57.36
30.0	70.70	63.74	53.54	51.17	51.73	53.43	55.71	58.30
35.0	77.56	70.43	58.95	55.22	54.93	56.06	57.94	60.24
40.0	83.55	76.34	64.07	59.25	58.16	58.74	60.22	62.23
45.0	88.87	81.65	68.86	63.17	61.37	61.43	62.53	64.24
50.0	93.70	86.48	73.34	66.96	64.54	64.11	64.84	66.27
55.0	98.13	90.93	77.54	70.60	67.63	66.76	67.15	68.31
60.0	102.26	95.06	81.49	74.09	70.64	69.37	69.43	70.33
65.0	106.12	98.94	85.22	77.44	73.56	71.92	71.68	72.33
70.0	109.78	102.60	88.75	80.65	76.40	74.42	73.90	74.32
75.0	113.25	106.07	92.13	83.74	79.15	76.87	76.08	76.28
80.0	116.56	109.38	95.35	86.72	81.83	79.26	78.22	78.21
85.0	119.74	112.56	98.44	89.59	84.42	81.59	80.33	80.12
90.0	122.79	115.61	101.42	92.37	86.95	83.88	82.39	81.99
95.0	125.74	118.55	104.28	95.05	89.41	86.11	84.42	83.84
100.0	128.60	121.40	107.06	97.66	91.80	88.29	86.41	85.66

The thermal conductivity of carbon dioxide near the critical point (λ /mW m^{-1} K^{-1})

T/K P/MPa	298	300	302	304	306	308	310
0.1	16.61	16.77	16.93	17.10	17.26	17.42	17.59
0.5	16.81	16.97	17.13	17.29	17.45	17.61	17.77
1.0	17.10	17.25	17.41	17.56	17.72	17.88	18.04
1.5	17.45	17.60	17.75	17.90	18.05	18.20	18.35
2.0	17.88	18.02	18.16	18.30	18.44	18.59	18.73
2.5	18.41	18.54	18.66	18.79	18.92	19.05	19.18
3.0	19.07	19.17	19.27	19.38	19.49	19.60	19.72
3.5	19.91	19.97	20.03	20.11	20.19	20.27	20.37
4.0	20.97	20.97	20.99	21.01	21.05	21.10	21.15
4.5	22.38	22.28	22.21	22.16	22.13	22.11	22.12
5.0	24.31	24.03	23.81	23.63	23.50	23.39	23.31
5.5	27.18	26.52	26.01	25.61	25.29	25.03	24.82
6.0	32.26	30.50	29.29	28.41	27.74	27.21	26.79
6.5	82.87	39.22	35.15	32.87	31.36	30.27	29.44
7.0	83.94	81.65	59.63	42.52	37.70	35.04	33.28
7.5	85.42	82.70	80.43	81.57	56.67	44.52	39.66
8.0	86.92	84.16	81.52	79.25	78.64	83.25	53.66
8.5	88.36	85.65	82.98	80.39	78.07	76.57	76.76
9.0	89.74	87.10	84.46	81.85	79.30	76.94	74.95
9.5	91.05	88.48	85.91	83.33	80.76	78.26	75.88
10.0	92.29	89.80	87.29	84.77	82.24	79.73	77.27
10.5	93.48	91.05	88.61	86.16	83.68	81.20	78.75
11.0	94.62	92.25	89.87	87.48	85.06	82.63	80.22
11.5	95.70	93.39	91.07	88.73	86.38	84.01	81.65
12.0	96.75	94.48	92.22	89.94	87.64	85.33	83.02
12.5	97.76	95.54	93.32	91.09	88.84	86.59	84.33
13.0	98.73	96.55	94.38	92.19	89.99	87.79	85.58
13.5	99.67	97.53	95.40	93.26	91.10	88.94	86.78
14.0	100.58	98.47	96.38	94.28	92.17	90.05	87.94

The thermal conductivity of carbon dioxide, (λ /mW m^{-1} K^{-1})

T/K P/MPa	750	800	850	900	950	1000
0.1	53.01	56.65	60.21	63.70	67.13	70.49
0.5	53.08	56.71	60.27	63.76	67.18	70.54
1.0	53.17	56.80	60.35	63.84	67.25	70.61
2.5	53.45	57.06	60.60	64.07	67.47	70.81
5.0	53.96	57.53	61.03	64.47	67.85	71.18
7.5	54.51	58.04	61.50	64.91	68.27	71.56
10.0	55.11	58.58	62.01	65.38	68.70	71.97
12.5	55.75	59.16	62.54	65.87	69.16	72.40
15.0	56.42	59.78	63.10	66.39	69.64	72.84
17.5	57.13	60.42	63.68	66.93	70.13	73.31
20.0	57.87	61.08	64.29	67.48	70.65	73.78
22.5	58.64	61.77	64.92	68.06	71.18	74.28
25.0	59.43	62.49	65.56	68.65	71.72	74.78
27.5	60.25	63.22	66.23	69.25	72.28	75.30
30.0	61.08	63.96	66.90	69.87	72.85	75.83
35.0	62.79	65.50	68.29	71.14	74.02	76.91
40.0	64.55	67.07	69.72	72.45	75.23	78.03
45.0	66.34	68.68	71.18	73.79	76.46	79.17
50.0	68.15	70.31	72.66	75.14	77.71	80.33
55.0	69.96	71.95	74.15	76.51	78.97	81.50
60.0	71.77	73.59	75.65	77.88	80.24	82.69
65.0	73.58	75.22	77.15	79.26	81.52	83.88
70.0	75.37	76.85	78.64	80.64	82.80	85.07
75.0	77.15	78.47	80.13	82.02	84.08	86.26
80.0	78.90	80.08	81.61	83.39	85.35	87.45
85.0	80.64	81.67	83.08	84.75	86.62	88.64
90.0	82.35	83.25	84.53	86.10	87.88	89.82
95.0	84.05	84.81	85.98	87.44	89.13	90.99
100.0	85.72	86.35	87.41	88.78	90.38	92.16

The viscosity of carbon dioxide near the critical point (η/μPa s)

T/K P/MPa	298	300	302	304	306	308	310
0.1	14.92	15.02	15.12	15.21	15.31	15.41	15.50
0.5	14.96	15.05	15.15	15.25	15.34	15.44	15.53
1.0	15.01	15.11	15.20	15.30	15.39	15.49	15.58
1.5	15.08	15.18	15.27	15.37	15.46	15.56	15.65
2.0	15.18	15.27	15.36	15.46	15.55	15.64	15.74
2.5	15.29	15.39	15.48	15.57	15.66	15.75	15.84
3.0	15.45	15.53	15.62	15.71	15.80	15.88	15.97
3.5	15.64	15.72	15.80	15.88	15.97	16.05	16.13
4.0	15.89	15.96	16.03	16.10	16.18	16.26	16.33
4.5	16.21	16.26	16.32	16.38	16.45	16.51	16.58
5.0	16.64	16.67	16.70	16.74	16.79	16.84	16.89
5.5	17.27	17.24	17.22	17.22	17.23	17.25	17.28
6.0	18.29	18.09	17.97	17.89	17.84	17.81	17.79
6.5	58.96	19.73	19.21	18.91	18.71	18.58	18.49
7.0	63.06	56.87	22.85	20.89	20.17	19.76	19.48
7.5	66.08	61.00	55.02	46.91	23.93	21.96	21.10
8.0	68.58	64.04	58.99	53.67	46.77	31.34	24.64
8.5	70.75	66.54	61.93	57.40	52.62	46.54	37.21
9.0	72.69	68.72	64.37	60.23	56.20	51.72	46.32
9.5	74.47	70.67	66.50	62.59	58.97	55.16	50.95
10.0	76.11	72.44	68.40	64.64	61.28	57.86	54.23
10.5	77.64	74.08	70.14	66.49	63.31	60.15	56.86
11.0	79.09	75.62	71.75	68.19	65.14	62.16	59.11
11.5	80.46	77.07	73.26	69.76	66.82	63.97	61.09
12.0	81.77	78.44	74.68	71.23	68.38	65.64	62.89
12.5	83.02	79.74	76.02	72.63	69.84	67.19	64.54
13.0	84.22	80.99	77.31	73.95	71.22	68.64	66.08
13.5	85.39	82.19	78.55	75.21	72.53	70.01	67.52
14.0	86.50	83.35	79.72	76.42	73.78	71.32	68.89

Transport properties along the saturation line

T/K	η_{gas} μPa s	η_{liq} μPa s	λ_{gas} mW m^{-1} K^{-1}	λ_{liq} mW m^{-1} K^{-1}
304	30.73	39.02	243.1	187.1
302	23.47	47.61	67.3	84.9
300	21.35	53.13	50.9	82.3
295	18.77	64.40	37.0	85.2
290	17.32	74.05	30.5	90.6
285	16.32	83.20	26.3	96.6
280	15.56	92.22	23.4	102.7
260	13.59	130.3	16.81	126.8
240	12.26	177.5	13.49	150.9
220	11.13	244.0	11.36	176.3
200	10.07	$\cdots$	9.75	$\cdots$

Values of λ and η given at T, P, ρ for checking computer code

T/K	P/MPa	ρ/kg m^{-3}	λ /mW m^{-1} K^{-1}	η/μPa s
220	0.1	2.440	10.90	11.06
300	0.1	1.773	16.77	15.02
800	0.1	0.662	56.65	35.09
304	7	254.3205	42.52	20.89
220	15	1194.86	187.50	274.22
300	50	1029.27	137.61	133.15
800	75	407.828	78.47	48.62